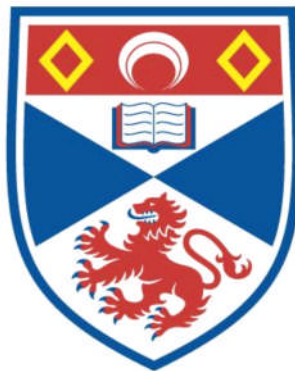# MECHANICAL PROPERTIES OF FISH MYOTOMAL MUSCLE

MELISSA LYNNE F. DAVIES

**A Thesis Submitted for the Degree of PhD
at the
University of St Andrews**

1995

Mechanical Properties of Fish Myotomal Muscle

A thesis submitted to the University of St. Andrews for the degree of Doctor of Philosophy.

By Melissa Lynne F. Davies.

School of Biological and Medical Sciences,

Gatty Marine Laboratory,

University of St. Andrews.

January 1995

To Barry

♥

for everything

Declaration

I hereby declare that the research reported in this thesis was carried out by me and that the thesis is my own composition. No part of this work has previously been submitted for a higher degree.

The research was conducted in the School of Biological and Medical Sciences, United College of St. Salvator and St. Leonard, University of St. Andrews, under the direction of Professor I. A. Johnston.

Signed: Date: 20/3/95

Certificate

I hereby certify that Melissa L. F. Davies has spent nine terms engaged in research under my direction and that she has fulfilled the conditions of General Ordinances No. 2 (Resolution of the University Court No. 1, 1967) and is qualified to submit the accompanying thesis for the degree of Doctor of Philosophy.

Signed: Date: 20/3/95

Contents

Summary

Chapter 1

Swimming ability is closely linked to the functional design of the locomotory system. The basic principles underlying motion in a fluid are summarised to outline the problems faced when moving through the aquatic environment. The mechanism underlying the generation of mechanical power is described and the ways in which fish have developed this basic design is explored in relation to mechanical and metabolic power. Finally, the conversion of muscular power into swimming movements is reviewed in terms of the musculo-skeletal system, the generation of thrust, efficiency of movement and adaptations of body form.

Chapter 2

Muscle fibres were isolated from myotomes of the Atlantic cod (*Gadus morhua* L) at points 0.35 and 0.90 from the snout to the caudal peduncle (L_S). Half times (ms) for force development (HPT) and relaxation (HFT) for isometric tetani were significantly shorter for muscle fibres from rostral than from caudal myotomes (24.7 ± 1.8 and 54.0 ± 2.9 and 42.1 ± 2.4 and 88.3 ± 8.0 at 5°C for fibres at 0.35 and 0.90 L_S respectively, mean ± SEM, n = 15). Maximum (unloaded) contraction velocities were found to be 2.4 times higher for rostral than for caudal muscle fibres (6.9 ± 1.3 and 2.9 ± 0.8 muscle lengths.s^{-1} respectively at 5°C; mean ± SEM, n = 8). Sinusoidal length changes approximating those found during steady swimming were imposed on isolated muscle fibres. Activation phase (defined in degrees

from the point that the muscle passed through the resting length while being stretched) was varied from 15° to 360° at oscillation frequencies of 4 Hz and 9 Hz. Caudal fibres, by virtue of their longer HPT and HFT, generate tension over a greater portion of the oscillation cycle and so produce net negative work at earlier values of activation phase than rostral fibres. Caudal muscle fibres are activated whilst lengthening during sub-carangiform swimming which, combined with the present results, suggests that they may play a role in propagating rostrally produced forces to the tail blade. No significant differences were found between the contractile properties of muscle fibres from summer and winter caught cod.

Chapter 3

The volume and surface densities of T-tubules and sarcoplasmic reticulum (SR) were investigated in fast muscle fibres isolated from rostral (0.35 L_S) and caudal (0.90 L_S) myotomes of Atlantic cod (*Gadus morhua* L.). No significant differences were found between rostral and caudal fibres for any of the components measured - SR and T-tubules constituted around 6% and 0.23% of myofibrillar volume respectively, comparing well to the literature. The results suggest that regional differences in membrane dimensions are unlikely to contribute to differences in contractile properties between rostral and caudal myotomes.

Chapter 4

The force-velocity (P-V) relationship was measured for slow and fast muscle fibre types isolated from the short-horned sculpin (*Myoxocephalus scorpius* L.). P-V curves were also compared for fast

fibres isolated from rostral (0.35 L_s) and caudal (0.90 L_s) myotomes of the sculpin and the Atlantic cod (*Gadus morhua* L.). In the sculpin, peak isometric force (P_0), maximum shortening velocity (V_{max}), maximum instantaneous power ($\dot{W}_{max}$) and the optimum shortening velocity for $\dot{W}_{max}$ were significantly greater in fast than in slow fibres, whilst half-times to activation (HPT) and relaxation (HFT) were 70-100% longer in slow fibres. Slow and fast fibre types thus generate maximum power at velocities relevant to the speeds at which they are recruited during swimming and the greater power output of fast fibres is consistent with their role in powering bursts of speed and acceleration where thrust requirements are large. Few regional differences were found in the contractile properties of sculpin fast fibres: P_0 and $\dot{W}_{max}$ were the same in rostral and caudal fibres (160 kN.m^{-2} and 146-180 W.kg^{-1} respectively) but caudal fibre V_{max} was 28% lower than that of rostral fibres. Since the optimum relative velocity (V/V_{max}) for power output was higher in caudal than in rostral fibres, $\dot{W}_{max}$ was generated at the same velocity of shortening in rostral and caudal fibres, despite their differing in V_{max}. In the cod, fast fibres isolated from rostral and caudal myotomes had similar peak tensions but HPT and HFT were up to 50% shorter in rostral fibres. $\dot{W}_{max}$ was 170 W.kg^{-1} in cod rostral fibres compared to only 88 W.kg^{-1} in caudal fibres. The P-V relationship of cod rostral fibres was less curved than that of caudal fibres, resulting in the generation of a greater relative power output for a given load in the former. The results suggest that sculpin, rostral and caudal fast fibres may be used under similar strain amplitudes and frequencies *in vivo* while in the cod, rostral fibres are capable of generating maximal power over the upper range of tail-beat frequencies observed *in vivo*. Cod caudal fibres may function primarily to stiffen the tail by resisting muscle lengthening and thus

have a reduced ability to generate power during isovelocity shortening as a result.

Chapter 5

The relationship between isometric force and sarcomere length was examined in bundles of fast muscle fibres isolated from rostral (0.35 L_s) and caudal (0.90 L_s) myotomes of the short-horned sculpin (*Myoxocephalus scorpius* L.). Force was strongly dependent on sarcomere length between 2.1 to 3.6 μm and rostral fibres produced relatively more force than caudal fibres at a given sarcomere length. Optimum sarcomere length was significantly longer in rostral than in caudal fibres (2.45 μm compared to 2.33 μm respectively) but peak forces at the optimum sarcomere length for force production (l_{osarc}) were the same. A simple sarcomere model was found to predict these results using measurements of sculpin sarcomere geometry corrected for shrinkage assuming a thick filament length of 1.6 μm. Deviations of the experimental length-tension curve from the predicted path at long sarcomere lengths coincided with an increase in passive force and relaxation rates decreased with sarcomere length above 2.4 μm in both rostral and caudal fibres. The influence of sarcomere geometry on power output during swimming is discussed.

Chapter 6

Short-horned sculpin (*Myoxocephalus scorpius* L.) were acclimated for 6 to 8 weeks to either 5°C or 15°C. The isometric properties of fast muscle fibres isolated from rostral (0.35 standard length [L_s]) and caudal (0.90 L_s) myotomes were compared between acclimation groups at 5, 10 and 15°C. At

each temperature, no regional differences were found in peak tension (P_0) or in the half-times to activation (HPT) and relaxation (HFT). In fibres from 5°C acclimated fish, a 10°C rise in temperature decreased tetanic P_0 by 55% but in fibre from 15°C fish, P_0 was relatively temperature independent. Rates of activation and relaxation at each temperature were not significantly affected by acclimation state: the temperature coefficient ($Q_{10[5-15°C]}$) for HPT and HFT was generally between 1.6 and 1.7 for both acclimation groups. The work loop technique was used to measure the power output of rostral and caudal muscle fibres isolated from 5°C acclimated fish under conditions of strain and activation calculated from the propulsive stroke of a fast start. Strain sequences were calculated at three positions down the trunk (035, 0.60 and 0.93 L_s) from prey capture events performed by a 5°C acclimated fish at 5 and 15°C. For the *in vitro* studies 5°C strain sequences were used at 5°C and 15°C sequences, at 15°C. The mean power output of rostral and caudal fibres was similar under each strain sequence and instantaneous power output peaked sequentially down the trunk during the tail beat cycle. At 5°C, mean power output was greatest at 0.60 and 0.93 L_s (21-23 W.kg^{-1}) while at 15°C, power output was greatest at 0.35 L_s (13 W.kg^{-1}). Power output at 0.35 L_s was similar at both temperatures. The potential for a high positive power output in post-anal myotomes at the temperature of acclimation may relate to the large thrust requirements during the propulsive stroke of a prey strike. At 15°C, the power output of fibres from cold acclimated fish at 0.60 L_s was 70% lower than that of 15°C acclimated fish (approximately 7 and 23 W.kg^{1} respectively). However, the power output of both acclimation groups was similar when each was measured at their respective acclimation temperature. In sculpin, acclimation to 5°C thus leads to a reduction in muscle performance at the higher temperature relative to muscle from warm acclimated fish.

Chapter 7

The findings of the individual Chapters are briefly summarised and discussed in relation to their possible role in generating different swimming movements in both species.

Chapter 1

GENERAL INTRODUCTION

Until the late nineteenth Century, the adaptation of living organisms to different environments was generally taken as evidence for the existence of a Creator, as it seemed to imply a conscious design of form and function. Then the publication of Darwin's "Origin of Species" in the 1850s provided a conceptual framework which showed how biological design could result from evolutionary development by natural selection. Survival is the ultimate target of the individual; design features that increase the likelihood of staying alive are rewarded with the passage of genetic information into succeeding generations. To ensure the survival of a species, enough individuals must be able to function sufficiently to meet the demands of the environment at any particular moment (Gans 1991). Function is limited by the physiological characteristics of the structure performing that function and these are in turn limited by the genotype (Lindstedt and Jones 1987). Since a structure often performs more than one task, the resulting phenotype will be compromise between various conflicting functional demands (Mayr 1976). The nature of the environment dictates what functional demands must be met and so is critical in determining the form of its inhabitants.

Water covers over seven-tenths of the planet's surface and was home to the first vertebrates some 450 million years ago (Romer 1959). From these ancestral creatures evolved the group of animals known collectively as Pisces - the fish. Fish are an evolutionary success story. They constitute around half of the 43500 extant vertebrate species and display a staggering variety of body forms and adaptations (Whitfield 1984). The

development of a variety of swimming strategies to meet locomotory demands within a particular habitat has played an integral part in their conquest of the waters and this chapter aims to show how swimming ability is closely linked to the functional design of the locomotory system.

1.1. The physics of motion

Motion of a body

Locomotion results from the physical interaction of a body with its surroundings. In order to understand the swimming strategies that fish have evolved, it is first necessary to examine the basic principles of motion and the design constraints acting on a body moving through a fluid.

The three basic laws governing the motion of a body were proposed by Sir Isaac Newton in his "Mathematical Principles of Natural Philosophy" (1687). These laws form the starting point for the design of any locomotory system and are as follows (taken from Medley 1982):

I Every body remains in its own original state of rest or of uniform motion in a straight line unless external forces oblige it to change that state.

II Change of motion is proportional to the impressed force, and acts along the same straight line.

III Action is always equal and opposite in direction to reaction.

The second law is fundamental to the study of the mechanics of locomotion and may also be expressed as:

$$F = ma \qquad (1.1)$$

which means the total force (F) acting on a body is equal to its mass (m) times its acceleration (a).

or in other words:

$$F = \frac{d}{dt}(mv)$$ (1.2)

which means that the total force (F) acting on a body is equal to the rate of change of momentum [mass (m) times velocity (v)] with respect to time (t)[1].

Using these two equations it is possible to explain what happens when two (or more) separate bodies interact. In the study of locomotion, these can represent the moving part of an organism (e.g. the fin of a fish) and the 'piece' of the environment (the water mass) which is in contact with it.

The effort expended (or work done) during a particular movement is a function of the force required to move a specific distance. If a force acting on a body at one point in space causes it to be displaced to a different point, the work done (in Joules) by the force in moving the body from position one (s_1) to position two (s_2) is given by:

$$W = \int_{s1}^{s2} Fds$$ (1.3)

---

[1] SI units: force in Newtons (N), mass in grams (g), velocity in metres per second (m.s^{-1}), acceleration in metres per second squared (m.s^{-2})

and the power used (in Watts) to move the body from s_1 to s_2 is the rate at which the work was done:

$$P = \frac{dW}{dt} = F \cdot v \qquad (1.4)$$

Therefore for locomotion to occur, work must be done to displace a body from one point to another. The power which is required to do this depends on the balance between the applied force and the velocity of displacement.

Motion in a fluid

As well as being bound by the laws of motion, a swimming fish is also subject to hydrodynamic constraints. The three main types of forces acting on a body submerged in a fluid are inertial, viscous and gravitational (Webb 1975a). The latter is insignificant for a fish submerged well below the surface and will not be dealt with here. Both inertial and viscous forces depend on the length and shape of the fish and its forward velocity (U). Inertial forces also depend on the density of the fluid (for water = 1.0 $g.cm^{-3}$ [0 ‰] to 1.03 $g.cm^{-3}$ [35‰]; fig. 1, Webb 1975a) while viscous forces depend on the resistance of the fluid to shear forces i.e. its viscosity (for water = 0.008 to 0.019 $kg.m^{-1}.s^{-1}$ over the range 0 - 30°C; fig. 3, Webb 1975a). Viscous forces occur because water resists distortion with a force known as **drag**. In order to move forward through the water, the fish must produce an opposing force (**thrust**) that is sufficient to overcome this drag. The amount of thrust required will vary depending on the size and body form of the fish, its swimming speed and the temperature of the water.

Drag forces originate in the water mass immediately surrounding the fish. This region, known as the boundary layer, was first described by Prandtl in 1904 to explain why hydro-mechanical theory incorrectly predicted flow patterns (see Prandtl 1952; Webb 1975a). He found that by taking viscous forces into account, new predictions closely agreed with observations. At the skin of a swimming fish, the velocity of water particles matches the fish's forward velocity, while a short distance away the particle velocity declines to that of the surrounding water mass. The distance over which this steep velocity gradient occurs marks the boundary layer and is the result of large viscous forces (Webb 1975a). The flow within the boundary layer can be laminar (drag forces low), turbulent (drag forces high) or transitional between the two. At any particular point along the body, the type of flow can be predicted from the size, body form and surface texture of a fish by the Reynolds number (Webb 1975a). Boundary layer flow lays important constraints on fish locomotion as it determines the total amount of thrust, and therefore the total power which is required for swimming.

1.2. Generation of mechanical power

The molecular motor

The mechanical power needed to overcome the resistance of drag is generated by skeletal muscle fibres. The basic structure of fish muscle fibres follows the vertebrate pattern. Interdigitating thick and thin filaments are arranged into serially repeating units (sarcomeres) to form myofibrils which are then packed into muscle fibres. Thick filaments are primarily composed of molecules of the protein myosin (Mw 500 000 Daltons) which consist of two pear-shaped 'heads' (S1 regions) connected *via* a flexible 'hinge' (S2 region) to a long tail (Rayment *et al.* 1993a;

Woledge, Curtin and Homsher 1985). The tails form the core of the thick filament, aligned so that they point to its centre, with the S1 heads projecting towards the adjacent thin filaments in a helical array (Woledge *et al.* 1985). Twelve thin filaments surround each thick filament (six per half sarcomere), each consisting of the proteins actin, tropomyosin and troponins I, T, and C.

Force is generated when the two types of filament slide past one another, resulting in active shortening of the muscle fibre (Huxley and Niedergerke 1954). In the classical hypothesis, this sliding action is the result of the cycles of attachment, shortening and detachment of 'crossbridges' between actin and the myosin S1 head, fuelled by the hydrolysis of ATP (Huxley 1974). Crossbridge shortening, termed the power stroke, is caused by a conformational change in part of the S1 region on the release of the products of ATP hydrolysis (Rayment *et al.* 1993*b*). The force generated per crossbridge as estimated from experiments with whole fibres is 4 pN (Woledge *et al.* 1985): the distance shortened during each power stroke ranges from 5 nm (calculated from the structure of the S1 head; Rayment *et al.* 1993*b*) to 204 nm (measured in motility assay; Harada *et al.* 1990 - see Burton 1992 for review). Measurement of the stepping of a single molecule of myosin along an actin filament with pN and nm precision using an optical trap gives a crossbridge force of 3-4 pN and an average step size of 11 nm. The latter value is comparable to that estimated from length transient experiments in whole muscle (10 nm; Huxley and Simmons 1971), which strengthens the evidence against the possibility of multiple steps per ATP hydrolysed (Finer, Simmons and Spudich 1994). Whether this measurement is truly due to the action of a single S1 head will depend on if and how the second head simultaneously contributes to filament translation.

The molecular motor is regulated in concert by the troponin complex and tropomyosin which interfere with crossbridge formation, possibly by sterically blocking the actin binding site (Squire 1981). The troponin complex consists of troponin I (actomyosin inhibitory subunit), troponin C (Ca^{2+} binding subunit) and troponin T (tropomyosin binding subunit) (Grabarek, Tao and Gergely 1992). Troponin C has four Ca^{2+} binding sites which when occupied, initiate a sequence of events that removes the inhibitory effect and allows crossbridge cycling to begin (Potter and Gergely 1975; Ebashi 1975; Grabarek *et al.* 1992). Calcium ions stored in the sarcoplasmic membrane (SR) system surrounding the myofibrils are released into the inter-myofibrillar space on fibre stimulation allowing fine control of the activation of muscle contraction (Rüegg 1988). At the end of the stimulus, calcium pumps restore the *status quo* by actively returning free calcium to the SR lumen. As free calcium levels decline in the sarcomere, troponin C gives up its bound calcium and the muscle relaxes as crossbridge formation is inhibited once more. The presence of calcium binding proteins (parvalbumins) may also aid relaxation by 'mopping up' excess calcium ions (Gerday and Gillis 1976; Pechère, Derancourt and Harech 1977).

Fibre types - a multi-geared system

The swimming performance of fish can be classified into three main categories (Beamish 1978):

(i) Sustained (> 200 min; no muscle fatigue)

(ii) Prolonged (20 s - 200 min; ends in fatigue)

(iii) Burst - maximum speed (< 20 s; ends in extreme fatigue)

For many fish, maximum speed is in the region of 10-20 body lengths/second ($L.s^{-1}$) depending on species, size and temperature (see Table IV, Beamish 1978). Fish muscle makes up to 60% of the total body mass compared to 40 - 45% in some mammals; this can be understood by considering the physical differences between air and water (Bone 1978; Munro 1969) - in water, the power needed to overcome drag forces increases in proportion with (velocity)^3 and as a result, fish tend to be slower than comparable vertebrates, even though a greater portion of their body mass is muscle (Bone 1978; Schmidt-Nielsen 1984). The geometric relationship of power and velocity mean that 80% of the muscle mass is only used to provide top speeds at moments critical for survival, such as prey capture or predator avoidance (Webb 1975a). Fish can afford to maintain this dormant power source with relatively little cost as water (by virtue of its density) provides structural support and removes the maintenance costs which limit muscle mass in land vertebrates.

At the upper and lower limits of performance, fish muscle fibres will thus face two quite different functional demands: a low, economical power output sustained over long periods of time and short bursts of high power at top speeds. The simplest solution to this problem is to have a series of different 'motors' geared structurally and metabolically to meet locomotory requirements at different swimming speeds, a strategy which fish have universally adopted.

Mechanical power

Modification of the basic muscle fibre design in vertebrates has led to fibre types specialised for the production of maximal power over different ranges of speed. Fish are unique amongst vertebrates in that these separate types are arranged in anatomically distinct zones. Because of

this, initial systems for the classification of fibre type were based primarily on muscle colour and location. Subsequently, the biochemical, structural and contractile properties of different types has been described, leading to a greater understanding of their roles in producing thrust (reviewed in Bone 1978 and Johnston 1981). Anatomical separation is most clearly observed in the trunk muscles, which are segmentally arranged into blocks (myotomes) on either side of the spine. When the trunk of a typical teleost is viewed in cross section, a wedge of red-coloured muscle fibres is visible lying just below the skin at the lateral line, forming an increasing percentage of the total area progressing towards the tail (fig. 1.1; Greer-Walker and Pull 1975). These are the *slow* twitch fibres (Bone 1975 *b*). The remaining 70-90% of the trunk muscle is white in colour and is made up of *fast* twitch fibres (Greer-Walker and Pull 1975; Altringham and Johnston 1988 *a*; Hudson 1969). Usually there is a transitional region of pink fast twitch or *intermediate* fibres between the slow and fast muscle zones (Johnston, Davison and Goldspink 1977) and in addition, a few benthic sharks have a thin sub-dermal layer of small diameter slow tonic fibres (*superficial* fibres) which have been implicated in maintaining head and tail posture (Bone 1978; Bone *et al.* 1986). The number of fibre types determined by histochemical methods ranges from three in the black mollie (*Molliensia* sp.) and sturgeon (*Acipenser stellatus*) to seven in the cod (*Gadus morhua*)(Patterson, Johnston and Goldspink 1975; Kryvi, Flood and Gulyaev 1980; Korneliussen, Dahl and Paulsen 1978). The division of muscle into different fibre types by this approach is somewhat subjective, as the precise number of fibre types will depend on the experimental protocol. For example, acid pre-incubation (pH 4.5) deactivates the myosin ATPase reaction in fast and intermediate fibres (e.g. Rome, Sosnicki and Choi 1992) while slow fibres are deactivated by alkaline pre-incubation (pH 10.2) (Tatarczuch and

Figure 1.1

Figure 1.1

Diagram of cross-section through the post-anal tail of a generalised teleost fish showing the location of slow (S), intermediate (I) and fast (F) muscle fibre types.
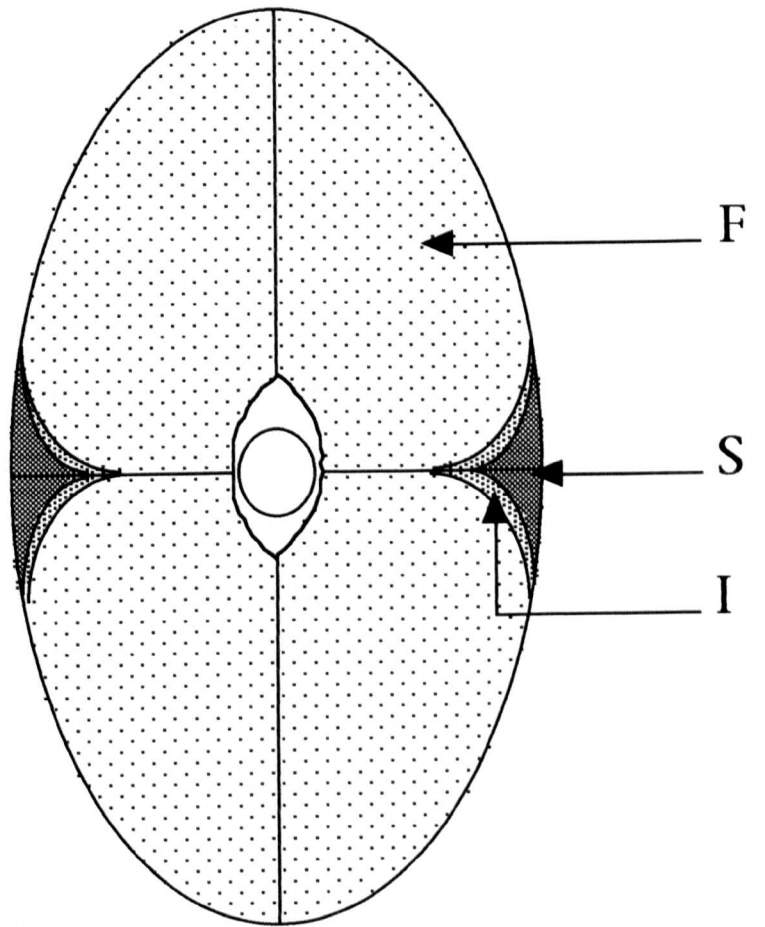
Kilarski 1982). In reality it may be that instead of a finite number of distinct types, muscle fibres vary to give a continuous spectrum of mechanical characteristics. However for most purposes, fibres are usually placed according to function into one of the three main categories: slow, fast or intermediate.

From equation 1.4, the demand for additional power at higher swimming speeds must be met by increases in both total muscle force and cycle frequency. During undulatory (periodic) swimming, the frequency of the tail-beat increases with velocity but the amplitude of lateral displacement does not (e.g. Grillner and Kashin 1976; Rome, Funke and Alexander 1990). To prevent a decline in work output per cycle and a subsequent drop in power, total muscle force must also increase (equation 1.3). Muscle force can be regulated either by varying the degree of activation of individual fibres or by recruiting more fibres to the force generating state (Aidley 1971). Electrical recordings (EMGs) of muscle activity during swimming in dogfish (Bone 1966) and carp (Johnston *et al.* 1977) show that up to the maximum sustainable speed, swimming is solely powered by the slow fibre type. In the carp, slow muscle EMG activity was found to increase by a factor of five between sustained speeds of 30 to 60 cm.s^{-1}, indicating an increase in total muscle force corresponding to the greater power requirements at the higher speed. Of this increase in EMG activity, 80% could be attributed to increased spike amplitude with the remaining 20% resulting from increased spike frequency, supporting the regulation of muscle force primarily by fibre recruitment with variation in fibre activation contributing to a much lesser degree (Rome *et al.* 1992). At the maximum sustainable speed (also termed the critical velocity, U_{crit}; Brett 1964) all the slow fibres are fully activated and the slow muscle mass will be generating its maximum force. As swimming speed increases, the

demand for additional power is met by the gradual recruitment of intermediate and fast fibres until at top burst speeds, all the muscle is activated (e.g. Johnston *et al.* 1977).

The pattern of fibre recruitment and the mechanical response of a fibre following activation depends upon its type of innervation. Slow muscle fibres are multi-terminally innervated and are activated by secondary motoneurons terminating in *en grappe* endings (Bone 1978; Westerfield, McMurray and Eisen 1986). Secondary motoneurons are relatively small, long latency neurons which are mainly active during slower swimming (Liu and Westerfield 1988). In slow fibres, a single sub-threshold stimulus *via* the motoneuron causes end-plate junction potentials resulting in a slow mechanical twitch (Mos, Maslam and Armée-Horvath 1988; Rome and Sosnicki 1990; Andersen, Jensen and Løyning. 1963; Hidaka and Toida 1969) with the magnitude of the tension response dependent on the frequency of stimulation (Aidley 1971). If the stimulation causes a depolarisation of 20-30 mV or more, a propagated action potential eliciting an all-or-none twitch is observed; multiple stimuli result in the summation of individual twitches to give a tetanus (Altringham and Johnston 1988*a*). The distance between individual end-plates remains a constant proportion of fibre diameter, ensuring a smooth, even contraction down the length of the fibre (Mos *et al.* 1988; Hoyle 1957). The tension response in isolated teleost slow fibres can be abolished by the application of acetylcholine antagonists showing that *in vitro* activation is *via* end-plate transmission (10^{-6} M curare, Rome and Sosnicki 1990).

In contrast to the slow fibre type, fast fibres show two main patterns of innervation:

(i) Chondrosteans, elasmobranchs, dipnoans and some primitive teleosts (gonorynchiformes, clupeiformes and anguilliformes) generally show the typical pattern found in higher vertebrates: fast fibres focally innervated by a single motor endplate (Bone 1964, 1970). Occasionally, the fibres may be dually innervated by different axons (Bone 1978). They respond to sufficient depolarisation with an all-or-none propagated action potential and a twitch (Altringham and Johnston 1988a). Variation in force is achieved by recruitment of additional fibres since each motor unit can only be recruited in an all-or-none fashion.

(ii) More advanced teleost orders have multi-terminal innervation and, like slow fibres, respond to sub-threshold stimuli in a frequency dependent manner with a graded contraction. A depolarisation of 20-30 mV is sufficient to elicit an action potential and an all-or-none twitch (Altringham and Johnston 1988a; Westerfield *et al.* 1986). The contractile response of teleost fast fibres is also blocked by the addition of an acetylcholine antagonist showing activation *via* endplate transmission (10^{-6} M, α-bungarotoxin; Johnson, Altringham and Johnston 1991). However, in focally innervated fast fibres of the eel *Anguilla anguilla*, 10^{-6} M, α-bungarotoxin did not measurably affect contraction (Johnson, Altringham and Johnston 1991) implying either the involvement of a neurotransmitter other than acetylcholine (which is unlikely) or that end-plate transmission was not necessary for *in vitro* fibre activation. In fast fibres, end-plates may frequently derive from more than one motoneuron, a condition known as polyneuronal innervation, and innervation by as many as 22 different axons has been reported (Hudson 1969). If the axons innervating a polyneuronally innervated fibre have different excitatory thresholds then over a

restricted range, the size of the elicited action potential will be proportional to the size of the stimulus, allowing greater control of force production (Hoyle 1957; Aidley 1971).

In zebrafish, two classes of motoneuron innervating fast fibres can be identified: each fibre is innervated by one of three primary motoneurons (fast conducting with a high threshold) and an average of two or three secondary motoneurons (slow conducting with a lower threshold) - 13% of fibres receive primary innervation only (Westerfield *et al.* 1986; Liu and Westerfield 1988). The primary motoneurons co-activate large specific groups of fibres within each myotome, unlike secondary motoneurons, which may also send axons into adjacent myotomes. Primary motoneurons produce high amplitude end-plate potentials on stimulation consistent with the production of an all-or nothing mechanical response and show a close association with the Mauthner axon prior to leaving the spine (Liu and Westerfield 1988; Westerfield *et al.* 1986). They are principally active during fast swimming, struggling behaviours and the startle response which suggests that they can be directly activated by the Mauthner neuron (Liu and Westerfield 1988; Diamond 1971). Both primary and secondary motoneurons show co-ordinated activity over a range of speeds (Liu and Westerfield 1988; Jayne and Lauder 1994). Motoneurons only become active when the activity level of the spinal neuronal network is greater than their excitability thresholds. As the activity level of spinal neurons (under the control of inputs from the brain) increases with swimming speed, a simple mechanism exists for the selective recruitment of muscle fibres as swimming speed increases (Wallén and Williams 1984; Grillner *et al.* 1993).

The transition from focal to distributed innervation observed in fish fast muscle fibres seems to indicate selective forces favouring the latter,

especially since transitional forms occur, as in the stomiiformes which show both focal and distributed innervation patterns (Bone and Ono 1982). Fish which have focally innervated fast fibres (such as the herring and dogfish [Bone, Kiceniuk and Jones 1978; Hudson 1973; Bone 1966]) show a marked cut-off point between sustained speeds and maximum burst speeds - their fast fibres must respond to activation with an all-or-none contraction and are therefore only activated at the highest swimming speeds. For example, the pacific herring is capable of swimming indefinitely at length-specific speeds of up to 3.4 $L.s^{-1}$ using its slow muscle but at speeds greater than 4.5 $L.s^{-1}$, the focally innervated fast fibres are recruited and exhaustion occurs within minutes (Bone *et al.* 1978). Multi-terminal innervation by a single axon would allow the use of sub-threshold stimuli (i.e. junction potentials) to produce a slow uniform contraction down the length of the fibres. This would allow fast fibres to additionally contribute to power output lower speeds. Fish such as carp and saithe, which have the multi-terminal pattern, have a much lower length-specific fast fibre recruitment threshold of 0.5 to 1.9 $L.s^{-1}$ compared to fish which have the focal pattern (Bone *et al.* 1978; Johnston and Moon 1980). Polyneuronal innervation with motoneurons of different excitability may allow the full activation of each fast muscle fibre over a greater range of speeds (Hoyle 1957), giving the fish an increased ability to modulate muscle force at intermediate speeds.

Tail-beat frequency increases with swimming speed so it is not surprising to find that the maximum shortening velocity (V_{max}) of different fibre types measured *in vitro* corresponds to their order of recruitment with increasing swimming speed i.e. slow <intermediate <fast. When the sarcolemma is made permeable by physical or chemical 'skinning', V_{max} of the fast fibres is around two and eight fold faster than

slow and superficial types respectively showing that differences in velocity between fibre types is not caused by varying degrees of fibre activation (Altringham and Johnston 1982; Altringham and Johnston 1986). The myosin S1 head, which contains both the actin and ATP binding sites, consists of a heavy chain fragment and 2 light chains (Rayment *et al.* 1993*a*). These light chains occur in a number of isoforms and although not essential for the splitting of ATP and generation of force, they have been shown to markedly affect the rate at which a muscle can contract (Lowey, Waller and Trybus 1993; Rome, Sosnicki and Goble 1990). Slow and intermediate fibres have similar light chain isoforms which differ from those found in fast fibres giving a structural basis for variation in the rate of crossbridge cycling (Johnston *et al.* 1977; Lowey and Risby 1971; Rome, Sosnicki and Goble 1990). In fast fibres, rapid relaxation due to a larger volume fraction of sarcoplasmic reticulum and greater quantities of parvalbumins further enhances the potential for a high frequency of contraction (e.g. Eisenberg, Kuda and Peter 1984; Eisenberg and Kuda 1985; Gerday and Gillis 1976; Pechère *et al.* 1977).

Fast fibres generate more than twice the isometric force per unit muscle mass (i.e. tension) than slow fibres (maximally activated skinned fibres e.g.: Johnston and Salmonski 1984; Altringham and Johnston 1982; Altringham and Johnston 1986). Myofibrillar content is generally significantly higher in fast fibres than in slow fibres (80-96% compared to 40-60%; see Johnston 1981) which could account for this difference, but even after correction for differences in myofibrillar density, fast fibres may still generate higher tensions than slow fibres (as in the dogfish, Altringham and Johnston 1986). Thus by generating high force at a high contraction frequency, fast fibres have the potential to generate large amounts of power which is in keeping with their recruitment at swimming speeds where thrust requirements are large.

Direct measurement of the amount of muscle power used to swim at a given speed is technically difficult. The total mechanical power required to swim at a given speed can be calculated indirectly from theoretical analyses, but investigation of the contractile properties of muscle fibres *in vitro* provides a direct way in which the performance of a given fibre type can be assessed. A measure of instantaneous mechanical power output during muscle shortening can be calculated from the force-velocity relationship, where the velocity of muscle shortening is measured during an isotonic release at different relative loads (Hill 1938). Slow fibres of the carp and scup generate maximum instantaneous power *in vitro* over a range of relative shortening velocities (i.e. V/V_{max}) corresponding to those experienced during sustained, steady swimming *in vivo* (Rome and Sosnicki 1990; Rome, Sosnicki and Choi 1992). Swimming remains periodic (or steady) within the optimum operating range for power and efficiency; outside of this range, behaviour switches to burst-and-coast (or unsteady) swimming to maintain muscle activity strictly between the limiting values of V/V_{max} (Rome, Funke and Alexander 1990). The importance of this constraint can be seen if the optimum range of V/V_{max} is shifted to a lower V by an acute drop in temperature. More fibres must be recruited at an earlier stage to provide the same power and so total fibre recruitment occurs at a lower speed, reducing maximum swimming performance ('compression of recruitment order' - Rome and Sosnicki 1990; Rome, Funke and Alexander 1990).

The maximum instantaneous power output predicted from the force-velocity relationship will tend to overestimate the average power output during swimming (Josephson 1993) as muscle fibres *in vivo* tend to shorten for around 50% of the tail-beat cycle and in addition, the work done on the muscle to re-extend it to its original length is not accounted

for during isovelocity shortening. Fast fibre power output under imposed sinusoidal length changes in the sculpin is only 10% (at 15°C, 17 Hz) and 20% (at 5°C, 6 Hz) of the maximum instantaneous power output (Altringham and Johnston 1990*a*; Johnson, Johnston and Moon 1991; Beddow 1993) and 50% lower in the dogfish (at 12°C, 3.5 Hz)(Curtin and Woledge 1993*a*; Curtin and Woledge 1988*a*). Power output during oscillatory experiments is influenced by the strain, the number and timing of stimulus pulses and the cycle frequency (Josephson 1985) and is likely to give a more accurate representation of the conditions of strain and activation found *in vivo* more accurately than an isovelocity release (Josephson 1993).

Metabolic power

In order to generate mechanical power, muscle fibres require a constant supply of ATP delivered *via* metabolic pathways. Muscular work is not the only energetic consideration for a fish and may only account for around 50% of the total available energy, with osmoregulation (up to 30%) and cardiovascular work (up to 15%) being other major energy sinks depending on relative demands (Driedzic and Hochachka 1978).

Slow fibres, which power sustained swimming speeds, have high activities of enzymes associated with the citric acid cycle, oxidative phosphorylation and the oxidation of fatty acids, indicating a large potential for the production of ATP by aerobic metabolism (Johnston *et al.* 1977) corresponding to their role in providing sustained power. Mitochondrial content, an indicator of aerobic capacity, is generally 25 to 35% of slow fibre volume in fish compared to around 5 to 7% in the soleus muscles of the guinea pig and rat (Johnston 1981; Johnston 1983; Eisenberg *et al.* 1974; Stonnington and Engel 1973). Glycogen and lipid are

present in large amounts, giving localised sources of fuel for the aerobic pathway (Greer-Walker 1970; Patterson *et al.* 1975; Johnston, Ward and Goldspink 1975); both lipid droplets and mitochondria are found within as well as between the fibre and may be closely associated (Beardall and Johnston 1983; Lin, Dobbs and DeVries 1974). Amino acids may also be utilised as an energy source, either directly or indirectly after prior conversion to glucose and glycogen (Driedzic and Hochachka 1978). In their mitochondrial content, fish slow fibres more closely resemble ventricular muscle in the mouse (34%), a muscle which also faces demands for sustained power (Bossen, Sommer and Waugh 1978).

Corresponding to this high mitochondrial density, fish slow fibres are well supplied with oxygen. Capillary density is high (2900-6000 capillaries per mm^2 fibre)(Eggington and Johnston 1982a; Beardall and Johnston 1983; Johnston and Bernard 1982; Kryvi *et al.* 1980; Totland *et al.* 1981) and in *Salmo gairdneri*, around 50% of total cardiac output goes to the slow muscle at 80% of maximum oxygen uptake (Daxboeck, Randall and Jones 1982, cited in Johnston 1983). In addition, a small fibre diameter (10-60 μm) acts to minimise the oxygen diffusion distance (Tatarczuch and Kilarski 1982; Korneliussen *et al.* 1978) and the possession of large quantities of myoglobin, giving the muscle its characteristic red colour, enhances the rate of oxygen delivery (Kryvi, Flatmark and Totland 1981).

Aerobic cost during sustained swimming (as a function of oxygen consumption) increases in direct proportion to $(velocity)^3$, as the growing demand for power requires an increase in the aerobic production of ATP (Beamish 1978; Driedzic and Hochachka 1978). At sustained speeds the rates of ATP supply and demand are balanced, buffered by stores of creatine phosphate (Driedzic and Hochachka 1978). Fatty acids give the most efficient yield of ATP and are preferentially oxidised as an energy source: in migrating fish, total body lipids have been found to decrease in

proportion to the distance travelled (coho salmon; Krueger *et al.* 1968). When the rate of ATP depletion can no longer be balanced by fatty acid oxidation, glycogen stores are mobilised to give a faster return of ATP. Slow fibres metabolise some glycogen anaerobically as U_{crit} is approached, but the production and oxidation rates of lactate reach an equilibrium, preventing the build up of lactic acid (Johnston and Goldspink 1973a; Wokoma and Johnston 1981; Duthie 1982).

As swimming speed increases beyond U_{crit}, the demand for ATP exceeds the rate of aerobic supply and there is a corresponding increase in anaerobic glycolysis as faster fibres are recruited and key enzymes are de-inhibited by the depletion of creatine phosphate and ATP stores (Driedzic and Hochachka 1978). Accordingly, fast fibres contain high concentrations of enzymes involved in anaerobic glycolytic pathways and the recycling of creatine phosphate, while concentrations of aerobic enzymes are relatively low (e.g. Johnston *et al.* 1977; Johnston and Moon 1981). The limited information on intermediate fibres shows that they are less well equipped in glycolytic enzymes than fast fibres, but they are between slow and fast fibres in aerobic capacity and ATPase activity in keeping with their place in the order of recruitment (Johnston *et al.* 1977; Johnston 1983).

The switch from aerobic to anaerobic metabolism between the slow and fast fibre type is apparent at the ultrastructural level in terms of mitochondrial and capillary volume densities. Compared to slow fibres, the mean mitochondrial content of fast fibres is much lower - around 2 to 9% in polyneuronally innervated fast fibres. However, this may vary considerably with fibre size. In the carp for example, the smallest fibres (area < 100 μm^2) contain 12-17% mitochondria compared to < 2% in the largest fibres (area > 1000 μm^2), indicating a small potential for aerobic

metabolism in some fast fibres (Johnston and Moon 1981). In focally innervated fast fibres mitochondrial content is $\leq$ 1% and it is likely that these fibres must meet their energy requirements entirely by anaerobic glycolysis (Kryvi 1977; Bone 1978). Capillary density is much lower in fast fibres (e.g. 12% of slow fibre density in saithe and 30% in tench) and a greater percentage of fast fibres (in comparison to the slow type) may completely lack capillary contact (Beardall and Johnston 1983; Johnston and Bernard 1982). However, the difference in the capillary area per *unit volume* of mitochondria between fast and slow muscles is relatively small, illustrating the close coupling of oxygen supply to aerobic demand (Johnston and Bernard 1982; Kryvi *et al.* 1980).

Rates of glycogen utilisation per unit mass in slow fibres when energy demands are high may be three-fold greater than that of fast muscle because of their greater aerobic capacity (Johnston and Goldspink 1973*b*) but because of the difference in total muscle mass, the higher rates of ATP turnover and the smaller ATP yield available from anaerobic pathways, depletion of glycogen stores is increasingly rapid once fast fibres begin to be recruited, with the total depletion of glycogen stores corresponding to fatigue (Driedzic and Hochachka 1978; Bone 1966). The mobilisation of glycogen to meet anaerobic demands is extremely rapid - in the trout up to 50% of the glycogen store may be used within fifteen seconds (Stevens and Black 1966) and there is a correspondingly large increase in white muscle lactate levels as the rate of lactate production far exceeds its removal.

The exhaustion of creatine phosphate stores causes an imbalance as the concentrations of free phosphate and ADP start to rise. To maintain the free energy available from ATP hydrolysis, fish convert excess ADP into ATP, AMP and GDP. This process is sustained by the production of IMP and NH_4^+ - unlike mammals, fish are able to tolerate high levels of NH_4^+ (see

Driedzic and Hochachka 1978 for review). Blood pH declines as levels of muscle and whole blood lactate and metabolic acid (H^+) rise (Wood 1991) but a potential reduction in the oxygen carrying capacity of the blood by the Root shift is prevented. Fish erythrocytes do not possess carbonic anhydrase which allows the maintenance of red blood cell pH by Na^+/H^+ exchange activated by catecholamines (Randall and Brauner 1991).

The energetic cost of using fast fibres is primarily associated with the return to pre-exercise conditions after the metabolic and physiological changes that take place during swimming and may be considerable following exhaustive exercise. Blood flow is increased to the white muscle tissue during recovery (Wardle 1978) and post-exercise oxygen consumption may remain elevated for some time, directly stimulated by the acid pH of the blood (Wood 1991). Catecholamines are only released once U_{crit} is passed, possibly in response to changes in blood CO_2 loading and/or psychological components and, unlike the situation in higher vertebrates, they may be more important in regulating processes during post-exercise recovery than during exercise itself (Wood 1991). Creatine phosphate, ATP and O_2 stores are restored within the first hour of recovery but during the long-term recovery phase, only one-quarter of the oxygen used can be accounted for by the reduction in lactate levels, contrary to the classical 'oxygen debt' hypothesis (Scarabello, Heogenhauser and Wood 1991). Wood (1991) suggested on the basis of several lines of evidence that the majority of lactate was actually actively retained in the fast muscle tissue for disposal during recovery, with other tissues such as the gills, kidney, red muscle, liver and heart also showing the ability to metabolise lactate, the whole process being mediated by catecholamines (Bilinski and Jonas 1972; Wood 1991; Weiser *et al.* 1987; Wardle 1978). Lactate is removed by either oxidative or gluconeogenic pathways and rates of clearance and glycogen re-synthesis are size

dependent: lactate levels return to normal in around two hours in a 2 g chubb compared to twelve hours in a 300 g rainbow trout (Lackner *et al.* 1988; Turner, Wood and Clarke 1983) while complete restoration of glycogen stores may take 24 hours for a 30 cm fish (*Onchorhynchus mykiss,* Milligan and Wood 1986*a*; Goolish 1991). The proportion of lactate which is finally re-converted to glucose varies with species, physiological condition and intra-cellular acidity (Scarabello *et al.* 1991; Milligan and Wood 1986*a*; Milligan and Wood 1987*b*). However, recovery may be further hampered as lactate levels continue to rise post-exercise for some time (Scarabello *et al.* 1991).

The cost of locomotion

Fish can afford to maintain such a large mass of 'expensive' muscle because the contribution of fast fibre activity is so much more important to the fitness of the fish in terms of immediate survival than the impact it has on energy resources (Goolish 1991). Energetic costs at sustained speeds can be quantified using rates of oxygen consumption and have been found to increase with both swimming speed and the distance travelled (Beamish 1978; Krueger *et al.* 1968). Above maximum sustainable speeds, the cost incurred over a given distance is much more difficult to measure as the work done by the fish is no longer proportional to oxygen consumption (Beamish 1978) but, once fast fibres begin to be recruited, costs will increase rapidly as efficiency of fuel conversion is sacrificed for a faster supply of ATP. There may also large 'hidden' costs associated with post-exercise recovery after swimming at prolonged and burst speeds (Wood 1991). In terms of survival, it will be important for the energetic costs[2] associated with locomotion to be minimised: a low locomotory cost

---

[2]Energetic cost = energy expenditure to travel a certain distance

will increase the energy available for growth and reproduction (e.g. Alexander 1967; Pennycuick 1991). By balancing mechanical and metabolic power output at different swimming speeds, fish ensure that the production of metabolic power is as efficient as possible over a range of velocities in order to minimise the impact of locomotion on their energy budget.

Costs can be further reduced by maximising the conversion of chemical energy into mechanical work by the muscle fibres. Both muscle *efficiency* - the metabolic input required for a given mechanical output[3] and muscle *economy* - the metabolic energy used to perform a certain task (Wilkie 1960; Curtin and Woledge 1993a; Full 1991) give a measure of conversion ability. Muscle contraction is never 100% efficient: of the free energy released by the splitting of ATP, only a part will be converted into mechanical work (Woledge *et al.* 1985). A large proportion is used by the sarcoplasmic reticulum (SR) calcium pumps (approximately 25% for an isometric contraction at l_r) with other ATP dependent processes and metabolic heat accounting for the rest (Wilkie 1974; Curtin and Davies 1975).

Since estimates of mechanical performance must only be used within the context they were defined, comparison of performance estimates between different studies is often difficult. However, within individual studies there is good agreement between the relative performance of isolated bundles of slow and fast fibres and their roles during swimming. For example, net work production by dogfish slow fibres under imposed sinusoidal length changes was more efficient (0.51 ± 0.05) than in fast fibres (0.41 ± 0.02)(conditions optimised for efficiency. Mean ± standard error, *n* = 9 and 13 respectively; Curtin and Woledge 1993a; Curtin and Woledge 1993 b). Fast fibre efficiency during isovelocity shortening was

[3] Thermodynamic efficiency = work output/heat + work; mechanical efficiency = work output per ATP split.

only 0.33 ± 0.01 by comparison, but by allowing for the difference in calcium pump ATP turnover an efficiency of 0.38 was obtained (Curtin and Woledge 1991; Curtin and Woledge 1993*a*). The studies of Curtin and Woledge calculated total energy input in terms of the heat produced during a contraction but did not take differences in myofibrillar content into account (75.5% and 62.2% in fast and slow fibres respectively [Bone *et al.* 1986]) - the mechanical efficiency of the myofibrillar apparatus is therefore likely to be greater than their results suggest. Net work output also includes the passive contribution of stretched elastic tissues, which can considerably increase mechanical efficiency (Heglund and Cavagna 1985; Cavagna, Heglund and Taylor 1977).

Positive work output (i.e. that produced during muscle shortening) under sinusoidal strains was 21-26% efficient in sculpin fast fibres (Johnson, Johnston and Moon 1991) and 12-23% in cod fast fibres at 4°C (Moon, Altringham and Johnston 1991)(conditions optimal for work output in both cases). In sculpin fibres, efficiency was reduced to 6-10% by an acute rise in temperature to 15°C (Johnson, Johnston and Moon 1991). In both studies, the Gibb's force free energy change of creatine phosphate splitting (55 kJ.mol^{-1}) was used as a measure of energy input. In fast skinned fibres from dogfish and *Notothenia neglecta*, isometric tension was maintained with 30-50% greater economy (tension per ATP per unit time) in slow fibres when compared to fast fibres, but peak tensions in fast fibres were up to 2.5 times greater (Altringham and Johnston 1986). The greater efficiency and economy of slow fibres is in keeping with their role in powering low swimming speeds. However there is a trade off between power and efficiency, as the mitochondria required for efficient energy production consume space within a fibre that would otherwise be occupied by myofibrils. Fast fibres are able to generate high force at a greater velocity than slow fibres and possess mechanisms for a

correspondingly high rate of ATP delivery. They are more costly to use, both in terms of fuel conversion and mechanical efficiency, but this is a necessary sacrifice which allows the fish to swim at speeds that would otherwise be unattainable.

1.3. Harnessing the motor

By possessing a functional spectrum of muscle fibres, fish have a source of mechanical power which is metabolically equipped for locomotion over a range of swimming speeds. However, both the timing and direction of this power must be controlled if it is to be usefully converted into motion. Motion through a fluid results from thrust, which is generated by the interaction between a moving body and the fluid surrounding it. Body movements are generated using muscular force and act to accelerate the quantity of water adjacent to the moving part (known as the added mass) away from the body in a perpendicular direction. A reaction force component (inclined forwards) results as the water pushes back on the moving body (Webb 1984). Over a whole cycle of movement, the sum of these reaction forces is directed towards the head, resulting in net thrust in the direction of motion - the magnitude of this longitudinal force component depends on the angle that the rearward face of each propulsive element makes with the direction of motion (known as caudal inclination).

The form of propulsive movements of the body is central to the way in which thrust is produced and can be classified into three main types (Breder 1926):

(i) those involving movements of the body and/or caudal fin
   (carangiform, sub-carangiform, anguilliform, thunniform and
   ostraciiform).

(ii) those involving undulations of long-based median fins (amiiform, balistiform, tetradontiform and gymnotiform).

(iii) those involving oscillations of the pectoral fins (rajiform, diodontiform and labriform).

Fish are not restricted exclusively to one category: the majority of teleosts use their fins to generated power at low speeds but switch to rapid undulations of the body and caudal fin when bursts of high speed are required (e.g. Blake 1983; Archer and Johnston 1989). Ultimately, the precise range of body movements available to an individual fish will depend on the relationship between muscle activity patterns, the passive mechanical properties of the body and the interaction between the body and the surrounding water (Blight 1977):

a) *Control of muscle activity*

The neuronal network responsible for the control of locomotory movements in fish follows the basic vertebrate design (Grillner *et al.* 1993). The pattern of undulatory body movements is generated by interneurons within the spinal chord. These are segmentally arranged into functional units and produce laterally alternating bursts of activity in an oscillatory rhythm (McClellan and Grillner 1984; Grillner *et al.* 1988). Each wave of activity is initiated by the brain stem in the anterior segments by a signal from the reticulospinal cells and passes in a wave down the body towards the tail (e.g. Grillner and Kashin 1976; Wardle and Videler 1992; He, Wardle and Arimoto 1991). Feedback from the spinal pattern generator ensures that the reticulospinal cells continue to fire in phase with the activation wave during subsequent cycles (Grillner *et al.* 1993). Reticulospinal input increases in both frequency and amplitude with swimming speed and sets the activity level of the spinal

interneurons. Motoneurons selectively convey this activity from the spinal network to the muscle fibres, thereby recruiting different fibres types at specific swimming speeds (Wallén and Williams 1984; Grillner *et al.* 1993).

The basic oscillatory activity pattern is modified by signals from the brain in response to visual and audiovestibular information to produce accelerating or turning manœuvres. When a threatening stimulus is received, a two stage escape response is typically observed (Eaton, Bombardieri and Meyer 1977). The size of the initial lateral displacement during stage one and the direction of the escape trajectory during stage two are determined by the relative size and timing of muscle activation on each side of the body (Foreman and Eaton 1993). Co-ordinated activation of the reticulospinal cells is thus able to simply and elegantly generate a whole range of swimming manœuvres at different speeds (Foreman and Eaton 1993).

b) Transmission of mechanical power into thrust

Force transmission follows a path determined by the muscle fibre arrangement and the passive mechanical properties of the surrounding skeletal network. Muscles do work by applying bending moments, either along the longitudinal axis (body and long-based fin undulation) or about pivot joint (paired fin oscillation), causing the movement of a propulsive element relative to some 'fixed' point. Fast fibre myotomes fill the bulk of the trunk in a series of overlapping, spatially complex shapes which are attached also to the spinal chord and septal sheets at specific points - their shape is often likened to a horizontal 'W', with a single point or 'cone' directed rostrally and two caudally (i.e. ←rostral ⋝caudal→). Each vertebra has two myotomes and each myotome may span from 3 to 12

intervertebral joints point-to-point (Wainwright 1983). With this arrangement, muscle contraction will run in a smooth wave down the trunk and several consecutive myotomes must contract simultaneously to produce a bend in the spine.

Within a single fast myotome, the orientation of the fibres can deviate by as much as 40° from the longitudinal axis (Alexander 1969). Two basic patterns of fast fibre orientation have emerged (Alexander 1969):

(i) In the selachian pattern, found in selachians, anguillids, salmonids and in the caudal peduncle of other teleosts, muscle fibres are aligned towards the points of the myomeric cones.

(ii) In the teleost pattern, found in the bulk of axial muscle in the remaining teleost groups, the path traced by muscle fibres aligned through successive myotomes results in a series of helical trajectories running towards the tail from the plane of the median septum out to the surface of the skin and back in to the median septum.

The complexity of fibre orientation has two important consequences. Firstly, it allows all the the fibres within a myotome to shorten an equal amount (and therefore at the same rate) for a given bend in the fish. Secondly, fast fibres have to shorten by a smaller amount to produce a given bend compared to the parallel oriented slow fibres (Alexander 1969; Rome *et al.* 1988). For example, a bend that requires slow fibres to shorten by 10% would require a shortening of 7-9% by fast fibres in the selachian pattern but only 2-3% by fast fibres in the teleost pattern (Alexander 1969). Thus fast fibres in the teleost arrangement have considerable mechanical advantage over the other two patterns, resulting in faster bending for a given rate of muscle contraction (Alexander 1969).

Tendons and both septal and myoseptal sheets are formed from arrays of collagen fibres and play key roles in the collection and transmission of muscular force. However, at the present date only a speculative account (based on observations of muscle and collagen fibre orientations) of the sequence of events following muscle activation can be given (see Wainwright 1983 for a review). The axial musculature is divided into two lateral halves by a tendinous sheet (the median septum) supported by vertebral spines and the spinal chord. Horizontal septa (one or more depending on the species) further divide the trunk into a series of compartments running longitudinally. Within each lateral half, the muscle fibres are grouped into myotomes bounded by more tendinous sheets (myosepta). In the region occupied by slow fibres, the myosepta tend to be firmly anchored to the skin (Videler 1993). On activation, each muscle fibre exerts a force on the myosepta adjacent to it as it attempts to shorten the distance between its points of attachment. The magnitude and direction of the transmission of this force through the elements of the skeletal network will then depend on:

(i) the angle subtended by one skeletal element (i.e. tendons, tendon sheets, skin and spinal chord) at its point of attachment to the next. Obtuse angles will direct force <u>along</u> the following element.

(ii) the orientation of collagen fibres over septal sheets, myosepta and tendons with respect to the next skeletal element. Collagen fibres aligned in parallel with the force component have low extensibility and high stiffness and are good transmitters of force.

In the anterior cone of a marlin myotome, collagen fibre tracts are oriented so that muscle force and shortening would be continually transmitted back towards the tail, firstly out to the skin, then along the skin before being guided back in *via* the horizontal septa to the backbone (Wainwright 1983). By these means, muscle force can create the necessary

bending moments needed to flex the spine and will propel the fish through the water.

c) Propulsive efficiency: the interaction of body and fluid

Propulsive efficiency (or Froude efficiency) can be defined as the amount of work done by a swimming fish that is converted into useful work (or thrust)(Webb, Kostecki and Stevens 1984). A proportion of muscular power will be lost during its transmission into bending moments and a further portion will be lost to the wake as kinetic energy or wasted as side forces (Blake 1983; Webb 1984). The amount of energy wasted in this way depends on the shape of the fish and the propulsive movements used to generate thrust. Propulsive efficiencies have been estimated at over 90% for a sub-carangiform swimmer (trout at maximum sustained speed; Webb 1971a), 50% for an ostraciiform swimmer (*Ostracion lentiginosum*; Blake 1981) and 60-65% for pectoral fin flying (*Cymatogaster aggregata*; Webb 1975b). These estimates would seem to suggest carangiform-type movements give the best conversion of muscular work into thrust. However, the Froude efficiency of this mode declines with swimming speed, so at low velocities propulsion by oscillations of the paired fins is likely to be more efficient (Webb *et al.* 1984); carangiform-type swimmers capable of using paired fin propulsion often switch swimming modes at low speeds, reducing the cost of locomotion. For an anguilliform swimmer, the highest propulsive efficiencies can be obtained when the waves of bending travel from rostral to caudal myotomes, the amplitude of oscillation increases towards the tail and the rearward velocity of the waves of contraction (V) is slightly greater than the forward swimming speed (U)(Lighthill 1960,

1969 and 1970). U/V should be around 0.80 for high propulsive efficiency (Webb 1971*b*).

Overall aerobic efficiency (thrust power/metabolic power) includes metabolic and mechanical energy losses as well as propulsive losses. A 50 cm trout swimming at the maximum speed it could maintain for 10 minutes without fatigue had an aerobic efficiency of 46% (Note: this was calculated using rates of oxygen consumption for sockeye salmon; Webb *et al.* 1984).

The successful colonisation by fish of a wide variety of niches has involved a considerable diversification of body form, since the optimum shape for propulsive efficiency may be compromised by other functional demands. Webb (1984) devised a 'plane of functional morphology' to describe the huge range of fish body form in terms of locomotory behaviour. Three specialised behaviours with corresponding morphological designs emerged: sprinters, manœuvrers and cruisers (represented by pike, banded butterfly fish and tuna respectively). Most fish are locomotory generalists, as body design will be a compromise that reflects the demands of a particular habitat. Their position within the morphological plane depends on the relative emphasis placed on the demands of efficiency, acceleration and manœuvre in their body design.

Morphological and physiological characteristics fix the basic cost of locomotion but considerable energetic savings may be made by behavioural adaptations. Reductions in thrust requirements can be made by using prevailing tidal streams (e.g. *Pleuronectes platessa*; Harden-Jones *et al.* 1978), schooling (Weihs 1975), maintaining the most economical cruising speed over long distances (Webb and Weihs 1983) and by alternating short bursts of acceleration with periods of coasting to reduce the cost of sustained (Weihs 1974) and prolonged (Videler and Weihs 1982) swimming.

1.4. Summary

The close link between swimming requirements and the functional design of the locomotory system is apparent at many levels, from the specialisation of different fibre types, each geared mechanically and metabolically to meet power demands at different speeds, to the development of a variety of methods for imparting thrust to the surrounding water. The aim of this thesis was to further explore the theme of functional design by studying regional differences in the contractile performance of isolated fast muscle fibres. The short-horned sculpin (*Myoxocephalus scorpius* L.) and the Atlantic cod (*Gadus morhua* L.) were chosen as experimental subjects as they give viable whole fibre preparations suitable for muscle mechanics experiments. During the present study, various approaches are used to study the mechanical characteristics of fast muscle fibres isolated from rostral and caudal myotomes: isometric contractions, isovelocity releases and imposed strains which approximate both steady and unsteady swimming *in vivo*. In addition, the isometric and isovelocity characteristics of fast and slow fibres of the sculpin are compared. To complement the mechanics experiments, sarcomere geometry and the volume and surface densities of sarcoplasmic reticulum and t-tubules are quantified to search for a relationship between structure and contractile performance. Finally, the results are discussed in relation to the generation of thrust *in vivo*.

MECHANICAL PROPERTIES OF MUSCLE FIBRES ISOLATED FROM ROSTRAL AND CAUDAL MYOTOMES OF THE ATLANTIC COD (*GADUS MORHUA* L.)

2.1. Introduction

Steady swimming in carangiform fish is powered by sinusoidal oscillations of the caudal fin (e.g. Gray 1933; Hess and Videler 1984). The contraction cycles that muscle fibres undergo *in vivo* can therefore be approximated *in vitro* by imposing sinusoidal strains on isolated preparations and stimulating at an appropriate phase during each cycle (Altringham and Johnston 1990*a*). High-speed cinematography synchronised with electrical recordings (EMG) from different points along the length of the fish has shown that the travelling wave of activation progresses towards the tail at a greater rate than the wave of mechanical bending (e.g. *Anguilla anguilla* and *Onchorhynchus mykiss* [Grillner and Kashin 1976]; *Lampetra fluviatilis* and *O. mykiss* [Williams *et al.* 1989]; *Cyprinus carpio* [Van Leeuwen *et al.* 1990]). As a result, the relationship between the strain cycle and muscle activation (activation phase) varies systematically along the length of the fish. For example, in a steadily swimming saithe (*Pollachius virens*), EMG onset occurs at an activation phase of 30° at 0.35 L_S (where L_S is the standard length) and

330° at 0.65 L_S (0° phase is defined as the point the muscle passes through its resting length whilst being stretched, with a full cycle equal to 360°)(Wardle and Videler 1993). Under conditions simulating swimming slow muscle fibres isolated from caudal myotomes of the scup (*Stenotomus chrysops*) produced net positive work and higher power outputs than fibres from rostral myotomes, which suggests that the majority of positive power is generated towards the rear of the fish at sustainable speeds (Rome, Swank and Corda 1993). However Altringham, Wardle and Smith (1993) working with fast muscle fibres isolated from the saithe found that the work done by caudal muscle fibres (0.65 L_S) was negative over most of the tail beat cycle. These authors suggested that under *in vivo* conditions, power generated by the more rostral myotomes is transmitted to the tail during the active lengthening phase of the caudal muscle fibres. The differing results of these studies may reflect differences in muscle properties between fibre types, between species or variations in the techniques used in obtaining *in vivo* parameters. Van Leeuwen *et al.* (1990) analysed body movements and recordings of EMG in red muscle at eight points along the body of the carp (*C. carpio*) and modelled work and power output during steady swimming. They found that rostral muscles in the carp were mainly active during shortening, a condition which produced net positive work in the model, whereas muscles in the tail were active mainly at and above their optimum length, producing mostly negative work (or work done on the muscle) with a small positive work output towards the end of the cycle. The contrast between the findings of Rome *et al.* (1993) and Van Leeuwen *et al.* (1990) is mainly due to the difference in strains used at rostral and caudal positions and the simplifying assumptions of the modelling approach. Van Leeuwen and co-workers also assumed that the duration of the mechanical active state of rostral and caudal fibres was the same whereas in both the saithe and

scup, caudal muscle fibres have a longer contraction duration than rostral fibres (Van Leeuwen *et al.* (1990); Altringham *et al.* 1993; Rome *et al.* (1993)).

Previous studies on the contractile properties of myotomal muscle fibres in the Atlantic cod have mainly been concerned with preparations isolated from the anterior abdominal myotomes (Altringham and Johnston 1990*b*; Archer, Altringham and Johnston 1990; Anderson and Johnston 1992). The aims of the present chapter were to compare the properties of fast muscle fibres in rostral and caudal myotomes during both isometric and cyclical contractions. Since contractile properties vary with acclimation temperature in a number of species (Johnston, Sidell and Driedzic 1985; Johnson and Johnston 1991*a*), experiments were conducted on both summer and winter caught fish.

2.2. Materials and Methods

Fish

Atlantic cod (*Gadus morhua* L.) were caught locally in St. Andrews Bay, Scotland and are referred to as 'winter' (November 1991-March 1992) and 'summer' (June 1992-October 1992) groups respectively. Fish were maintained in sea water aquaria at ambient temperature of 4-8°C during the winter and at 12-15°C during the summer at a photoperiod of 12h light: 12h dark, and were fed regularly on shrimps and fish flesh. Cod of standard length (L_s) 30-40cm were used to minimise scaling effects. The mean L_s and wet weight of the experimental groups are presented in table 2.1.

Table 2.1

Table 2.1

Standard length (L_S) and wet weight (W_W) of 'winter' and 'summer' caught *Gadus morhua* L. The mean preparation length (paired within each fish) of rostral and caudal muscle fibre preparations isolated is also shown.

All values are means ± SD. A two-tailed Student's t-test with H_A $\mu_1 \neq \mu_2$ was used to compare winter and summer standard lengths and a paired t-test was employed to compare rostral and caudal preparation lengths. Significant differences are indicated at the 0.05 (*), 0.001 (**) and 0.0001 (***) levels.

| GROUP	POSITION	n	Standard Length (cm)	Wet Weight (g)	Prep. Length (mm)
WINTER	Rostral	9	32.7 ± 2.1	438.0 ± 87.3	6.7 ± 1.2
	Caudal	9			4.2 ± 1.2 *
SUMMER	Rostral	6	35.1 ± 2.7 *	539.1 ± 116.4	7.4 ± 1.2
	Caudal	6			4.6 ± 0.5 ***
TOTAL	Rostral	15	33.7 ± 2.7	478.4 ± 108.8	7.0 ± 1.2
	Caudal	15			4.3 ± 0.8 **

Isolation of muscle fibres

Fish were killed by a blow to the head followed by transection of the spinal chord. Rostral blocks of muscle tissue were dissected from the abdominal wall and caudal blocks from each side of the tail (fig. 2.1). Caudal blocks were removed by making a deep transverse cut anteriorly, cutting the skin dorsally and ventrally and carefully freeing the block from the skeleton with a sharp scalpel. Muscle blocks were pinned out at their resting lengths on a silicone elastomer base (Sylgard 184, Dow Corning, Midland MI, USA) and immersed in Ringer solution containing (in $mmol.l^{-1}$): NaCl, 132.3; sodium pyruvate, 10.0; KCl, 2.6; $MgCl_2$, 1.0; $NaHCO_3$, 18.5; NaH_2PO_4, 3.2; $CaCl_2$, 2.7; pH 7.2-7.4 at 5°C adjusted using 1M HCl/NaOH (Hudson 1969). Further dissection was carried out in a dish under a stereomicroscope (SV11, Zeiss, West Germany) on a metal dissecting stage which was cooled with crushed ice (< 5°C). The Ringer solution was changed regularly during dissection to prevent the build-up of ions liberated from cut fibres.

Rostral preparations were isolated from a strip of muscle tissue (approx. 0.5 cm wide) taken from the abdominal block, cut parallel to the longitudinal axis of the fibres. The strip was pinned peritoneum-side down in a Sylgard-lined petri-dish and the skin was removed to reveal the underlying myotomes. The myotome closest to 0.35 L_s was identified and the flanking myotomes were trimmed back to their myosepts. The peritoneum was then removed from underneath the chosen myotome and the fibre bundle was carefully pared down to leave around 10-20 live muscle fibres. Aluminium foil clips were folded around the remains of the peritoneum, as close to the myosepts as possible to minimise the influence of tendenous structures.

Figure 2.1

Figure 2.1

Isometric tetanic contractions of fast muscle fibre bundles isolated from rostral and caudal myotomes of the Atlantic cod, *Gadus morhua* L. The rows of dots represent the stimulus train. Number of fibres: rostral = 6 and caudal = 13. Scale bars: horizontal = 80 ms, vertical = 5 mN.

40 Hz

90 Hz
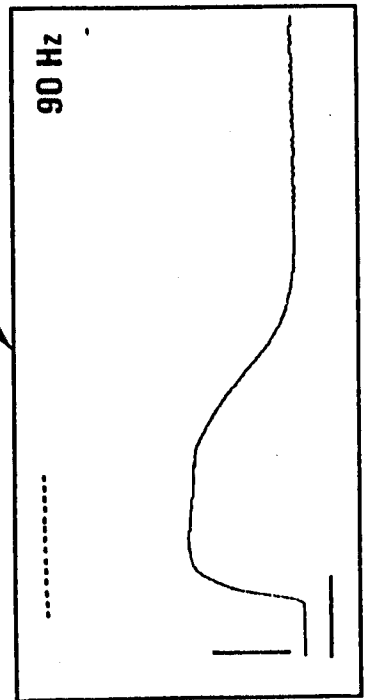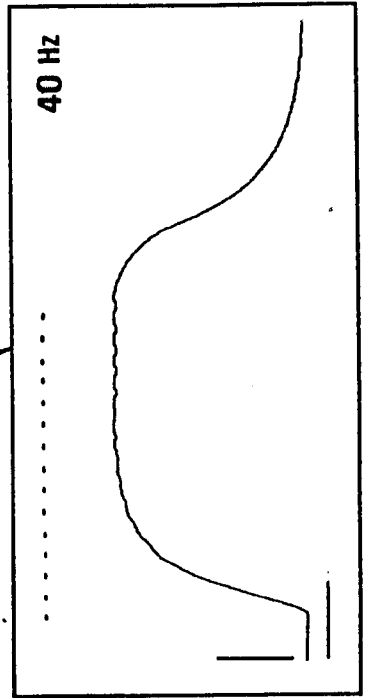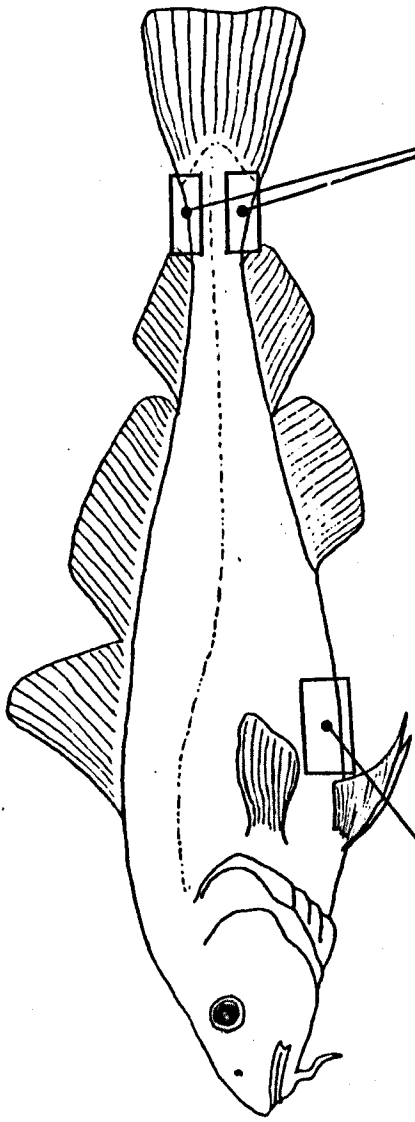
Caudal preparations were isolated from the caudal muscle block by tracing dorsal and lateral myotomes from the base of the caudal fin anteriorly until the tip of the myotome was reached (0.90 L_s). The tendenous insertion into the skin was detached and lifted up and back, allowing the myotome to be freed from the skin with a scalpel. This myotome was then placed in a separate dish and a bundle of 10-20 fibres was formed from the tip of the myotome. Foil clips were folded around the myosepta as close to the insertion point of the fibres as possible. Preparations were maintained in Ringer solution prior to an experiment and remained viable for 2-3 days. Experiments were usually completed within 8 h.
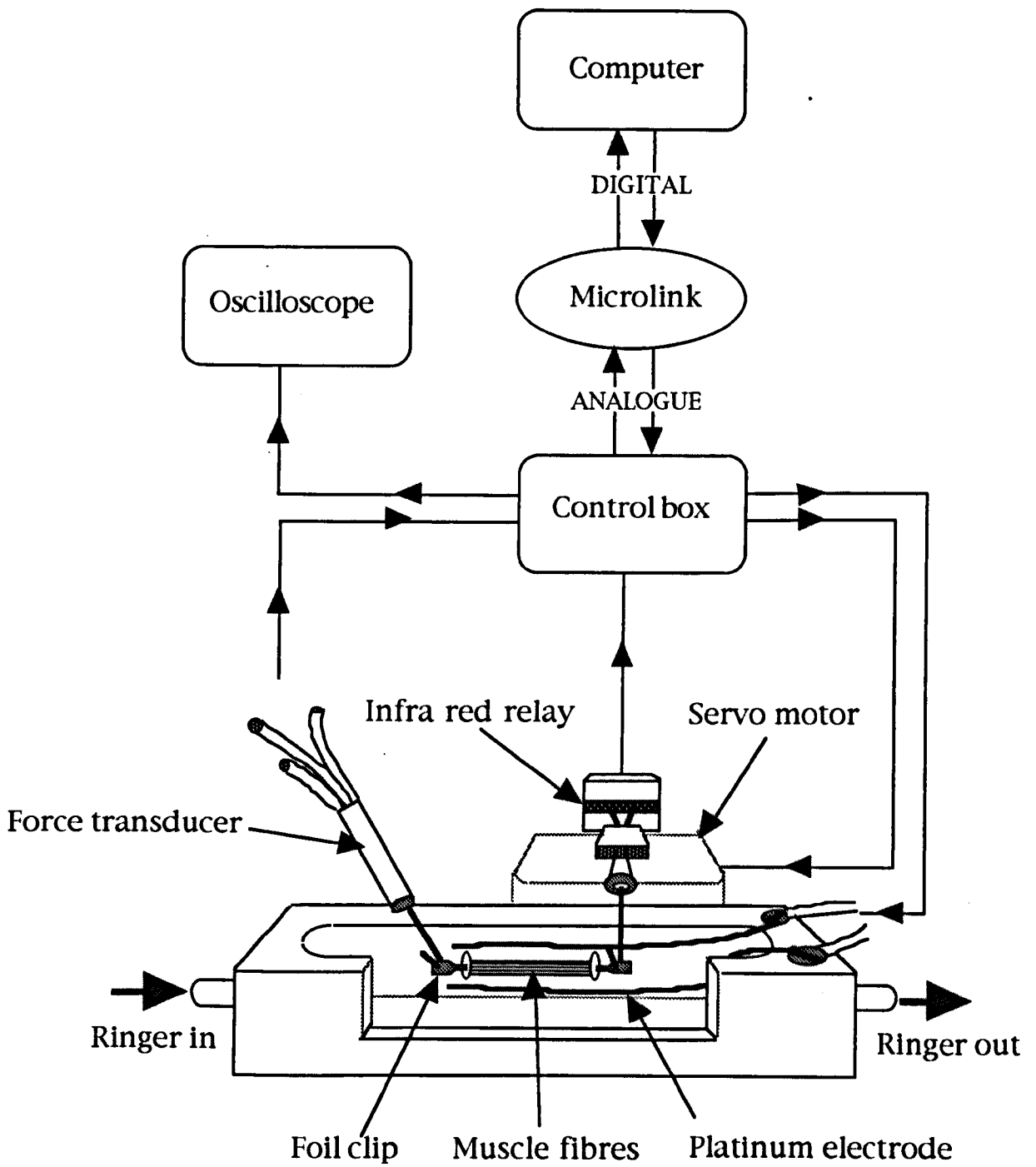
Experimental Apparatus

Fibre preparations were mounted in a perspex chamber (5 x 1 x 1 cm), attached *via* their foil clips to a pair of stainless steel hooks (fig. 2.2). One hook was connected to a servo-motor (MFE model R4-077, Emerson Electronics, Bourne End, Bucks) and the other to a silicon beam strain gauge (sensitivity 0.5 mN.V^{-1}, noise < 2 mV, drift < 1 mV.hr^{-1}; AME 801, SensoNor-as, Horten, Norway). The strain gauge (or force transducer) was contained within a stainless steel tube (waterproofed with silicon grease) which was mounted on a micro-manipulator to allow fine adjustment of preparation length. Ringer was circulated through the chamber by a peristaltic pump (Watson-Marlow), passing through a coil of plastic tubing immersed in a thermostatically controlled water bath (Grant LTD 6) maintaining the temperature in the chamber at 5 ± 0.1 °C. Chamber temperature was regularly checked using a thermal probe (KM220, Kane-May Ltd, Hertfordshire) and Ringer solution was changed every 2-3 h during the course of an experiment to compensate for increasing pH.

Figure 2.2

Figure 2.2

Diagramatic representation of the experimental set-up used to control stimulation patterns and muscle length during the work loop experiments.

Computer

DIGITAL

Microlink

Oscilloscope

ANALOGUE

Control box

Infra red relay

Servo motor

Force transducer

Ringer in

Ringer out

Foil clip   Muscle fibres   Platinum electrode

The experimental system was designed to calculate the work done by an isolated fibre bundle under varying conditions of length and activation. The system consisted of four main sections (fig. 2.2):

1. Live fibre chamber with associated servo motor and force transducer units

2. Control Box (M. McCandless, Department of Psychology, University of St. Andrews)

3. Microlink (Biodata Ltd., Manchester)

4. An IBM compatible PC with hard copy facilities (COMPAQ PortableII, Houston, USA; Hewlett Packard ColorPro plotter and Epson FX-80f/T+ line printer)

Experiments were controlled by in-house software (GENLOOP v. 3.02 by J. C. Eastwood) which enabled nine experimental parameters to be varied: the amplitude and width of each stimulus pulse, the number of pulses, the timing of the stimulation relative to the start of the length cycle (the phase) and the number, amplitude and frequency of sinusoidal oscillations. For isometric contractions, the length remained fixed (amplitude set to 0) whilst the stimulus parameters were varied. On initiating an experimental run, the parameter values set up the operating conditions in the Control box which then delivered the appropriate stimulus/length pattern to the live fibre chamber. Information received from the servo motor/force transducer units was constantly monitored and downloaded to the computer for processing and storage. The Microlink acted as a mediator, translating the information between analogue and digital formats. Servo/transducer output was monitored visually during the course of an experimental run using an oscilloscope (Gould 1602 or Tektronik).

Isometric contractions

Fibre length was adjusted to give the maximum isometric twitch corresponding to a sarcomere length of 2.2 μm as measured by the diffraction of a He-Ne laser beam (Barr and Stroud, Hughes) - the resting length of the fibre was termed l_r. The diffraction pattern was projected onto a thin perspex screen positioned at a known height above the fibre bundle. The distance between the zero and first order diffraction lines was related to sarcomere length using Bragg's equation (Bragg 1913):

$$L_s = \frac{m\lambda}{\sin \alpha_m} \tag{2.1}$$

where L_s = sarcomere length (μm)

   m = diffraction order number (with $m = 1, 2, 3,$)

   λ = wavelength of laser (μm)

 α_m = angle between zero and line of diffraction order m (°)

Supramaximal broad field stimuli were delivered *via* two platinum electrodes (Goodfellow) running parallel to the fibre bundle. Preparations were stimulated at 10 minute intervals enabling reproducible results to be obtained over the duration of the experiment. The amplitude, duration and frequency of pulses were adjusted to give a maximal fused tetanus and peak force was allowed to stabilise before proceeding with the experiment. Peak force (F_o), the time from delivery of the first stimulus to half peak force (HPT) and the time from the final stimulus to half relaxation (HFT) were measured for each preparation (fig. 2.3).

Figure 2.3

Figure 2.3

Records of an isometric twitch and tetanus indicating where the half-times to peak force (HPT) and relaxation (HFT) were measured. Peak force (F_O) is taken to be the highest force attained.

HPT in both twitch and tetanus is taken to be the time from the first stimulus pulse to $1/2$ F_O as force increases. Twitch HFT is the time from F_O to $1/2$ F_O as force declines while tetanic HFT is the time from the last stimulus pulse to $1/2$ F_O. Upper trace represents stimulus train during tetanus.

shpt | HPT | hft | HFT | 5mN | 50ms
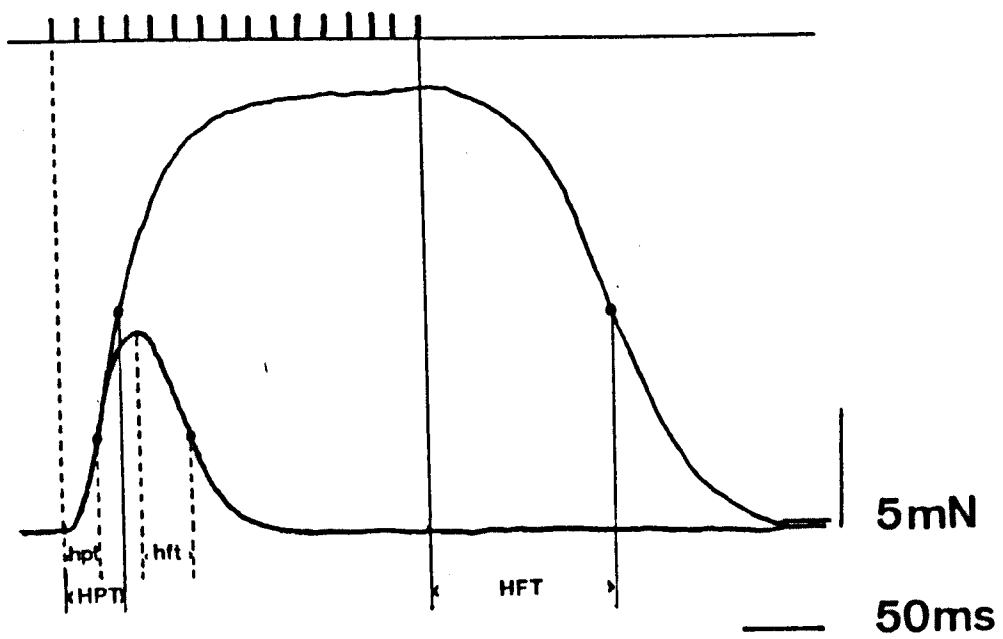
Estimation of maximum contraction speed (V_o)

V_o was determined at 5°C using the slack test method (Edman 1979) on fibres isolated from a group of 'winter' fish (L_s = 34.78 cm ± 0.71; mean ± SEM, *n* = 8). Fibres were given a step release (1-2 ms) during the plateau phase of an isometric tetanus causing the isometric force (F_o) to fall to zero (fig. 2.4). The contracting muscle fibres were then allowed to shorten at V_o until tension was recovered. The time interval between the step release and the re-development of force (slack time, T_s) was measured for 6-10 length steps for rostral and caudal muscle fibres. Plots of step length against slack time were linear and lines were fitted using the least-squares method. The equation of the line is of the form $\Delta L = m (T_s) + C$ where the gradient m represents V_o and the intercept ΔL is a measure of the series elasticity.

Work loop experiments

Rostral and caudal preparations were subjected to sinusoidal length changes about *in situ* resting length and phasically stimulated during each cycle. Activation phase was defined in degrees from the point the fibres passed through their resting length (0°) whilst being stretched to the delivery of the first stimulus, a full cycle being equal to 360°. The stimulus number, duration and frequency remained constant during the experiments (2 stimuli, 12 volts, 2 ms duration, 50 Hz per cycle: train duration 42 ms) as did the strain amplitude (± 5 % l_r) while the activation phase and oscillation frequency were varied. The chosen values had previously been shown to produce maximum positive work output in fast muscle fibres isolated from rostral myotomes (Altringham and Johnston 1990*b*; Anderson and Johnston 1992). Four consecutive cycles were

Figure 2.4

Figure 2.4

(a) The change in time to tension recovery (slack time: T_1 and T_2) after two step releases of different amplitude (L_1 and L_2) in fast fibres isolated from a caudal myotome in *G. morhua.* at 5°C. (b) An example of the linear relationship between slack time and the amplitude of the length step (ΔL) for muscle fibres isolated from both rostral and caudal myotomes. Note that the gradient of the rostral line is steeper than that of the caudal line indicating a faster V_0. Rostral and caudal preparations differed in both resting length and cross-sectional area.

a.

L₁
L₂ | 0.5mm

2mN

T₁ T₂

— 20ms

b.

rostral

caudal

ΔL (Muscle lengths)

Slack time (ms)
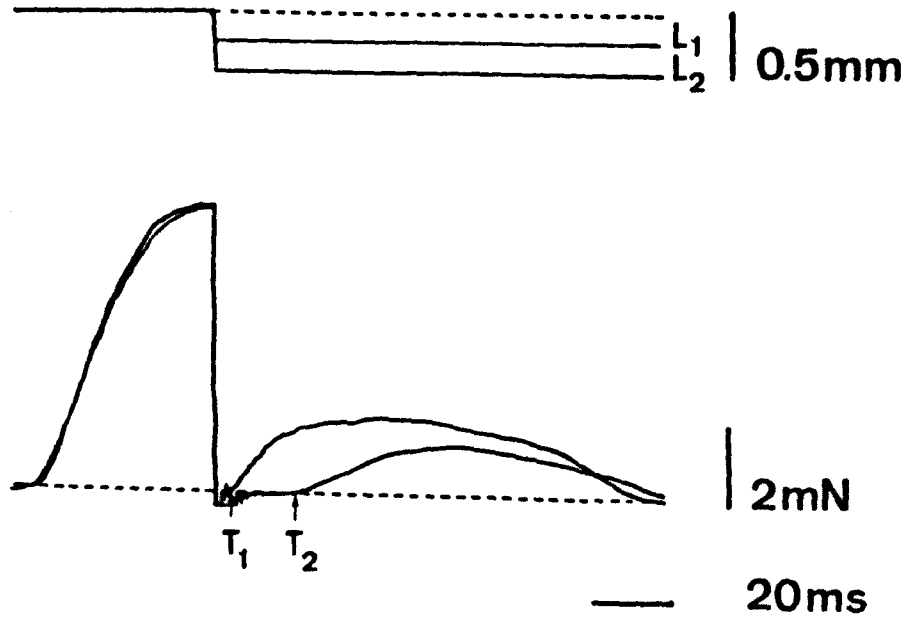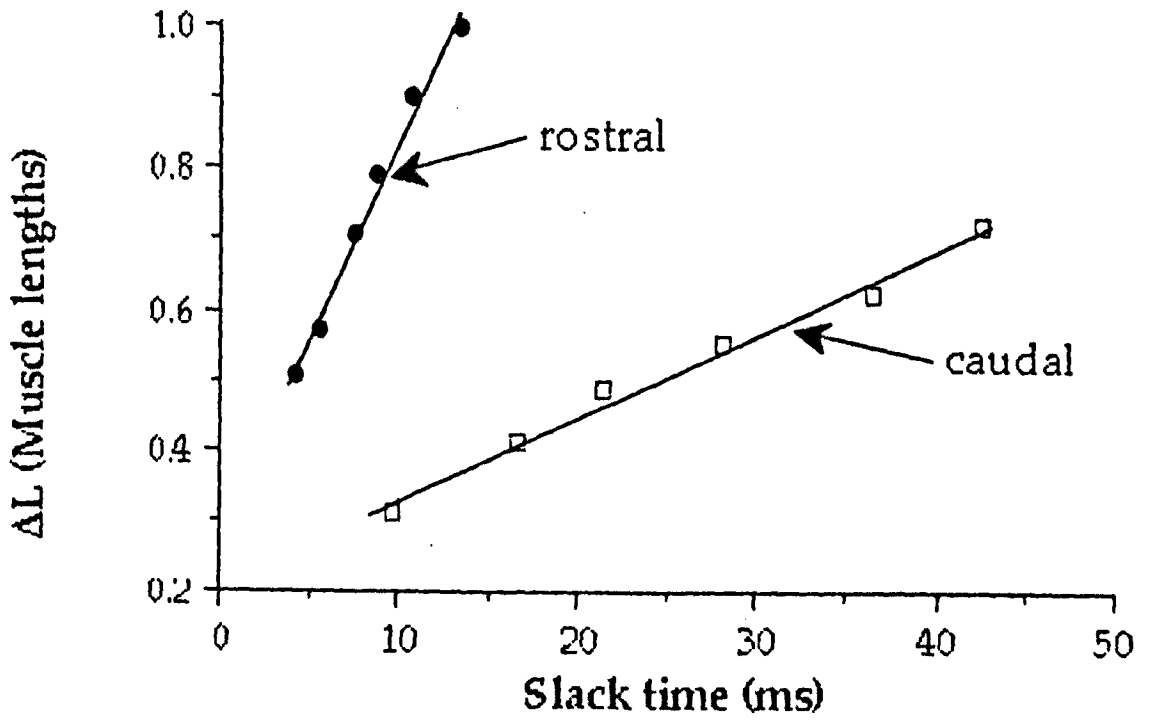
delivered in each experimental run. The work done during each cycle was obtained by numerical integration of plots of force against muscle length (work loops); anticlockwise components indicate positive work - that done by the muscle, clockwise components indicate negative work - that done on the muscle (Josephson 1985). Mean power is the work per cycle multiplied by the cycle frequency. The work done by the unstimulated preparation (that due to elastic and viscous components) was constant for a specific strain (usually less than 5%) and was subtracted from the net work produced by the activated preparation. Values of force and work were calculated from the mean of the second and third cycles so that the effect of preceding and following cycles was included. The results were then expressed as a percentage of maximum positive values and plotted against activation phase. As a quality control criterion, if the values of force and work were found to decline or increase by more than 10% at an activation phase of 15° over the course of an experiment, the results for that preparation were not used in the final analysis.

Determination of cross-sectional area

After each experiment, the cross-sectional area of the muscle fibre bundle was determined in order to convert the results into standard units. Preparations were placed on a disc of cork (1 cm diameter, 0.5 cm thick) and were anchored at one end by a metal staple pressed over the foil clip. The second foil clip was hooked over a bent steel insect pin which had been pushed through the cork and the suspended preparation was adjusted to its resting length. The preparation was coated in mounting medium (Tissue-Tek, Miles Scientific, Illinois, USA) and then the cork was quickly inverted and plunged into liquid iso-pentane cooled to near its freezing point in liquid nitrogen (N_2, -159°C). The frozen preparation

Figure 2.5

Figure 2.5

Cross-sectional profile of a bundle of rostral fast muscle fibres stained for myosin ATPase activity (pH 9.4). A single dead fibre is identified by a 'D'. Scale bar = 0.1 mm.
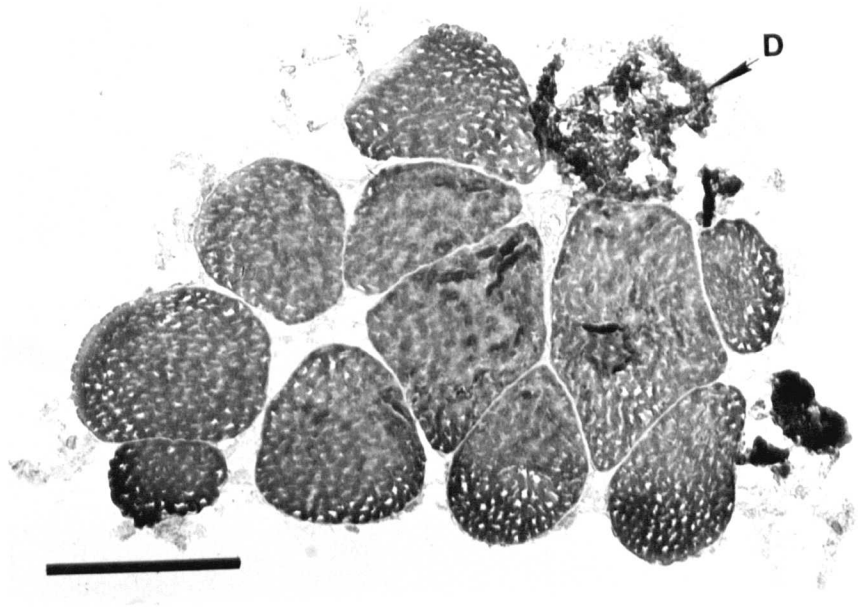
transreferred to a cryostat (Cryocut 1800, Reichert-Jung, West Germany) and allowed to equilibrate with the chamber temperature (-16 to -18°C) for at least 2 hours prior to cutting. Transverse sections (10-20 μm) were cut, lifted onto cover slips (22 mm^2) and dried in air for approximately 45 minutes. Sections were stained for myosin ATPase activity (Johnston *et al.* 1974) and then mounted on slides using glycerol gelatine (Sigma). Fibre outlines were traced using a microscope drawing arm (Nikon, Labophot) and the cross-sectional areas obtained by digital planimetry (Kontron Elektronic GmbH, West Germany). Dead and damaged fibres could be identified by their irregular, broken outlines and were excluded from the total area (fig. 2.5).

Statistics

Values are presented as mean ± standard error of the mean (SEM) with *n* representing the sample size. Isometric HPT and HFT were obtained for rostral and caudal preparations and grouped into 'winter' and 'summer' fish. A model for a nested and crossed multifactorial analysis of covariance was constructed (Cochran and Cox 1957; Winer 1962):

$$Y'_{j(i)jk} = Y_{j(i)jk} - \beta(X_{j(i)k}) = \mu + S_i + F_{j(i)} + P_k + (SP)_{ik} + (FP)_{j(i)k} \qquad (2.2)$$

where Y = the criterion mean

Y'= the criterion mean adjusted for the effect of the covariate

μ = general mean

S = the effect of season group (subscript i: winter=1, summer=2)

F = the effect due to the individual fish (subscript j; = n)

P = the effect of muscle isolation site (k: rostral =1, caudal =2)

$\beta(X_{j(i)k})$ = the effect of the covariate

The significance level was set at $\alpha_{(1)}=0.05$ as the criterion for the rejection of H_0 with $H_0 : \mu_1=\mu_2$ and $H_A : \mu_1 \neq \mu_2$. Analysis of covariance was performed using General Linear Interactive Models (GLIM). Data for V_0 was also tested using multifactorial analysis of covariance, excluding the seasonal factor. Comparisons of standard length, wet weight and preparation length between seasonal groups was performed with a Student's t-test using MINITAB 8.1. (Minitab Inc., Philadelphia, USA).

2.3. Results

Isometric contractile properties

Compared to rostral preparations, muscle fibres from caudal myotomes were found to require a lower stimulus frequency to produce a fused isometric tetanus (40 Hz compared to 90 Hz; fig. 2.1). Tension output in rostral fibres tended to decline during the tetanic plateau whereas caudal fibres could maintain steady tension over a longer period of stimulation (fig. 2.1). Average peak tetanic tensions (P_0) obtained were 123.5 ± 7.2 kN. m^{-2} and 78.2 ± 6.6 kN. m^{-2} for rostral and caudal preparations respectively (mean $\pm$ SEM; $n = 11$ and 7). In addition, a significant difference was found in fibre l_r; mean rostral fibre l_r was 2.7 mm longer than that of fibres isolated from caudal myotomes (table 2.1).

Although fish of similar size were studied, mean L_s of the 'summer' group was significantly greater than that of the 'winter' group (table 2.1). The mean contraction times of caudal muscle fibres were slower by 70% for HPT and 63% for HFT relative to fibres from rostral myotomes (table 2.2). Analysis of covariance with standard length as the covariate showed

a significant relationship of L_s with HPT and HFT (table 2.3a and b). The interaction term for length and position also had a significant effect on HPT indicating that the relationship between position and HPT varied for fish of different lengths. The model was then re-fitted after assigning a weight to the factor 'position' which allowed a separate analysis of the effects of the factors 'length', 'season' and 'fish' on the data for rostral and caudal muscle fibres (table 2.4). The variance due to the covariate length for caudal data was 38 times greater for HPT and 11 times greater for HFT than for rostral data showing that the effect of the covariate length on contraction times in caudal fibres accounts for a major part of the overall effect of L_s on HPT and HFT (tables 2.3 & 2.4).

Isometric contraction times were not found to be significantly influenced by season at an experimental temperature of 5°C (table 2.3). Position (rostral or caudal) was by far the most influential factor in determining contraction time. Both tetanic half time to peak tension (HPT) and half time to relaxation (HFT) were significantly greater in caudal preparations and a major proportion of the variance in HPT and HFT was due to position of the fibre in the fish (tables 2.3a & b).

Maximum contraction speed - V_O

Maximum contraction speed was 2.4 fold higher for muscle fibres from rostral (6.9 ± 1.34 muscle lengths.s^{-1}) than caudal myotomes (2.9 ± 0.81 muscle lengths.s^{-1}) (mean ± SEM, $n = 8$. See also fig. 2.4b). Analysis of covariance showed a significant difference in V_O due to position with a significant interaction between fish and position indicating that there was some variation between individuals in the effect of position on V_O.

Table 2.2

Table 2.2

Half-time to peak tension (HPT) and half relaxation time (HFT) during isometric tetani at 5°C of fast muscle fibres isolated from *Gadus morhua.*

All values are mean ± SEM

GROUP	POSITION	*n*	HPT (ms)	HFT (ms)
WINTER	Rostral	9	26.5 ± 2.9	50.8 ± 3.6
	Caudal	9	40.1 ± 2.7	77.7 ± 8.9
SUMMER	Rostral	6	22.1 ± 1.2	58.9 ± 4.6
	Caudal	6	45.2 ± 4.3	104.3 ± 13.0
TOTAL	Rostral	15	24.7 ± 1.8	54.0 ± 2.9
	Caudal	15	42.1 ± 2.4	88.3 ± 8.0

Table 2.3

Table 2.3

ANCOVA of isometric tetanic half time to peak tension (HPT) and half relaxation time (HFT) of fast muscle fibres isolated from *Gadus morhua*.

$H_O : \mu_1 = \mu_2$ and $H_A : \mu_1 \neq \mu_2$, $\alpha_{(1)} = 0.05$.

Symbols: d.f. = degrees of freedom, SS = sum of squares, MS = mean square, F = variance ratio, p = probability of F with $Group_{(1)}$ and $Error_{(2)}$ d.f., NS = not significant $(p < 0.05)$.

a) HALF TIME TO PEAK TENSION (HPT)

SOURCE	d.f.	SS	F	*p*
Due to length	1	213.2	6.64	*p*>0.025
Due to season	1	44.4	1.38	NS
Between fish	12	385.1	0.46	NS
Betw. Position	1	2261.7	32.19	p>0.0005
L x P	1	408.8	5.82	p>0.05
S x P	1	14.2	0.20	NS
Residual	12	843.4		
Total	29	4170.9		

b) HALF TIME TO RELAXATION (HFT)

SOURCE	d.f.	SS	F	*p*
Due to length	1	3025.0	5.86	p>0.05
Due to season	1	558.6	1.08	NS
Between fish	12	6197.0	1.42	NS
Betw. Position	1	8803.0	24.14	p>0.0005
L x P	1	865.8	2.37	NS
S x P	1	161.7	0.44	NS
Residual	12	4375.3		
Total	29	23987.0		

Table 2.4

Table 2.4

Change in variance due to the exclusion of first rostral and then caudal data from the ANCOVA, showing the effect of fibre position on the distribution of variation in the analysis for both half time to peak tension (HPT) and half relaxation time (HFT).

Symbols: d.f. = degrees of freedom, SS = sum of squares.

SOURCE	d.f.	Rostral (caudal excluded)		Caudal (rostral excluded)	
		HPT SS	*HFT* SS	*HPT* SS	*HFT* SS
Length	1	15.8	327.2	606.2	3564.0
Season	1	54.5	59.6	4.2	660.7
Fish	12	642.7	1432.6	585.7	9139.6
Total	14	713.0	1819.4	1196.1	13364.0

Work loop experiments: the effect of varying activation phase

Activation phase was varied from 15° to 360° whilst all other parameters were held constant. Relative values of force and work were calculated as a percentage of maximum positive values. A cycle frequency of 9 Hz was initially chosen on the basis of the following scaling equation (Altringham and Johnston 1990b):

$$f_{opt} = 1.67 L_s^{0.52} \qquad\qquad (2.3)$$

which describes the cycle frequency (f_{opt}) for optimum power output in the cod.

Starting from 15° phase, work output was initially positive with the maximum work output occurring at around 15° phase (fig. 2.6). As stimulus phase was increased, net work declined steadily, with the transition to net negative work occurring at 81 ± 6° for caudal and 121 ± 10° for rostral fibres (mean ± SEM, $n = 9$). Net work continued to decrease until approximately 270° phase and then returned towards positive values as the phase cycle progressed. A smaller number of experiments was used to check that the work output curve was continuous throughout the 360° cycle (inset, fig. 2.6). Varying the activation phase produced similar patterns from both rostral and caudal preparations, but the curve representing the work output given by caudal fibres showed a displacement to the left of the rostral curve (fig. 2.6). Maximum net negative work was substantially greater than maximum net positive work and peak forces were greater for the latter part of the phase cycle in caudal fibres (fig. 2.6 & 2.7). Negative work output was higher in caudal fibres than in rostral fibres at an equivalent phase (fig. 2.6).

Figure 2.6

Figure 2.6

Mean relative work per cycle produced with variation in activation phase by rostral (n = 8) and caudal (n = 11) fast muscle fibres of *G. morhua* at 5°C at an oscillation frequency of 9 Hz. Inset shows the continuity of the change in work over 360° for a single rostral preparation. The work loops are representitive of (a) maximum positive work (+3.1 μJ); (b) transition from positive to negative work (+0.082 μJ) and (c) maximum negative work (-3.38 μJ) in rostral fibres (note: not to the same scale; Force = vertical axis, strain = horizontal axis with arrows indicating direction of loop). Symbols: rostral work, —○—; caudal work, --■--. Values represent mean ± SEM.

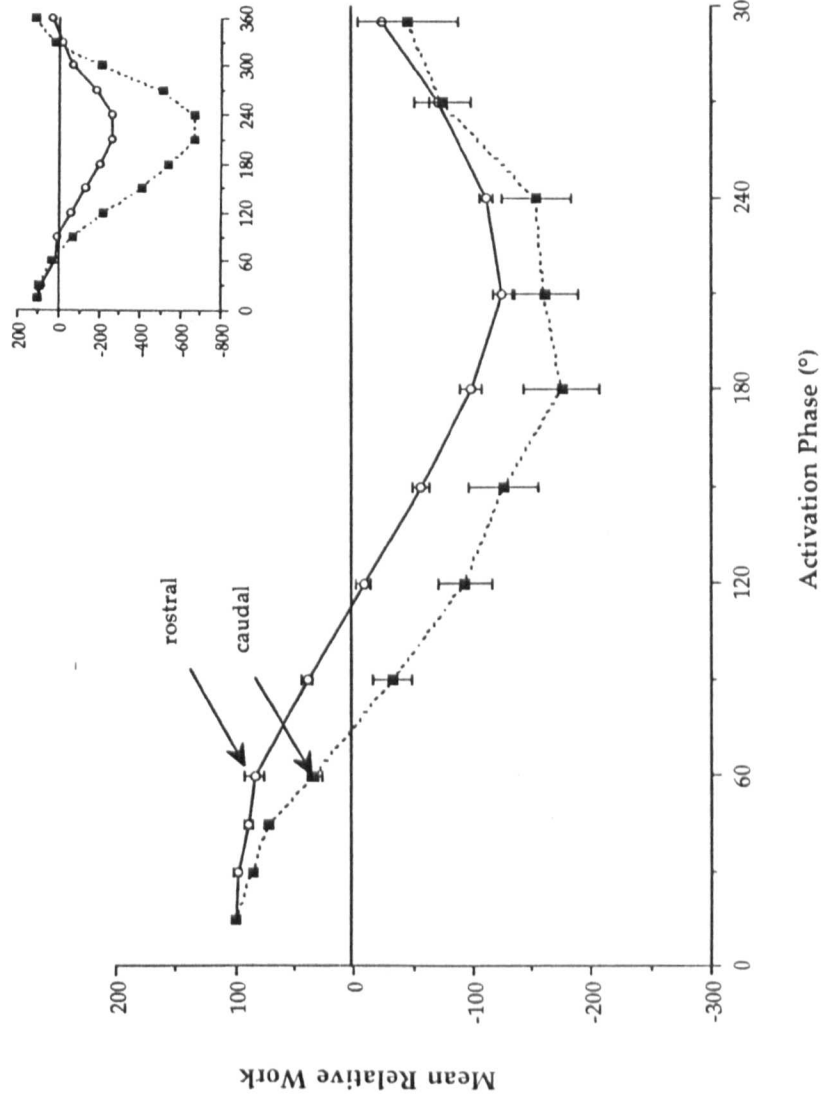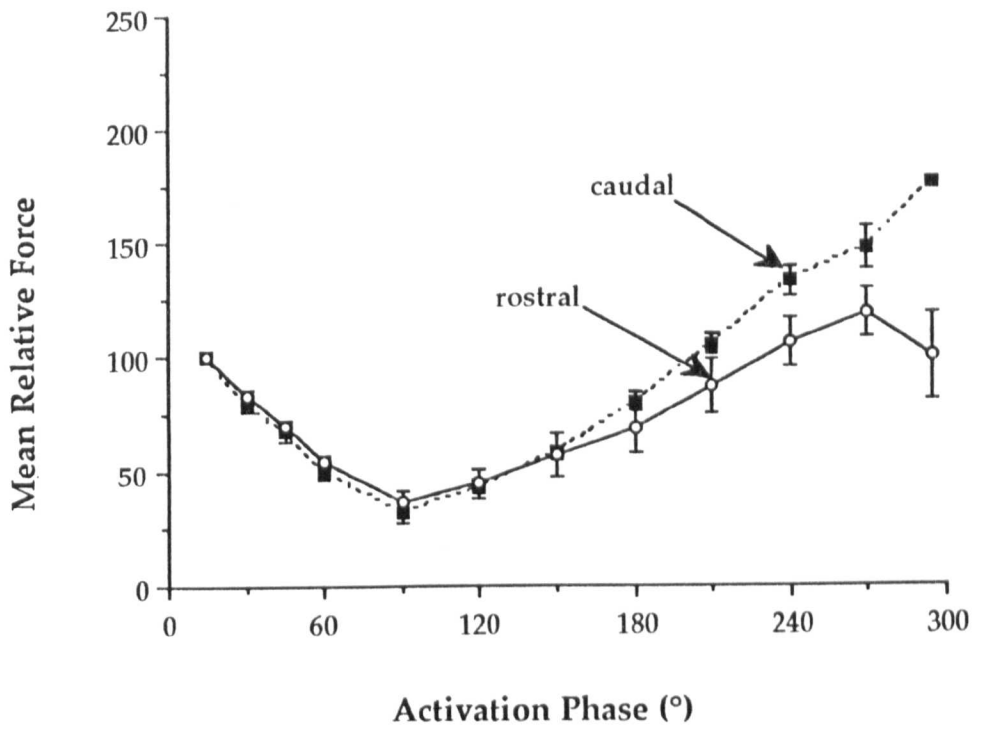Mean Relative Work

Activation Phase (°)

Figure 2.7

Figure 2.7

Mean relative force per cycle produced by rostral (n = 8) and caudal (n = 11) fast muscle fibres of *G. morhua* at 5°C at an oscillation frequency of 9 Hz with variation in activation phase. Symbols: rostral work, —o—; caudal work, --■--. Values represent mean ± SEM.

The change in work was closely related to changing peak forces (fig. 2.7). Comparing the changes in mean relative work and force in caudal fibres, it can be seen that F_o reaches its lowest values at around the transition point between positive and negative work and then rises to its maximum at 300° for rostral and 270° for caudal fibre preparations.

The effect of reducing cycle frequency

A 30-40 cm cod swimming at a cycle frequency of 9 Hz will be moving at a velocity that is approaching its maximum performance. Videler and Wardle (1991) formulated an equation which describes the ratio of the maximum tail beat frequency (TBF) in the cod to each 10 cm change in body length (Q_{10cm}):

$$TBF_{max\,cod} = 15.32\,(0.886^{(L_s-20)/10})(2.057^{(t-10)/10}) \qquad (2.4)$$

where L_s = standard length in cm and t is the temperature in °C. For a body size range of 30-40 cm, this gives a maximum tail-beat frequency of 8.4 to 9.5 Hz at a temperature of 5°C. This level of performance is required for behaviours when short bursts of high velocity are required, such as feeding, escape and kick-and-glide swimming.

The recruitment of anaerobic muscle during swimming occurs when the maximum sustainable specific speed is exceeded (Rome, Funke and Alexander 1990). For 35-37 cm cod, the maximum sustainable length-specific swimming speed has been variously reported as approximately 2 L_s^{-1} (Videler 1981; Videler and Wardle 1991) and 2.1-3.7 L_s^{-1} at 5°C (Beamish 1966; n = 40). Videler (1981) found that a 30 cm cod had an

average stride length of 0.60 L_S over a range of swimming speeds at 12°C. Since one tail-beat cycle moves the fish forward one stride length (Wardle 1977), the cycle frequency at the maximum sustained speed can be estimated by:

$$f_{sust} = U_S / A \qquad\qquad (2.5)$$

where U_S is the maximum sustainable specific speed in $L.s^{-1}$ and A is the stride length as a proportion of L_S. Using $U_S = 2\ L.s^{-1}$ and A = 0.6 L_S, a cycle frequency of 3.33 Hz is obtained. A slightly higher cycle frequency of 4 Hz was chosen to represent the lower limits of fast fibre activity *in vivo* and was imposed on rostral and caudal fibre preparations. The length of the stimulus train was kept constant, resulting in a decrease in the duty cycle (the percentage of the length cycle covered by the stimulus train) from 38% to 17%.

At 4 Hz, the activation phase for the transition from positive to negative work increased to 149° in caudal and 199° in rostral fibres, a change of 84% and 64% respectively, causing a shift of the work output curve to the right (average of 3 experiments; Fig. 2.8). Changing the number of stimuli per cycle from 2 to 4 extended the duty cycle from 17% to 33%, which increased the period of active tension generation and resulted in a reduction in the shift in the curve to 131° for caudal and 169° for rostral preparations (fig. 2.9).

Rostral fibres produced positive work over about 50% of the phase cycle at both 4 Hz and 9 Hz, but at 4 Hz the activation phase for maximum positive work (and thus power output) occurred approximately 70° later (figs. 2.6 and 2.8). At 4 Hz, the period of positive work output in caudal fibres was

Figure 2.8

Figure 2.8

Mean relative work per cycle produced by caudal fibres at 9 Hz (—■—) and 4 Hz (—□—) and rostral fibres at 4 Hz (··°··) with two stimuli and varying activation phase. All preparations were isolated from the same fish.

Figure 2.9

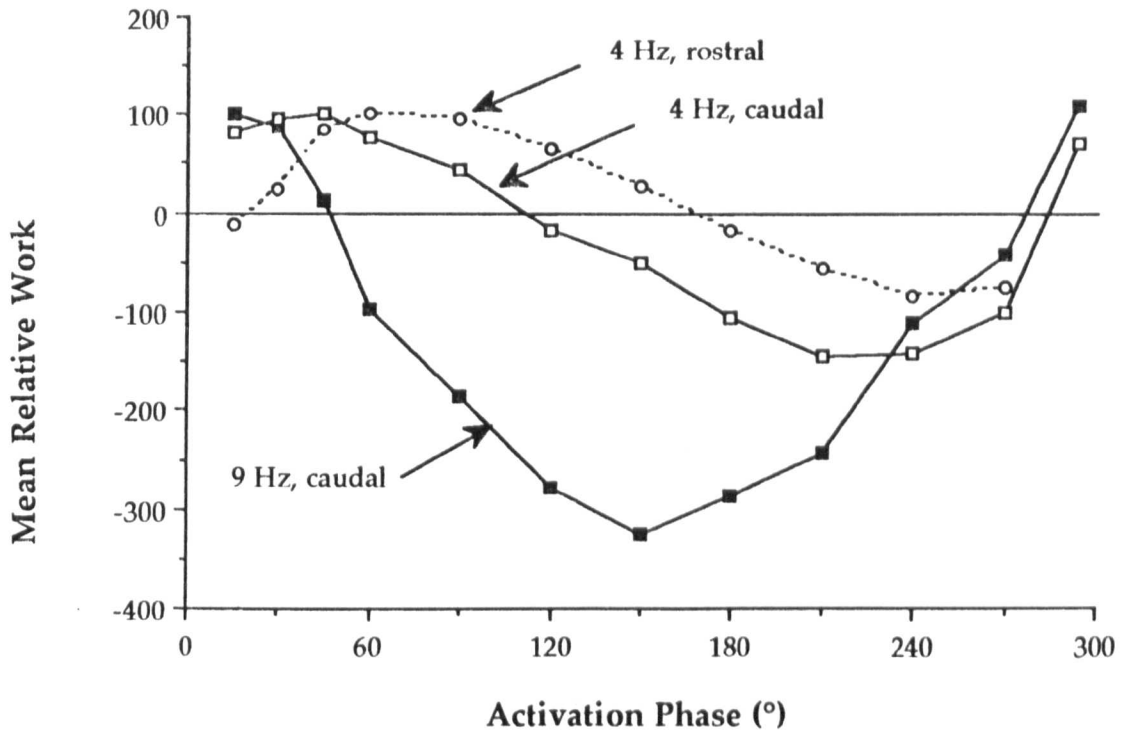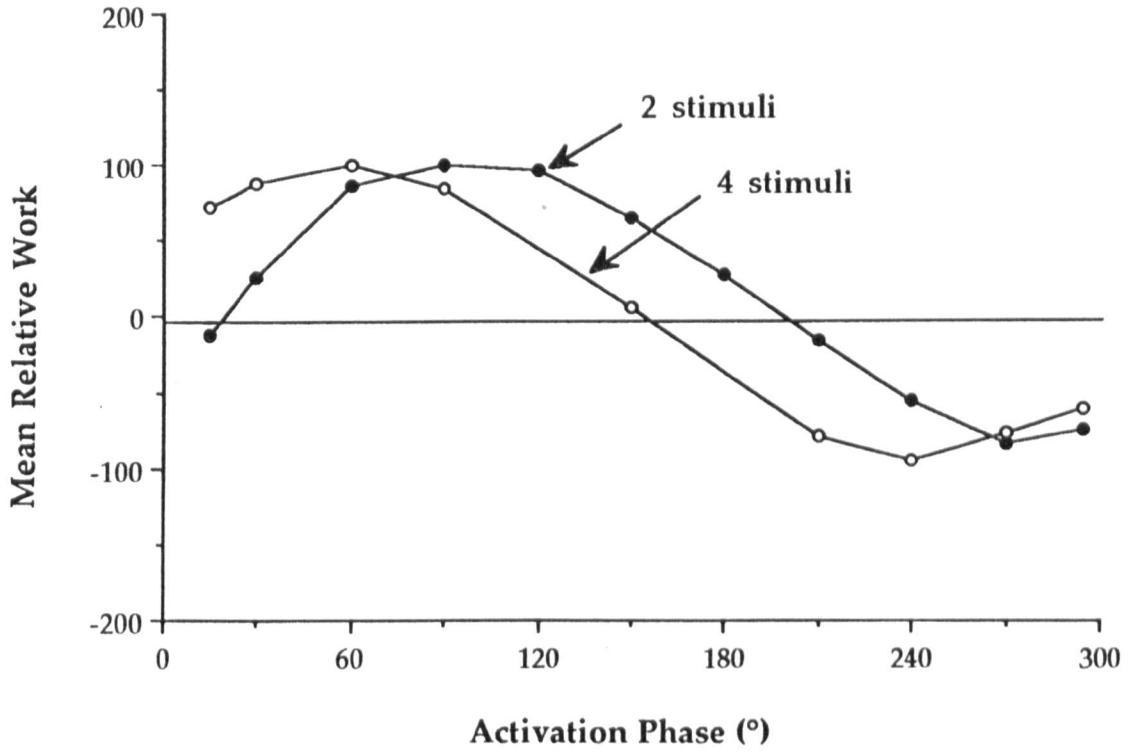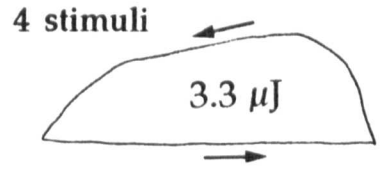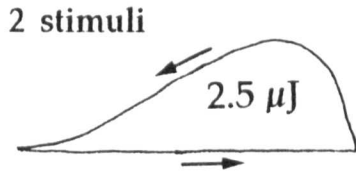# Figure 2.9

Mean relative work per cycle at 4 Hz oscillation frequency produced by two rostral preparations from the same fish with varying activation phase. Symbols: 4 stimuli (o), 2 stimuli (•). Work loop insets show the effect of increasing the number of stimuli from 2 to 4 on the area of the work loop.

2 stimuli   2.5 μJ

4 stimuli   3.3 μJ

Mean Relative Work

Activation Phase (°)

increased from approximately 42% to 58%, with maximum positive work occurring at a later phase as in rostral fibres (fig. 2.8).

2.4. Discussion

Regional differences in contractile properties

The contractile properties of fast muscle fibres isolated from rostral and caudal myotomes in the cod are intrinsically different. Maximum peak tensions decrease and contraction times increase from rostral to caudal myotomes (tables 2.2 and 2.3). Significant differences in peak tensions between rostral and caudal myotomes were also found in the saithe (Altringham *et al.* 1993) and in muscle blocks excised from a number of marine fish (Wardle 1985). In contrast, the contractile properties of muscle fibres isolated from rostral and caudal myotomes of the short-horned sculpin were not significantly different, perhaps reflecting differences in swimming style between species (Johnston, Franklin and Johnson 1993). The values for peak tensions obtained for fast fibres in the present study are lower than reported previously (Anderson and Johnston 1992; Archer *et al.* 1990).

V_0 was also found to be significantly lower in caudal than rostral preparations, agreeing with the longer HPT found in caudal fibres. Since the speed at which a muscle can shorten is a function of both myosin heavy chain (Greaser, Moss and Reiser 1988) and myosin light chain (Lowy, Waller and Trybus 1993), the present study suggests that tthere may be changes in myosin composition along the length of the fish.

Cyclical contractions

Imposing cyclical length changes decreases half times to peak tension and relaxation and increases maximum peak forces relative to isometric contractions (Altringham and Johnston 1990*b*). Higher peak tensions were produced when the activated muscle was lengthened as opposed to shortened. One possibility is that during forced lengthening, the cross-bridge attachments may be broken while in the strong-binding configuration - before they complete the ATPase cycle and detach (Lombardi and Piazzesi 1990). In order to lengthen the preparation, the apparatus must therefore exert a force on the fibres which is great enough to overcome this additional resistance. Since caudal fibres produce higher forces during the negative part of the work cycle, this suggests that either more of their cross-bridges are detached in a high energy state or that each individual cross-bridge is capable of resisting detachment with more force than in rostral myotomes.

When the muscle is stimulated, there is a delay between the arrival of the stimulus and the generation of tension so that the activation phase is not the phase at which maximum tension occurs. The timing and duration of tension relative to muscle lengthening and shortening will determine the final net work output. Caudal fibres, by virtue of their longer HPT and HFT, generate tension over a greater portion of the oscillation cycle and so produce net negative work at earlier values of activation phase than rostral fibres (figs. 2.6 and 2.8). A longer contraction duration also increases the amount of work that has to be done to lengthen caudal fibres resulting in higher values of negative work than rostral fibres at an equivalent phase (figs. 2.6 and 2.8). At an oscillation frequency of 4 Hz the cycle period is more than doubled, such that the period of tension

generation is a much smaller percentage of the cycle period and the transition to net negative work therefore occurs at a higher activation phase in both rostral and caudal fibres (fig. 2.8). Increasing the number of stimuli increases the period of tension generation (by increasing the duty cycle) and causes the observed shift of the positive-negative transition towards lower values of activation phase (fig. 2.9).

During steady swimming, the change in activation phase down the trunk remains constant with varying tail beat frequency (Grillner and Kashin 1976). The results presented here suggest that as tail beat frequency decreases, the duration of the stimulus train must increase in order to maximise positive work output over the appropriate range of activation phase. In trout, dace, eel and dogfish, the burst duration (or duty cycle) at a given position on the trunk was found to stay a constant proportion of the tail beat cycle, supporting this view (Grillner and Kashin 1976). Since the phase of EMG onset is constant with swimming speed, adjustment of the duration of EMG burst at a given position along the trunk may act to maintain the timing of force and work output in relation to muscle length in order to optimise power output during steady swimming at different speeds.

In agreement with Altringham *et al.* (1993), caudal fibres produced maximum force between 300° and 15° activation phase with work reaching maximum positive values as force declined (figs. 2.6 and 2.7). These authors proposed that since the moment of maximum force in isolated caudal muscle fibres coincides with maximum power output of rostral fibres, caudal fibres initially act to transmit rostrally produced power to the tail blade by stiffening the tail and only contribute positive power towards the end of the cycle. Although positive work occurred over

a similar range of phases in rostral and caudal fibres when compared on the same axis (figs. 2.6 and 2.8), the strain cycle in caudal myotomes *in vivo* lags behind that of rostral myotomes - in the saithe this delay is approximately 110° (Altringham *et al.* 1993). If the delay in cod is similar, then peak positive work in rostral myotomes (15-30°) would coincide with high forces and net negative work in caudal myotomes (280-300°; figs. 2.6, 2.7 & 2.8). Muscle activation while lengthening also occurs in caudal myotomes during unsteady swimming behaviours in the carp (Van Leeuwen *et al.* 1990) and bluegill sunfish (*Lepomis macrochirus*; Jayne and Lauder 1993). In light of such studies on the timing of EMG onset *in vivo*, the present findings for cod suggest that caudal muscle fibres may play a role in propagating rostrally produced force to the tail blade during swimming.

When interpreting kinematic data or extrapolating experiments with isolated fibres to the *in vivo* situation, the possible influence of the complex three-dimensional arrangement of myotomes and tendons on net power output must be considered. The interaction of muscle and tendon in the medial gastrocnemius muscle of the cat during walking and trotting allows the muscle fibres to actively shorten even though the whole muscle-tendon complex is lengthening (Griffiths 1991). Tension exerted on the muscle-tendon complex is high but at the expense of tendon, rather than muscle fibre lengthening (see van Leeuwen 1992). The present study shows that rostral and caudal muscle fibres of the Atlantic cod have different *in vivo* contractile properties when compared under similar conditions but the consequences of this for the generation of thrust during swimming will require experiments using more realistic strain and stimulation patterns which also take into account muscle architecture and the role of tendons and other elastic components.

Influence of season and body size on muscle contractile properties

Fish caught in summer and winter had similar contractile properties at 5°C. In the carp, muscle contractile properties are modified after several weeks cold acclimation which acts to partially compensate for the drop in muscle performance at low temperatures (Crockford and Johnston 1990). Cold acclimation results in changes in the expression of myosin heavy and light chains (Crockford and Johnston 1990) and is associated with an increase in sarcoplasmic reticulum Ca^{2+}-ATPase activity at low temperatures (Flemming *et al.* 1990). The contractile properties of cod fibres may show a seasonal acclimation effect when measured at higher experimental temperatures, as has been reported for the demersal marine fish the short-horned sculpin (Johnson and Johnston 1991a). Another possibility is that cod may undergo local migration to stay within a preferred temperature range during summer and winter months (Rose 1993).

Even over the restricted range of sizes used in this study, fish standard length was an important factor influencing muscle contraction times. As cod length increases, there is an increase in twitch 90% contraction time (Archer *et al.* 1990), tetanic HFT (Altringham and Johnston 1990b) and a decrease in maximum tailbeat frequency, power output and V_o (Altringham and Johnston 1990b; Anderson and Johnston 1992). The present study shows that the duration of muscle activation will tend to increase with increasing fish size and indicates that this relationship is different for rostral and caudal preparations, particularly for relaxation times. As fish size, and therefore cycle period increase, extending the

duration of tension generation would help to optimise power output throughout the tail-beat cycle. However, the range of sizes in this study which were selected specifically to minimise scale dependent effects are not sufficient to draw any firm conclusions.

STEROLOGICAL ANALYSIS OF MUSCLE: REGIONAL DIFFERENCES IN MYOTOMES OF THE ATLANTIC COD (*GADUS MORHUA* L.)

3.1. Introduction

The contractile properties of a muscle fibre are determined in part by its ultrastructure. Fibre types may vary in myofilament length (e.g. Akster, Granzier and ter Keurs 1984), mitochondrial content (Kryvi, Flood and Gulyaev 1980) and in patterns of vascularisation and innervation (Kryvi et al. 1980; Bone 1972) in addition to differences in protein composition (e.g. Focant, Huriaux and Johnston 1976; Huriaux and Focant 1977) and enzyme activities (Johnston, Davidson and Goldspink 1977) and these characteristics may be related to the function of a particular fibre type during swimming.

Slow muscle fibres in fish power low swimming speeds and have been shown to have significantly longer activation and relaxation times than fast fibres (e.g. Akster, Granzier and ter Keurs 1985). The decreased contraction duration in fast fibres has been correlated with their possessing higher volume and surface densities of terminal cisternae and T-tubules in a number of fish species (Nag 1972, Flemming et al. 1990, Akster et al. 1985) and in the guinea pig (Eisenberg, Kuda and Peter 1974; Eisenberg and Kuda 1975). However, many studies provide quantitative data on the relative amounts of T-system and sarcoplasmic reticulum (SR) but fail to relate these to measurements of the contractile characteristics

of the muscle concerned (e.g. Eisenberg et al. 1974; Eisenberg and Kuda 1975).

Stereology provides a theoretical basis for the calculation of the volume and surface area of a component in three dimensions from a two-dimensional image (see Weibel 1972 and 1973). Muscle fibres isolated from rostral and caudal myotomes in the cod have different contractile properties (see Chapter 2). The aim of this chapter was to quantify the T-system and sarcoplasmic reticulum from electron micrographs to investigate the structural basis of the observed difference in mechanical characteristics.

3.2. Materials and Methods

Electron microscopy

Preparation of samples

Bundles of fibres (10-20) were isolated from rostral and caudal myotomes of fish used in the V_{max} experiments (n = 8; Chapter 2) and pinned out *via* the remains of their myosepts on blocks of silicon elastomer base (Sylgard 184, Dow Corning, Midland, MI, USA) at their resting lengths. Tissue was fixed using a 2% solution of gluteraldehyde in 0.15 M sodium cacodylate buffer, 10 mM $CaCl_2$, pH 7.2 at 4°C for 2 hours and then rinsed in cacodylate buffer for a further hour. Small pieces of muscle 2-3 mm in length containing 1-3 fibres were dissected from the surface of the fixed bundles and placed in fresh cacodylate buffer. The material was post-fixed for 1 hour in 2% osmium tetroxide, 10mM $CaCl_2$, 0.8% potassium ferricyanide, 0.15 M sodium cacodylate, pH 7.2 which gives selective staining of sarcoplasmic reticulum and transverse tubule systems (Peachy 1965; Flemming *et al.* 1990) and rinsed overnight in fresh

cacodylate buffer. Samples were dehydrated in a series of alcohols from 50% through to absolute and embedded in Araldite CY212.

Sectioning

Longitudinal sections were cut parallel to the long axis of the muscle fibre on an ultramicrotome (OM-U2, Reichert, Austria). Semi-thin (1 μm) sections stained with Toluidine blue were used to check the orientation and progress of sectioning. Thin sections showing a gold interference pattern (80-90 nm) were picked up on 400 mesh copper grids and double-stained with uranyl-acetate and lead citrate. Sections were viewed under a Phillips 301B electron microscope at 60kV and 5 micrographs per block at a magnification of x 9100 (actual magnification x 7776) were randomly taken giving a total of 10 micrographs per fish (5 rostral and 5 caudal).

Quantitative analysis

Stereology

Micrographs were projected onto paper using a photographic enlarger (x 4) and the outlines of terminal cisternae, T-tubules, sarcoplasmic reticulum and myofibrillar space were traced. At the same time, a calibration scale (projected with the micrograph) was marked on each drawing to cancel out the enlarger magnification. The order in which the micrographs were traced was randomised by thorough shuffling, each micrograph being identified by plate number only to reduce bias on the part of the measurer. The surface area of terminal cisternae, T-tubules and sarcoplasmic reticulum longitudinal tubules (SR-tubules) were quantified using digital planimetry (Kontron Elektronic GmbH, West Germany). The volume density (V_v) of components (i.e. volume of component per unit

volume) were calculated after Weibel (1972) using myofibril volume as the reference space:

$$V_{v(i)} = \sum a_i / \sum A_t \qquad (3.1)$$

where a_i = surface area of component

A_t = surface area of myofibril

Surface densities were estimated using a 25 cm^2 coherent square double lattice test system with a fine line spacing of 0.2 cm and with a fine-to-heavy line ratio of 5 (i.e. 25 fine squares within each heavy square; Weibel 1973); T-tubule intersections were counted using the fine lines. The test grid was placed at 19° and 71° to the fibre axis to optimise sampling (Eisenberg, Kuda and Peter 1974). Surface densities (i.e. surface area of component per unit volume) were calculated after Weibel (1973) and were related to total muscle fibre volume:

$$S_{v(i)} = 2 \cdot I_i / L_t \qquad (3.2)$$

where L_t = total length of test line (μm)

I_i = intersection of test line with component

The length of the T-tubule SR junction relative to myofibrilar volume was calculated after Akster (1985), using a method adapted from Eisenberg and Salmons (1981):

$$J_t = Q_t / A_f \qquad (3.3)$$

where J_t = Relative T-SR contact length (μm^{-2})

Q_t = Number of T-SR contact profiles per unit fibre area

A_f = myofibrillar area

In the original formula, Q_t was multipied by an integration constant of 2 (Weibel 1979; equation 2.64) which was derived assuming that the tubules were randomly orientated. The T-system is orientated perpendicular to the long axis of the fibre, rendering this assumption invalid. Since this orientation is not strictly adhered to, the integration constant is difficult to calculate and the uncorrected equation is used (Eisenberg and Salmons 1981).

Statistics

All experimental values are presented as mean ± standard error of the mean (SEM). Volume and surface densities and relative T-SR contact length were tested by analysis of covariance with standard length as the covariate and fish and position within fish as factors.

Estimation of error

Measurement error was estimated for both methods of collection: direct digtisation from the enlarger image (method 1) and digitisation of the traced image (method 2). A micrograph was selected and a size range of objects for area and perimeter measurements (terminal cisternae and T-tubule profiles) were identified. Error for method 1 was estimated by digitising each object 30 times and calculating the coefficient of variation (V) for each object, giving an estimate of variability that is independent of object size (Zar 1984):

$$V = \frac{s}{\overline{X}} \cdot 100\% \qquad (3.4)$$

where s = sample standard deviation

$\overline{X}$ = sample mean

The measurement error for method 2 was estimated by tracing each object 30 times and then digitising each traced profile once before calculating V. A linear regression was used to test for a relationship between object size and V. The coeffient of variation was compared between different collection methods for each size class (equation 3.4; Zar 1984):

$$F = \frac{(s^2{}_{\log})_1}{(s^2{}_{\log})_2} \quad \text{or} \quad F = \frac{(s^2{}_{\log})_2}{(s^2{}_{\log})_1}, \text{ whichever is larger} \qquad (3.5)$$

where F = variance ratio (critical F value is $F_{0.05(2),v1,v2}$)

$s^2{}_{\log}$ = sample variance of the logarithms of the data

3.3. Results

Volume and surface densities of membrane components

Post-fixation in osmium ferricyanide clearly differentiated the sarcoplasmic reticulum and the T-system in muscle fibres isolated from both rostral and caudal myotomes (fig. 3.1). There was no difference in the volume densities obtained for total SR and T-tubules between fast fibres from rostral and caudal myotomes. The results for both the volume and

Figure 3.1

Electron micrographs (longitudinal sections) of fast muscle fibres stained with osmium tetroxide and potassium ferricyanide taken from rostral (a) and caudal (b) positions along the trunk of *Gadus morhua*. Abbreviations: A, A-band; I, I filament; M, M-line; SR, sarcoplasmic reticulum; T, T-tubules; TC, terminal cisternae; Z, Z-line. Scale bar = 1 μm
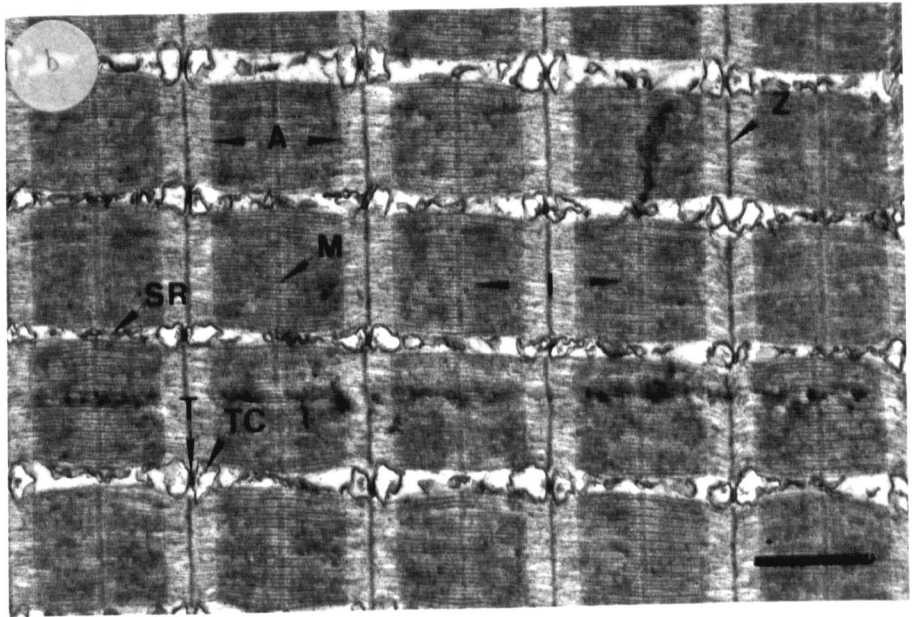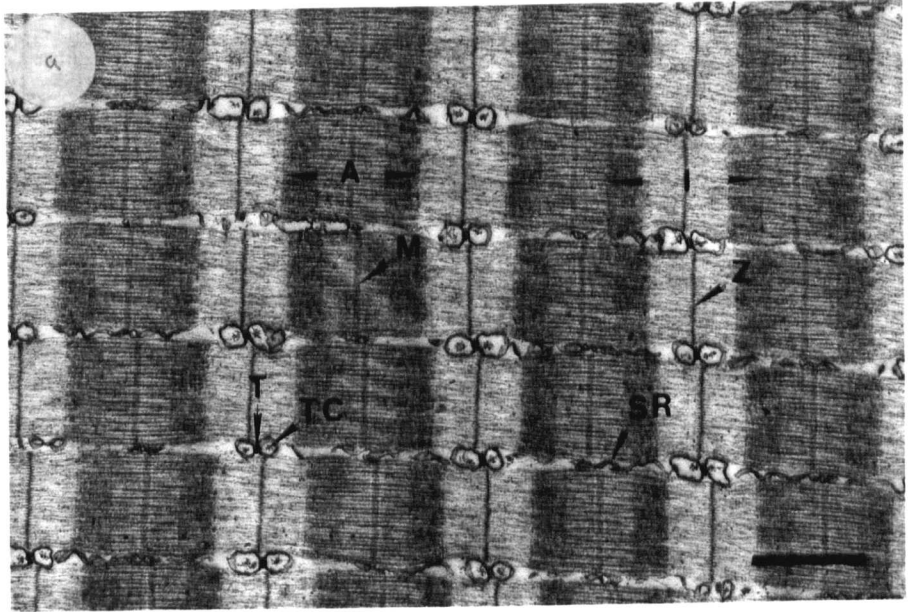
surface densities compared well to those in the literature for other vertebrate twitch fibres, despite differences in the methods of fixation and quantification that were employed (table 3.2). The surface densities of the elements of the triad were 0.78 to 0.90 μm^{-1} for terminal cisternae and 0.17 to 0.19 μm^{-1} for T-tubules in caudal and rostral fibres respectively and although mean volume and surface densities of terminal cisternae were 12-14% lower in muscle fibres isolated from caudal as opposed to rostral myotomes, the surface area-to-volume ratio was around 0.23 for both positions (table 3.1). No significant difference was found between rostral and caudal muscle fibres in the volume and surface densities of any of the components quantified (ANCOVA; $\alpha_{(1)}=0.05$).

T-SR contacts

The relative length of T-SR contact in caudal fibres was 20% less than that in rostral fibres (0.99 $\pm$ 0.03 μm^{-2} and 1.24 $\pm$ 0.08 μm^{-2} respectively [mean $\pm$ SEM; n = 25 for each position]) but this was not significant at the 0.05 level (ANCOVA; $p = 0.064$).

Estimation of error

A significantly greater measurement error was associated with the digitisation of pre-traced T-tubule and SR profiles (method 2) than for direct digitisation of the projected image (method 1) for all except the smallest and largest areas sampled (fig. 3.2). The error associated with both methods remained below 5% for profile areas between 0.01 μm^2 to 0.08 μm^2, but rose steeply to over 20% for areas less than 0.01 μm^2 (such as the T-tubule profiles)(fig. 3.2). Assuming that the measurement error associated with a given sarcomere component is the same for rostral and caudal samples, comparisons between rostral and caudal measurements will not be affected.

Table 3.1

Table 3.1

Volume and surface densities of sarcoplasmic reticulum and T-tubles in rostral and caudal fast muscle fibres of the Atlantic cod.

[a] measured by digital planimetry

[b] estimated using intersection counts

[c] correction factor of 1.06 assumes that Sr - tubules are only partially orientated within the sampled longitudinal sections (Eisenberg and Kuda 1975).

All values are mean ± SEM, n = 5 fish with 5 plates for each position within a fish (total of 50 plates). Analysis of covariance did not demonstrate a significant difference between muscle position for any of the quantified components at the 0.05 level.

Component	Position	Volume density (V_V) % [a]	Surface density (S_V) μm^{-1} [b]	Corrected S_V μm^{-1} [c]
Terminal Cisternae	Rostral	3.73 ± 0.33	0.90 ± 0.04	
	Caudal	3.29 ± 0.32	0.78 ± 0.06	
SR - tubules	Rostral	2.75 ± 0.50	1.38 ± 0.12	1.47 ± 0.12
	Caudal	2.68 ± 0.66	1.74 ± 0.08	1.84 ± 0.08
Total SR	Rostral	6.48 ± 0.78	2.26 ± 0.14	2.34 ± 0.14
	Caudal	5.97 ± 0.96	2.57 ± 0.10	2.67 ± 0.10
T - tubules	Rostral	0.26 ± 0.04	0.19 ± 0.02	
	Caudal	0.20 ± 0.01	0.17 ± 0.01	

Table 3.2

Table 3.2
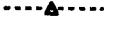
Summary of volume and surface densities of fast muscle fibre types.

All values are mean ± SEM. References: a - fast trunk fibres, this study; b - m. levator operculi anterior, Akster *et al.* 1985; c - anterior dorsal trunk fibres, fish acclimated to 7°C or 23°C for a minimum of 1 month, Flemming *et al.* 1990; d - superficial white trunk fibres, Eggington and Johnston 1982*b*; e - Nag 1972; f & g - Kryvi 1977; h - white vastus, Eisenberg and Kuda 1975; i - Luff and Atwood 1971.

SPECIES	SITE	Volume density %		Surface Density μm^{-1}	
		Tot. SR	T-tubule	Tot. SR	T-tubule
FISH					
Gadus morhua [a]	rostral (0.35 L_S)	6.48±0.78	0.26±0.04	2.34±0.14	0.19±0.02
	caudal (0.90 L_S)	5.97±0.96	0.20±0.01	2.67±0.10	0.17±0.01
Perca fluviatilis [b]	operculum	5.5 ±0.4		2.8 ±0.2	
Cyprinus carpio [c]	dorsal - 7°C	5.1 ±0.3		3.3 ±0.2	
	dorsal - 23°C	5.4 ±0.3		3.7 ±0.2	
Anguilla anguilla [d]	superficial	6.81±1.55	0.37±0.07		
	mid	4.75±1.39	0.30±0.14		
	deep	5.95±1.66	0.38±0.10		
O. mykiss [e]		13.7	0.40	2.42	0.34
Etmopterus spinax [f]	fast axial	6.00±2.23	0.50±0.37		
Galeus melastomus [g]	fast axial	6.80±1.64	0.89±0.45		
MAMMAL					
Guinea pig [h]	vastus muscle	4.59±0.29	0.27±0.02		
Mouse [i]		5.5			

Figure 3.2

Figure 3.2

Change in coefficient of variation (V) with cross-sectional area of measured profile for two different measurement methods. Symbols: method 1 = ———•———; method 2 = ····▲····.

V (%) vs. Mean area (μm^2)
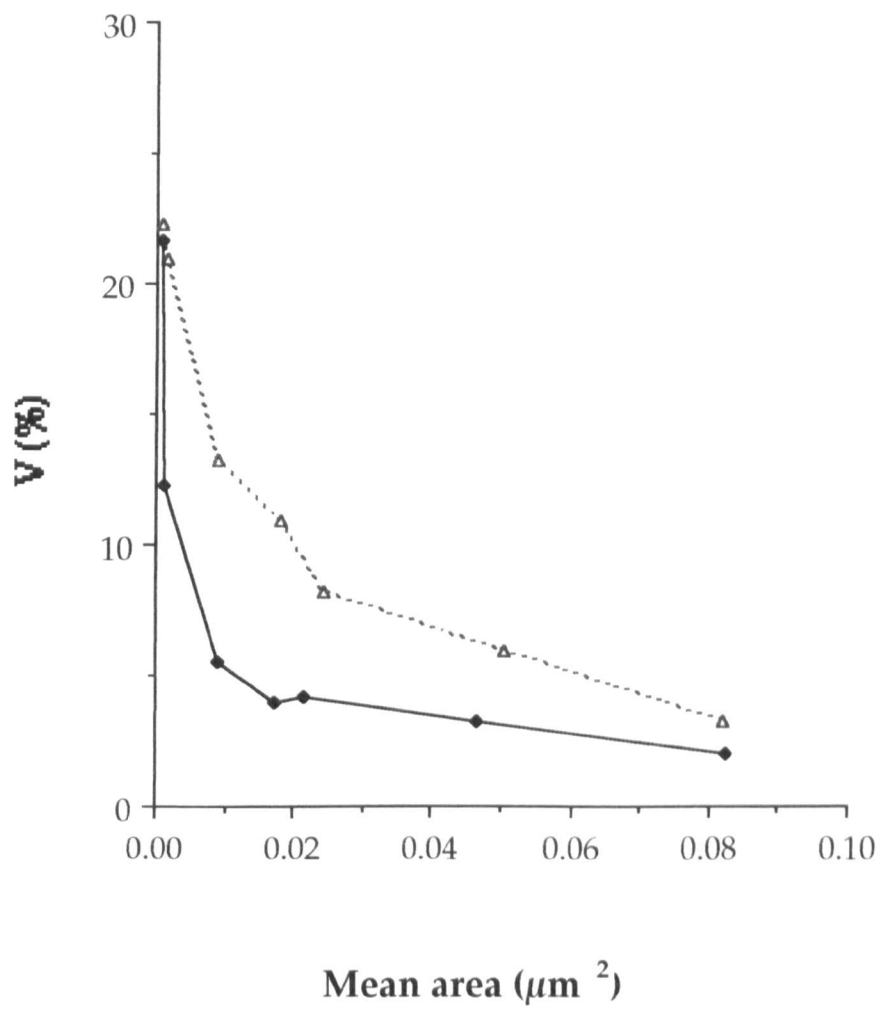
3.4. Discussion

Fast muscle fibres isolated from rostral and caudal myotomes of the Atlantic cod do not differ significantly in their volume and surface densities of T-tubules and sarcoplasmic reticulum (table 3.1) despite possessing differences in their contractile properties (Chapter 2, tables 2.2 and 2.3). Slow muscle fibres in both fish and mammals have been shown to have characteristically longer contraction times than fast fibres (e.g. Akster *et al.* 1985) which usually correlates well with lower volume and surface densities of terminal cisternae and T-tubules (e.g: Akster *et al.* 1985; Eisenberg *et al.* 1974; Eisenberg and Kuda 1975; Barnard *et al.* 1971).

Muscle fibre activation results from the release of free calcium from the terminal cisternae (Ebashi 1991) and terminal cisternae volume has been correlated with twitch contraction time in the rat (Kugelberg and Thornell 1983) and the carp (tables 2 and 3 in Akster *et al.* 1985). Although not statistically different, the surface and volume densities of the terminal cisternae in caudal fibres in the cod were indeed lower than in rostral fibres (table 3.1). However, even though the terminal cisternae in rostral fibres may contain a greater volume of free calcium ions, the similarity of surface area-to-volume ratios indicates that other factors must be involved to ensure a faster rate of calcium release (e.g. Dulhunty 1986). During excitation-contraction coupling, depolarization of the T-system causes the release of calcium ions from the terminal cisternae and it is likely that the length of T-SR contact, the region where the T-system is thought to initiate calcium release from the terminal cisternae, will affect the rate of calcium release and thus the rate of muscle fibre activation (Ebashi 1991, Eisenberg and Eisenberg 1982). Twitch activation time in the opercular muscles of the perch was found to decrease with increasing length of the T-SR contact: the time to peak tension of pink fibres in the perch was over twice that of white fibres, corresponding to a 19% decrease in T-SR contact

length (Akster *et al.* 1985). A similar relationship between T-SR contact length and half activation time was observed between rostral and caudal muscle fibres in the present study which may contribute to differences in the rate of force development.

Muscle relaxation is due to the removal of free calcium ions to the terminal cisternae over the whole surface of the SR (Ebashi 1991). Since the surface area and volume of membrane are not primarily responsible for the observed differences in relaxation rates of cod fast fibres, changes in either the specific activity of the SR Ca^{2+} pump (see Flemming *et al.* 1990 or Ushio and Watabe 1993) or the membrane density of pumps (see Dulhunty 1990) between rostral and caudal locations may be involved.

THE CHANGE IN FORCE-VELOCITY CHARACTERISTICS OF FISH MUSCLE FIBRES WITH LOCOMOTORY DEMAND

4.1. Introduction

The speed at which a muscle fibre shortens varies with load (Hill 1938). Early studies with whole frog sartorius muscle found that the relationship between muscle velocity and tension during isotonic shortening could be described by a simple hyperbolic curve (Hill 1938; Jewell and Wilkie 1958), providing estimates of maximum muscle shortening velocity (V_{max}) and instantaneous power output (Hill 1938, 1964). Subsequently, many studies found that in muscles of a number of vertebrates, force-velocity data points tended to deviate from Hill's hyperbola at high relative tensions (>0.8 P_O)(e.g. Edman, Mulieri and Scubon-Mulieri 1976; Lännergren 1978; Allen and Stainsby 1983; Marsh and Bennett 1985; Curtin and Woledge 1988*b*). In some cases, the tactic of omitting points above 0.8 P_O from the fitted curve was adopted to allow the comparison of the 'Hill constants' with other studies (e.g. Rome 1983). However, an accurate description of the P-V relationship is important when relating muscle contractile properties to their function *in vivo* (Marsh and Bennett 1986). By ignoring data points above 0.8 P_O, shortening velocity (and therefore power output) are overestimated at loads of between 0.8 and 1.0 P_O (e.g. Edman *et al.* 1979) and the predicted V_{max} may be

unreliable (Caiozzo, Herrick and Baldwin 1992). The hyperbolic-linear equation proposed by Marsh and Bennett was found to give a more accurate description of the P-V relationship than Hill's 'characteristic' equation in fast twitch muscle fibres of both lizards (Marsh and Bennett 1986) and fish (Langfeld, Altringham and Johnston 1989; Langfeld, Crockford and Johnston 1991; Beddow and Johnston 1995).

Slow fibre types tend to have a lower P_0 and V_{max} and a more curved P-V relationship than the fibres of the fast type (e.g. Rall and Schottelius 1973; Lännergren 1978; Ranatunga and Thomas 1990) and thus have a lower maximum power output as a result. Variations in P-V curvature (Bottinelli, Schiaffino and Reggiani 1991) and in V_{max} (Bottinelli, Schiaffino and Reggiani 1994) between different fibre types of the rat have been shown to be related to their relative proportions of myosin heavy chain isoforms and the ratio of light chain 1 to light chain 3. The P-V characteristics of fast and slow fibres in fish have been previously compared using skinned fibre preparations (e.g. Altringham and Johnston 1982 & 1986; Johnston and Salmonski 1984; Johnston, Sidell and Driedzic 1985; Langfeld *et al.* 1991) but since the process of skinning can impair mechanical function, these studies may not accurately represent intact fibre performance (e.g. Altringham and Johnston 1982; Bone *et al.* 1986; Curtin and Woledge 1988*b*).

The force-velocity characteristics and power output of fast fibres isolated from the short-horned sculpin (*Myoxocephalus scorpius* L.) have been examined in relation to acute (Langfeld *et al.* 1989) and prolonged (i.e. acclimatory) changes in temperature (Beddow and Johnston 1995). The aim of the present chapter was to characterise the force-velocity relationship of fast and slow fibre types in sculpin whole fibres. Sculpin fast fibres isolated from separate myotomes have the same isometric contractile properties (Johnston, Franklin and Johnson 1993) while in

the Atlantic cod (*Gadus morhua* L.), fast fibres show significant regional differences in P_O, rates of activation and contraction and V_{max} (Chapter 2). Therefore fast fibres were isolated from rostral and caudal myotomes of sculpin and cod in order to compare regional P-V characteristics within each species. The results are discussed in relation to crossbridge action and the locomotory lifestyle of the fish.

4.2. Materials and methods

Fish

Short-horned sculpin (*Myoxocephalus scorpius* L.) and Atlantic cod (*Gadus morhua* L.) were caught locally in St. Andrews bay, Scotland. Sculpin were caught during October 1993 (fast fibre experiments) September 1994 (slow fibre experiments) whilst cod were obtained during April and May 1994. The standard lengths (L_S) and wet weights (W_W) of the experimental groups are presented in table 4.1. As muscle contractile properties are known to be influenced by scaling (e.g. Anderson and Johnston 1992) fish standard length was restricted to a narrow range within species. Fish were maintained at ambient temperature (October/April/May = 10°C; September = 13-14°C) under a constant photoperiod (12 h light: 12 h dark) prior to use and fed on a diet of shrimps and fish flesh.

Isolation of muscle fibres

Fast muscle fibre preparations were isolated from rostral (0.35 L_S) and caudal (0.90 L_S) myotomes in both cod and sculpin following the method in Chapter 2: these are referred to as 'rostral' and 'caudal' throughout.

Sculpin slow fibres (15-20) were similarly isolated from the caudal myotomes (0.90 L_s) at the level of the mid-line just beneath the skin.

Experimental apparatus

The fibre chamber has previously been described (Chapter 2). Stimulus parameters (pulse magnitude, pulse width, pulse frequency and stimulus train duration) were set during both isometric and force-velocity experiments with a Grass stimulator (Grass S48, Grass Instruments). Muscle shortening was controlled during the force-velocity experiments with a control box designed to allow a two-stage release during the plateau of an isometric tetanus (Altringham and Johnston 1988 *b*). All experiments were carried out at 10°C.

Isometric contractions

Fibre length was adjusted to give the maximum isometric twitch - this was termed the resting length of the fibre (l_r). Resting length corresponded to a sarcomere length of 2.2 μm in cod rostral and caudal and in sculpin caudal fibres as measured by laser diffraction while in sculpin rostral fibres, sarcomere length at l_r was 2.4 μm. Clear diffraction patterns were not obtained for slow preparations.

The frequency of stimulation was adjusted until tetanic fusion occurred. The preparation was then allowed to rest for 1 h (or until the force plateau had stabilised) before continuing with the experiment. Peak force (F_o), the time from the first stimulus to half activation (HPT) and the time from the final stimulus to half relaxation (HFT) were measured for each preparation (see fig. 2.3). Preparations were stimulated at 10 minute

Table 4.1

Table 4.1

Standard lengths (L_s), wet weights (W_w) and fibre lengths (l_r) of the different experimental groups.

All values are mean ± standard deviation ($n = 6$). * indicates significant difference between rostral and caudal positions (paired t-test, $\alpha_{(2)} = 0.05$).

Species	Fibre Type	Standard Length L_s (cm)	Wet Weight W_w (g)	Fibre Length l_r (mm)
Cod	Fast rostral	36.9 ± 3.7	676.9 ± 187.6	8.48 ± 0.96[*]
	Fast caudal			3.67 ± 0.69
Sculpin	Fast rostral	16.1 ± 0.3	127.1 ± 19.9	5.83 ± 1.19
	Fast caudal			4.65 ± 0.39
	Slow	19.8 ± 4.1	255.0 ± 109.8	4.0 ± 2.17

intervals over the course of an experiment, enabling reproducible results to be obtained.

The force-velocity relationship

The force-velocity (P-V) relationship was determined for each preparation by giving a two-stage length release during the plateau of an isometric tetanus (fig. 4.1a). Firstly, a small step release (2 ms duration) was imposed which reduced force to some fraction (F) of the maximum (F_0). A second, slower release at a constant velocity (ramp release) immediately followed. The magnitude of the velocity (V) was adjusted until tension remained steady for at least 20 ms following the initial step release i.e. until the velocity of the ramp release was equal to the shortening velocity of the muscle fibres. The fibres were then returned to their resting length before the end of the stimulus train, allowing tension to rise towards its initial level.

Determination of cross-sectional area

Following each experiment, cross-sectional area was determined following the method in Chapter 2 to convert force (F, F_0 in N) into tension (P, P_0 in $kN.m^{-2}$). Fibre type was confirmed by staining for myosin-ATPase and SDH activities (Johnston *et al.* 1974; Nachlas *et al.* 1957).

Fitting the force-velocity curve

At least ten points were obtained for each P-V relationship by varying the amplitude of the initial step release (i.e. varying P/P_0) and adjusting

Figure 4.1

Figure 4.1

a. Traces showing the change in fibre length (upper traces) and force
(lower traces) during two isovelocity releases (1 and 2) in fast fibres
isolated from the sculpin. b. Each combination of relative tension (P/P_o)
and velocity (V) is then plotted to produce a force-velocity curve. The
force-velocity curves shown for fast rostral ($\triangle$), fast caudal ($\circ$) and slow
($\blacktriangledown$) fibres isolated from short-horned sculpin were fitted using the
hyperbolic-linear equation (Marsh and Bennett 1986).

a.
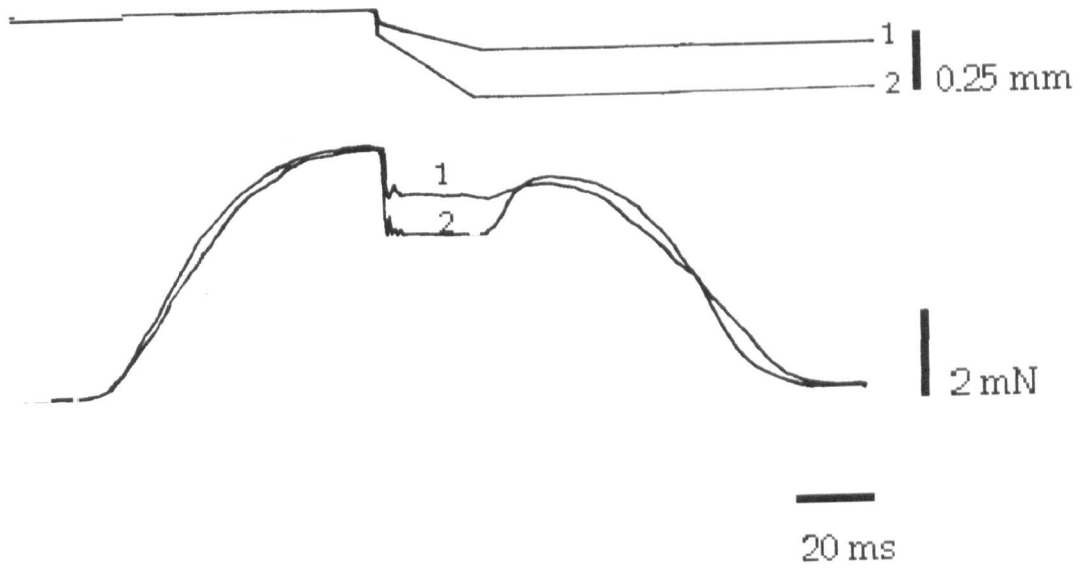
b.
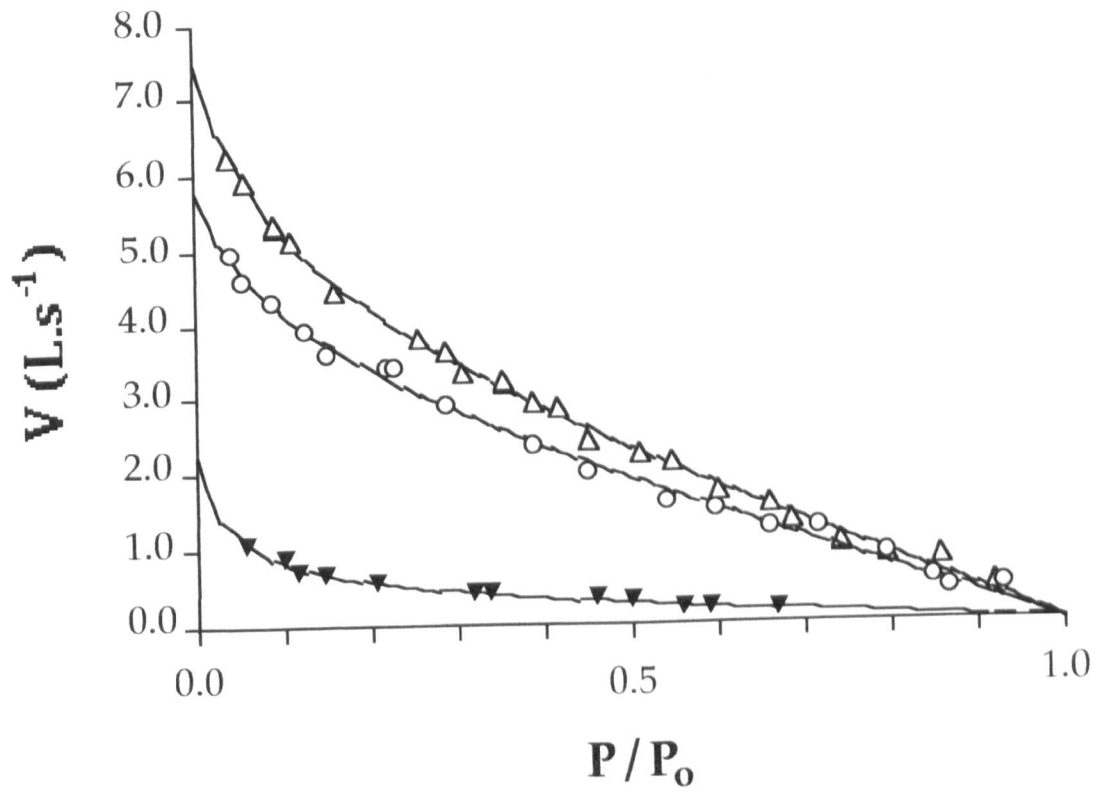
the ramp velocity until force remained constant during shortening. Relative tension (P/P_O) was plotted against the velocity of the ramp release in muscle lengths per second (V in $L.s^{-1}$) and fitted with the hyperbolic-linear relationship proposed by Marsh and Bennett (1986):

$$V = [B\ (1\text{-}P/P_O)/(A\text{+}P/P_O)] + C(1\text{-}P/P_O) \tag{4.1}$$

where A is a dimensionless constant and B and C are constants with dimensions of velocity. Equation 4.1 has been shown to describe force-velocity data in fish fast twitch fibres with greater accuracy than the traditional Hill equation (e.g. Marsh and Bennett 1986; Beddow 1993). Data was iteritively fitted with the least-squares regression of the hyperbolic-linear curve using the software package Regression (Blackwell Scientific Software, Oxford, England). The initial values of A, B and C were estimated. The program then iteritively adjusted these values until the best fit between observed and predicted curves was obtained and then returned the optimum values for the three constants (Altringham and Johnston 1988b; Beddow and Johnston 1995).

The maximum contraction velocity (V_{max}) was calculated by the program by extrapolating the curve to zero load (i.e. $P/P_O = 0$). Instantaneous power output ($W.kg^{-1}$) was the product of muscle tension (P) and velocity (V) at each point. The curvature of the P-V relationship was described by using the dimensionless power ratio $\dot{W}_{max}/V_{max}P_O$, where $\dot{W}_{max}$ is the maximum instantaneous power output (Marsh and Bennett 1986).

Statistics

All experimental values are presented as mean ± standard error (SEM). For each parameter, differences between rostral and caudal fast fibres were compared with a paired t-test. For the sculpin data, differences between fast (n = 12: 6 rostral, 6 caudal) and slow (n = 6) fibre types were tested for with an two sample t-test (H_o $\mu_1 \neq \mu_2$; α=0.05). If rostral and caudal fast fibres had been shown to be significantly different for a particular parameter, slow fibre data was separately compared with rostral and caudal data in turn. The accuracy with which the fitted P-V curve predicted the experimental relationship was measured with the standard error of the estimate (SEE; Zar 1984):

$$SEE = \sqrt{Residual\ MS} \qquad (4.2)$$

All analyses were carried out using the statistical package MINITAB 8.1. (Minitab Inc., Philadelphia, USA).

4.3. Results

Isometric contractile properties

<u>Sculpin</u>

The ability of sculpin muscle fibres to generate tension varied with fibre type: fast fibres produced around 160 $kN.m^{-2}$ compared to only 72 $kN.m^{-2}$ in slow fibres, a reduction of 55% (table 4.2). Fast fibres isolated from rostral and caudal myotomes showed no difference in P_o, HPT or HFT (table 4.2). Lower peak tensions in slow fibres were accompanied by a

two-fold greater tetanic half-activation (HPT) time and a 70% greater half-relaxation (HFT) time relative to fast fibres (rostral and caudal data combined, table 4.2). The resting lengths of rostral fast, caudal fast and slow fibres isolated from sculpin were similar ($p > 0.05$; table 4.1) and tetanic fusion at l_r was achieved at a stimulus frequency of 60 to 80 Hz.

Cod

Peak tensions were similar in fast fibres from rostral and caudal myotomes, but large regional differences in isometric contraction times were apparent. Activation and relaxation half-times were up to 50% faster in rostral fibres when compared to caudal fibres (table 4.3). Resting length in cod rostral fibres was significantly longer than in caudal fibres ($p = 0.000$; table 4.1) and a stimulus frequency of 80-100 Hz was required for fusion of the tetanic plateau.

Force-velocity relationship

The hyperbolic-linear function gave an accurate fit of the data and over 97% of the variation in V was accounted for by the fitted P-V relationship (shown by SEE and r^2 values)(tables 4.2 and 4.3). Typical P-V curves are presented in fig. 4.1b using sculpin fast and slow fibres as an example. The difference in contraction velocity at a given relative force between slow and fast fibres in sculpin tended to increase as relative load decreased (fig. 4.1b).

In sculpin, the maximum contraction velocity (V_{max}) in fast fibres was 2.9-4.0 times greater than in slow fibres (table 4.2; fig. 4.1b). In addition, V_{max} was 28% lower in fast fibres isolated from caudal than from rostral

Table 4.2

Table 4.2

Summary of the isometric and force-velocity characteristics of slow, rostral fast and caudal fast muscle fibres isolated from the short-horned sculpin (mean ± SEM).

SEE = standard error of the estimate. Rostral and caudal positions compared with a paired t-test ($H_A: \mu_1 \neq \mu_2$). Level of significance: $*$ = $p \leq 0.05$; $**$ = $p \leq 0.01$; $***$ = $p \leq 0.001$. Slow and fast fibres compared with a two sample t-test ($H_A: \mu_1 \neq \mu_2$). Level of significance: † = $p \leq 0.05$; †† = $p \leq 0.01$; ††† = $p \leq 0.001$. Where fast fibres showed significant regional differences, slow fibres were compared with rostral (®) and caudal (©) fibres separately ($H_A: \mu_1 \neq \mu_2$). Level of significance: ® = rostral and © = caudal $p < 0.001$.

| | SLOW | FAST | |
		Rostral	Caudal
n	6	6	6
Tetanic P_O (kN.m^{-2})	72.1 ± 5.8 †††	159.9 ± 8.2	160.5 ± 5.1
HPT (ms)	60.4 ± 5.5 ††	27.5 ± 2.8	33.0 ± 2.7
HFT (ms)	131.1 ± 7.3 †††	73.2 ± 10.3	84.8 ± 6.5
$\dot{W}$ max (W/kg)	19.5 ± 2.0 †††	179.7 ± 18.9	145.7 ± 16.9
Vmax (L.s^{-1})	1.9 ± 0.1 †††	7.6 ± 0.7*	5.5 ± 0.5
P/P_O at $\dot{W}$max	0.57 ± 0.05	0.591 ± 0.03	0.487 ± 0.02
V at $\dot{W}$max (L.s^{-1})	0.48 ± 0.09 †††	1.85 ± 0.24	1.90 ± 0.21
V/Vmax at $\dot{W}$max	0.25 ± 0.04 ®©	0.221 ± 0.02**	0.344 ± 0.02
$\dot{W}$max/Vmax.P_O	0.149 ± 0.02	0.138 ± 0.01	0.166 ± 0.01
A	0.039 ± 0.01 †	0.149 ± 0.07	0.146 ± 0.06
B (L.s^{-1})	0.036 ± 0.01 ††	0.793 ± 0.27	0.322 ± 0.13
C (L.s^{-1})	0.976 ± 0.15 †††	3.49 ± 0.47	3.02 ± 0.34
r^2	0.985 ± 0.009	0.992 ± 0.002	0.993 ± 0.003
SEE	0.045 ± 0.004	0.106 ± 0.015	0.096 ± 0.008

myotomes (table 4.2). In cod, V_{max} in rostral fibres was 13% greater than in caudal fibres (table 4.3). The shape of the P-V relationship (i.e. its curvature) is described by the dimensionless power ratio $\dot{W}_{max}/V_{max}P_O$, where increasing curvature is signified by a lower ratio (Marsh and Bennett 1986). Curvature was found to be the same in slow and fast fibre types of the sculpin (table 4.2) but was significantly lower in rostral than in caudal fast fibres of the cod (table 4.3).

Power output

Sculpin

Fast fibres generated over eight times more maximum instantaneous power ($\dot{W}_{max}$) than the slow fibre type, corresponding to the relatively low P_O and V_{max} found for slow fibres (table 4.2). $\dot{W}_{max}$ was not significantly different between the two isolation sites (table 4.2).

The relative tension (P/P_O) at which $\dot{W}_{max}$ occurred was between 0.47 and 0.59 (table 4.2). Slow and rostral fast fibres produced maximum power at relative velocities (V/V_{max}) of 0.25 and 0.22 respectively, but in caudal fibres the optimum V/V_{max} for power was significantly greater at 0.344 (table 4.2). Since V_{max} decreased significantly from fast to the slow fibre type, the shortening velocity (V) at which $\dot{W}_{max}$ occurred in slow fibres was around 25% of the fast fibre value (table 4.2). However, rostral and caudal fast fibres generated maximum power at the same velocity of shortening, despite a difference in V_{max} (table 4.2). A plot of relative power output (i.e. $P/P_O * V/V_{max}$) against relative force shows the similarity of the curvature of rostral and caudal fibre P-V relationships (fig. 4.2b).

Table 4.3

Table 4.3

Summary of the isometric and force-velocity characteristics of fast fibres isolated from rostral and caudal myotomes of the Atlantic cod (mean ± SEM).

SEE = standard error of the estimate. Rostral and caudal positions compared with a paired t-test (H_A: $\mu_1 \neq \mu_2$). Level of significance: * = $p \leq 0.05$; ** = $p \leq 0.01$; *** = $p \leq 0.001$.
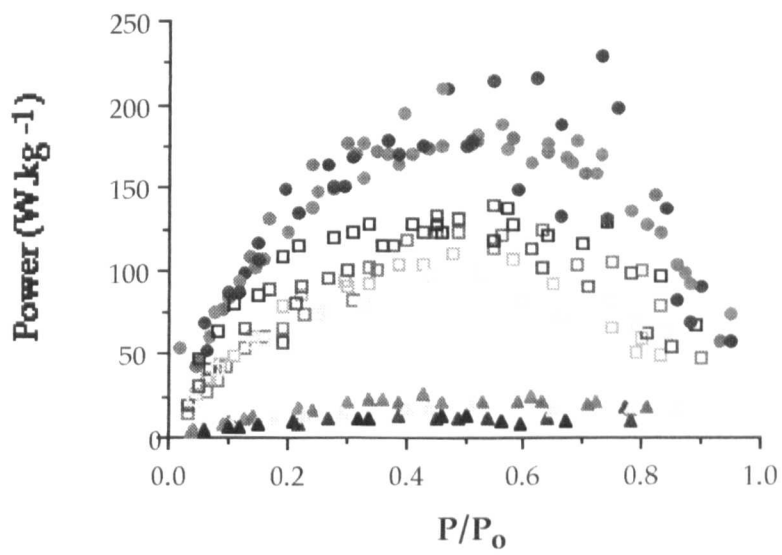
	FAST	
	Rostral	Caudal
n	6	6
Tetanic P_O $(kN.m^{-2})$	157.8 ± 15.9	123.2 ± 7.0
HPT (ms)	$13.2 \pm 1.0^*$	25.9 ± 2.9
HFT (ms)	$29.7 \pm 7.6^*$	58.6 ± 10.3
$\dot{W}$max (W/kg)	$170.5 \pm 10.5^{**}$	87.5 ± 5.2
Vmax $(L.s^{-1})$	$7.9 \pm 0.4^*$	6.9 ± 0.3
P/P_O at $\dot{W}$max	0.468 ± 0.02	0.466 ± 0.06
V at $\dot{W}$max $(L.s^{-1})$	$2.38 \pm 0.08^*$	1.57 ± 0.14
V/Vmax at $\dot{W}$max	$0.308 \pm 0.01^{**}$	0.229 ± 0.02
$\dot{W}$max/Vmax.P_O	$0.141 \pm 0.01^*$	0.105 ± 0.01
A	0.060 ± 0.01	0.053 ± 0.01
B $(L.s^{-1})$	0.261 ± 0.03	0.218 ± 0.06
C $(L.s^{-1})$	2.52 ± 0.35	3.74 ± 0.29
r^2	0.979 ± 0.010	0.995 ± 0.003
SEE	0.155 ± 0.027	0.113 ± 0.031

Figure 4.2

The change in (a) instantaneous power output in fast fibres isolated from rostral (●) and caudal (□) myotomes and slow (▲) fibres and b) relative power output in rostral (●) and caudal (□) fast fibres of the short-horned sculpin (*Myoxocephalus scorpius* L) with relative load (P/P$_0$).
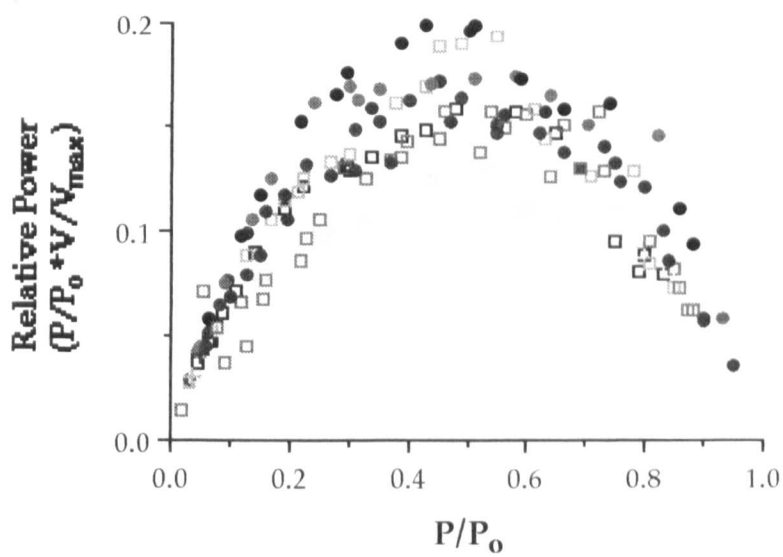
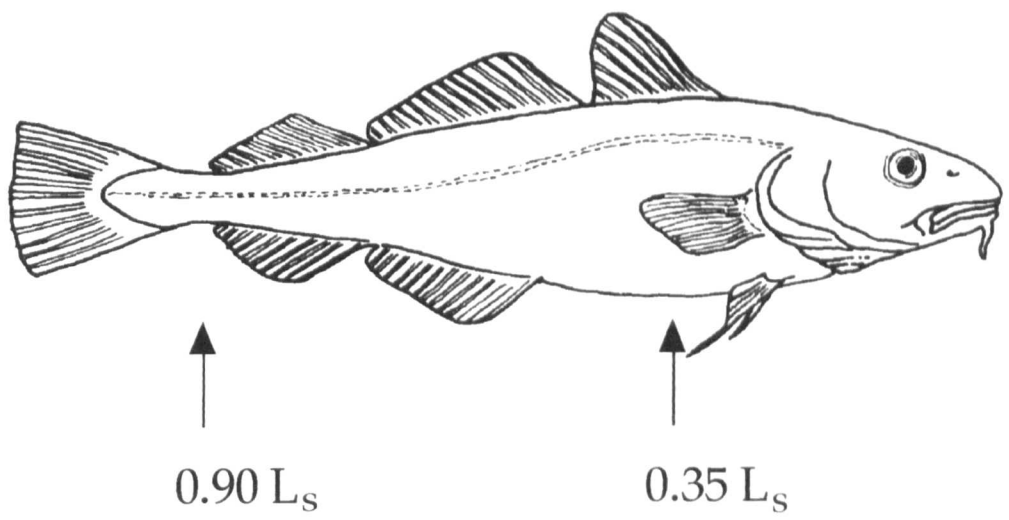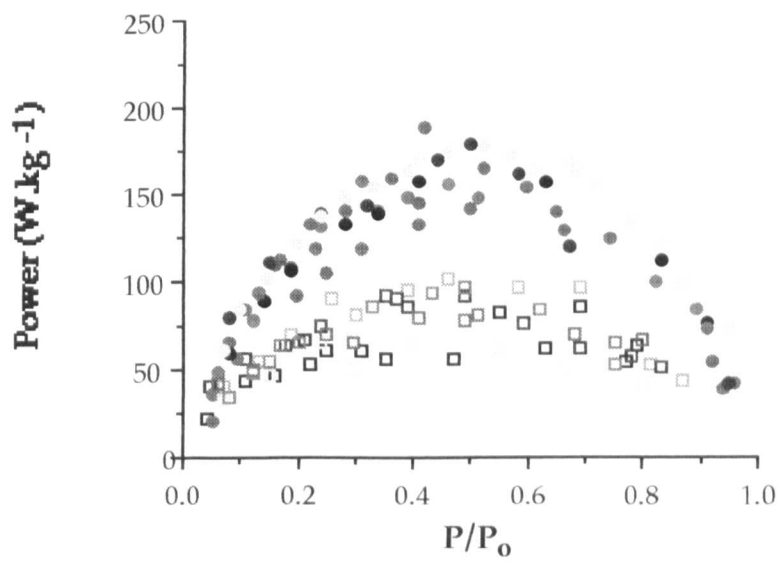0.90 L$_S$ 0.35 L$_S$
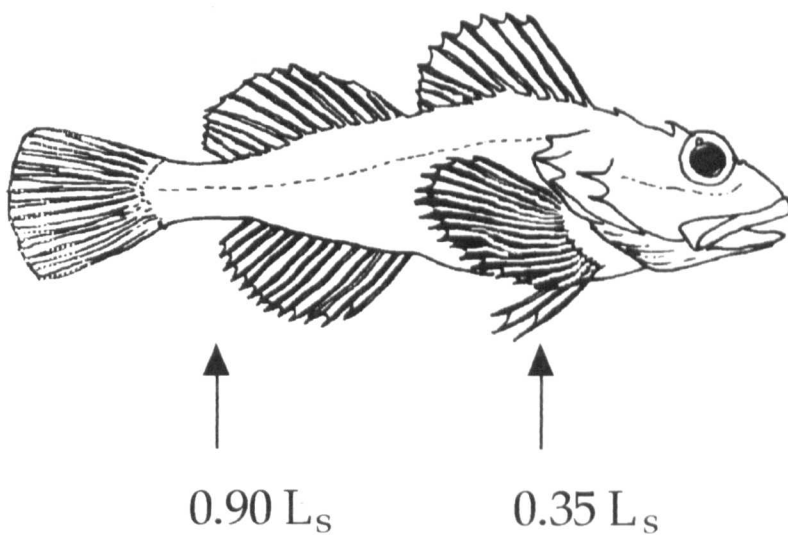
a.

b.
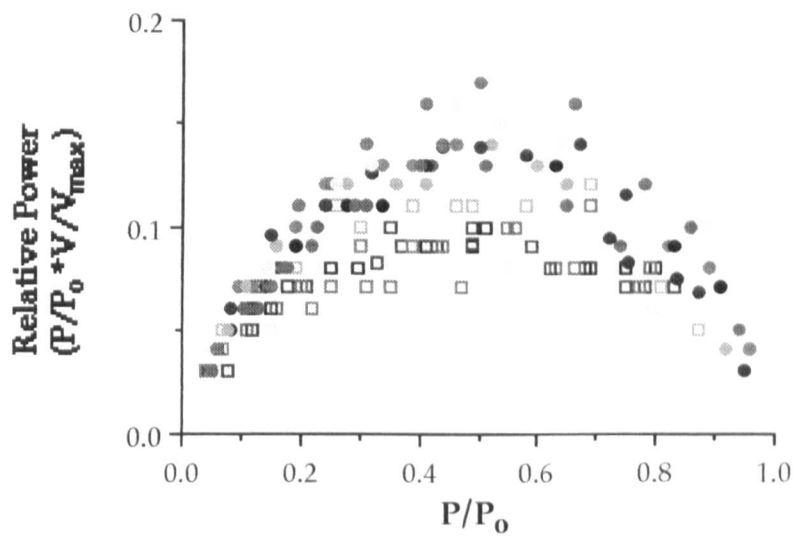
Figure 4.3

Figure 4.3

The change in (a) instantaneous power output and (b) relative power output with relative load (P/P_0) in fast fibres isolated from rostral (●) and caudal (□) myotomes of the Atlantic cod (*Gadus morhua* L.).

0.90 L$_S$ 0.35 L$_S$

a.

b.

<u>Cod</u>

The relative tension (P/P_o) at which $\dot{W}_{max}$ occurred was 0.47 in fibres isolated from both rostral and caudal myotomes (table 4.3). Fibres also showed regional differences in the relationship between relative velocity and $\dot{W}_{max}$, with $\dot{W}_{max}$ occurring at a higher V/V_{max} in rostral (0.31) than in caudal (0.23) fibres (table 4.3; paired t-test, $p \le 0.01$). As a result, the velocity of shortening at which $\dot{W}_{max}$ was generated in rostral fibres was 0.81 $L.s^{-1}$ greater than in caudal fibres.

The relative difference in the curvature of the P-V relationship in rostral and caudal fibres can clearly be seen from the change in relative power with P/P_o (fig. 4.3b). A lower curvature allows rostral fibres to contract at a higher V/V_{max} for a given relative force, thus generating greater relative power over a range of P/P_o (fig. 4.3b).

4.4. Discussion

Sculpin

<u>Contractile properties of fast and slow fibre types</u>

Fast and slow fibre types isolated from the sculpin show significant differences in contractile properties. Peak tension (P_o) and the maximum shortening velocity (V_{max}) increase by between two and four times from the slow to fast type (table 4.2). As a result, maximum instantaneous power output ($\dot{W}_{max}$) in slow fibres is only 12% of the fast fibre value (table 4.2). Electrical recordings (EMGs) show that fibre types are recruited in the order slow→ intermediate→ fast with increasing swimming speed (e.g. Johnston *et al.* 1977). The increase in $\dot{W}_{max}$ from the slow to fast fibre type matches the rising demand for mechanical power with increasing

swimming speed (as drag is proportional to [swimming velocity]^3; Webb 1975a; table 4.2).

Maximum power output of rostral fibres in the present study was 180 $W.kg^{-1}$ compared to a net power output (the product of net work per cycle and cycle frequency) of between 20 and 30 $W.kg^{-1}$ measured under conditions approximating steady swimming (table 4.2; Altringham and Johnston 1990a; Johnson and Johnston 1991a; Johnston *et al.* 1993). $\dot{W}_{max}$ is considerably greater than net power as it is the product of a single combination of force and velocity whilst during an oscillatory cycle, muscle length and velocity are being constantly varied. Net power values thus represent the *average* power output and, unlike P-V estimates, includes the work done in re-lengthening the muscle (Josephson 1993). Instantaneous power output during oscillatory work may actually be greater than that estimated from the P-V relationship. Stevens found that for a given shortening velocity, more force is generated during an oscillatory cycle between around 0.3 P_0 and P_0 than during isovelocity shortening (Stevens 1993), as the latter does not take account of the enhancement of force output by an active pre-stretch (e.g. Edman, Elzinga and Noble 1978).

Rome has suggested that relative velocity (V/V$_{max}$) is an important constraint in muscle fibre design and that muscle fibres operate *in vivo* over a range of V/V$_{max}$s where their efficiency and power output are high (Rome 1990; Rome, Sosnicki and Choi 1992). Below 0.18 V$_{max}$, efficiency declines sharply (Curtin and Woledge 1988b; Hill 1938; Hill 1964) while above 0.36 V$_{max}$ power output is reduced (Rome, Funke and Alexander 1990; Rome 1990). The optimum V/V$_{max}$ for power output in both sculpin and cod muscle fibres lies between 0.18 and 0.344, falling within the proposed optimal range (tables 4.2 and 4.3).

Sculpin fast and slow fibres generate maximum power at similar V/V_{max}s but fast fibres can shorten three to four times faster than slow fibres (table 4.2). As a result, the optimum shortening speed for power output is greater in fast fibres, corresponding to relative swimming speeds at which each fibre type is first recruited (table 4.2). In addition, isometric activation and relaxation half-times are 40-50 % lower in the fast fibre type (table 4.2). The structural differences underlying these differences in rates of activation and relaxation are likely to be complex, involving increases in the volume and surface densities of t-tubule and sarcoplasmic reticulum (SR) membranes (e.g. Eisenberg, Kuda and Peter 1974; Eisenberg and Kuda 1975) and the concentration of parvalbumins, which act to enhance rates of relaxation (Gerday and Gillis 1976; Pechère, Derancourt and Harech 1977). Maximum tail-beat frequency (TBF) is limited by the minimum duration of muscle contraction (Wardle 1975) and TBF has been shown to be linearly related to swimming speed over a range of velocities (Bainbridge 1958). A potentially shorter contraction duration combined with a high rate of shortening in fast fibres correlates well with their recruitment at higher speeds and their role in powering top burst speeds.

Regional P-V characteristics in sculpin fast fibres

Few regional differences were found in the contractile properties of sculpin fast fibres (table 4.2). Peak tension, half-times to activation and relaxation and $\dot{W}_{max}$ were the same in rostral and caudal fibres but caudal fibre V_{max} was 28% lower than that of rostral fibres (table 4.2). However, since the optimum V/V_{max} for power output was greater in fibres from caudal than in rostral myotomes, $\dot{W}_{max}$ occurred at the <u>same</u> shortening velocity in both rostral and caudal fibres, despite a difference

in V_{max} (table 4.2). Under imposed sinusoidal strains, rostral and caudal fibres isolated from the sculpin have been shown to have similar net power outputs and require the same conditions of strain and oscillation frequency to generate maximum power (Johnston *et al.* 1993). Johnston and co-workers proposed that *in vivo*, fast muscle power output would be positive down the body of the fish under most conditions (Johnston *et al.* 1993) and the results of the present study show that fibres isolated from rostral and caudal myotomes are equally capable of generating positive power (table 2). The fact that maximum power output in rostral and caudal fibres occurs at the same velocity of shortening during an isovelocity release (table 4.2) combined with their similar optimum conditions for power output during oscillatory work (Johnston *et al.* 1993 strongly suggests that sculpin fast fibres may operate under similar conditions of strain and activation during swimming, regardless of their location on the body.

Cod

Regional differences in isometric contractile properties

Fast fibres isolated from rostral and caudal myotomes of the cod gave similar peak tensions but both HPT and HFT in rostral fibres were around half of caudal values (table 4.3). Longer activation and relaxation rates in cod caudal fibres were not based on differences in the volume and surface density of t-tubules or sarcoplasmic reticulum membrane (Chapter 2). Other factors which may influence the relative relaxation rates of rostral and caudal fibres include the density (Dulhunty 1986) and specific activity (Ushio and Watabe 1993) of Ca^{2+}-ATPase pumps in the SR-

membrane and the concentration of parvalbumins (Gerday and Gillis 1976).

Regional differences in force-velocity characteristics

V_{max} is 13% greater in fibres from rostral than from caudal myotomes (table 4.3) - a much smaller difference than was previously found between rostral and caudal fibres isolated from winter fish at 5°C (Chapter 2). This discrepancy may be due to differences between the experimental groups or may reflect regional differences in the temperature sensitivity of V_{max}.

In cod, the P-V relationship for fast fibres is significantly less curved (higher power ratio) in fibres isolated from rostral than from caudal myotomes (table 4.3). The consequence of a decrease in curvature is that muscle fibres are able to shorten more quickly for a given relative load (i.e. the optimum V/V_{max} for power output is shifted to higher values) and therefore generate more power than if the P-V relationship was more curved. Because of a lower P-V curvature, rostral fibres are able to generate maximum power at a relatively faster shortening velocity compared to caudal fibres than would be possible by a regional difference in V_{max} alone. The shape of the P-V curve depends on the relative net rates of cross-bridge attachment and detachment with a greater curvature corresponding to a lower ratio (Huxley 1957). This implies that in cod rostral fibres, the relative rate of cross-bridge detachment is low in comparison to that in caudal fibres resulting in rostral fibres cross-bridges being attached for a longer period of time during fibre shortening. A way of testing this theory would be to compare the relative stiffness of rostral and caudal fast fibres at different shortening velocities, since the stiffness of an active muscle fibre is related to the

number of attached cross-bridges (e.g. Ford, Huxley and Simmons 1985). Cross-bridge detachment could be delayed in a number of ways: (i) a difference in the composition of myosin heavy chain (MHC) isoforms between rostral and caudal fibres (Bottinelli *et al.* 1991), resulting in reduced myosin ATPase activity; (ii) regional differences in the relative composition of myosin light chain (MLC) isoforms resulting in rostral/caudal differences in V_{max} and the shortening velocity for a given relative load (Lowey, Waller and Trybus 1993; Bottinelli *et al.* 1994); (iii) Differences in the regulation of the cross-bridge cycle by the troponin-tropomyosin complex (Landesberg and Sideman 1994); (iv) Prolonged rates of relaxation due to lower rates of calcium uptake and release (e.g. Flemming *et al.* 1990), a lower concentration of parvalbumins (Gerday and Gillis 1976) or an increased troponin C affinity for $[Ca^{2+}]$. The latter is unlikely as the rate of relaxation in caudal fibres is significantly longer than that in rostral fibres (table 4.3).

Maximum rostral power output was 170 $W.kg^{-1}$, but $\dot{W}_{max}$ in caudal fibres was only 50% of rostral values (table 4.3). The optimum V/V_{max} for power output in rostral fibres was 0.31 compared to 0.23 in caudal fibres which, combined with a higher rostral V_{max}, resulted in rostral fibre $\dot{W}_{max}$ occurring at a 50% higher shortening velocity (table 4.3). The orientation of teleost fast fibres allows rostral and caudal fibres to shorten around 25% and 70% respectively of the distance shortened by fibres in a longitudinal orientation for a given bend in the fish (Alexander 1969). The four-fold mechanical advantage of rostral fibres, in addition to their ability to generate maximal power at high shortening velocities and their fast rates of activation and relaxation, will enable them to generate their greatest power at the highest tail-beat frequencies *in vivo*. It is likely that the main role of caudal fast muscle fibres in the cod is to resist

lengthening, thereby transmitting rostrally produced forces to the tail blade (Chapter 2) and thus they may have a reduced ability to generate power during shortening as a result.

LENGTH-TENSION CHARACTERISTICS OF MUSCLE FIBRES ISOLATED FROM ROSTRAL AND CAUDAL MYOTOMES OF THE SHORT-HORNED SCULPIN

5.1. Introduction

According to the sliding filament theory, the total force generated during a muscle contraction is the sum of the individual crossbridge forces (Huxley and Hanson 1954; Huxley and Niederkerke 1954). Subsequent experimental evidence showing that isometric tension in length-clamped sections of a frog muscle fibre was dependent on the degree of overlap between the thick and thin filaments compared well to theoretical predictions and gave further credence to the sliding filament theory (Ramsey and Street 1940; Gordon, Huxley and Julian 1966). As predicted, force was maximal at sarcomere lengths where unimpeded crossbridge formation could occur along the full length of the thick filament (Gordon *et al.* 1966).

Thick filament length in vertebrates shows little variation, with reported values ranging from 1.44μm (*Cyprinus carpio* - red axial fibres; Van Leeuwen *et al.* 1990) to 1.74μm (*C. carpio* - m. hyohyoideus pink fibres; Akster 1985); the standard reference length is frequently taken to be 1.6μm (*Rana*; Page and Huxley 1963). Actin filament length is more variable between species (∎

0.8-1.3μm; taken from fig. 9, Van Leeuwen 1991) and measures between 0.85 to 0.95μm in the fast and slow axial muscles of the carp (Van Leeuwen *et al.*1990; Sosnicki, Loesser and Rome 1991). Due to the apparent regularity of thick filament length, it is actin filament length which determines the range of sarcomere lengths over which a muscle fibre can actively generate tension.

The optimum sarcomere length (l_{opt}) for force production during an isometric tetanus was found to be different for rostral and caudal fast fibres isolated from the sculpin, suggesting that they may differ in their length-tension characteristics (see Chapter 4). The aim of this study was therefore twofold: firstly, to compare the sarcomere length-tension curves of fast fibres isolated from rostral and caudal myotomes in the sculpin. Secondly, since the shape of the length-tension curve can be theoretically determined using ultrastructural measurements (Van Leeuwen 1991), to determine the sarcomere dimensions of rostral and caudal fibres and then to calculate a theoretical length-tension relationship for rostral and caudal fibres. It was predicted that a difference in length-tension curves would coincide with a difference in actin filament length. The results are discussed in relation to sarcomere length changes during swimming.

5.2. Materials and Methods

Fish

Short-horned sculpin (*Myoxocephalus scorpius* L.) were caught locally in St. Andrews Bay, Scotland during October 1993. Fish of standard length (L_s) 117.8$\pm$ 14.2 cm and wet weight (W_w) 161.9 $\pm$ 0.99 g (mean $\pm$ standard deviation (SD)) were maintained in sea water aquaria at 10°C for a period of five weeks

prior to use under constant photoperiod (12 h light :12 h dark) and were maintained on a diet of shrimps and fish flesh.

Isolation of muscle fibres

See Chapter 2.

Experimental apparatus

The fibre chamber and stimulator have previously been described (Chapters 2 and 4 respectively. The servo-system was not used as sarcomere length was set by manually adjusting the preparation using a micromanipulator until the desired sarcomere length was obtained. All experiments were carried out at $10 \pm 0.1°C$.

Experimental determination of sarcomere length-tension curve

Sarcomere length was determined by laser diffraction using the method described in Chapter 2. The distribution of sarcomere lengths along an single muscle fibre becomes increasingly inhomogeneous at long sarcomere lengths (e.g. Altringham and Pollack 1984) so the laser beam was directed through the central region of the preparation to avoid sampling widely divergent sarcomere populations. The fibres were stimulated to give an isometric twitch via two platinum electrodes (Goodfellow) running parallel to the fibre bundle and preparation length was adjusted using a micromanipulator until maximal peak force was attained. The preparation length at which maximal force occurred was designated as the resting length (l_r) of

the fibre. The magnitude, width and frequency of pulses were then optimised to give a maximal fused tetanus and the preparation was then allowed to rest until tetanic peak force (F) had stabilised before proceeding further. Tetanic peak force, half-time to peak tension (HPT) and half-time to relaxation (HFT) were measured for a range of sarcomere lengths in random order and the active force (F_a) was calculated:

$$F_a = F - F_r \qquad\qquad\qquad (5.1)$$

where F_r = resting tension at a given sarcomere length

Fibres were stimulated at ten minute intervals and set to their new sarcomere length from l_r just prior to stimulation. After relaxation had occurred, the fibres were then returned to l_r. In this way, reproducible results could be obtained during the course of an experiment. Relative active force (F^*) was calculated as a proportion of the maximum tetanic force (F_0) and the results expressed as the mean ± standard error (SEM) for each sarcomere length. The length-tension relationship was fitted with a fifth-order polynomial curve using a graphics package (CricketGraph, Cricket Software).

Determination of cross-sectional area

After each experiment, the cross-sectional area of the muscle fibre bundle was determined following the method used in Chapter 2.

Electron microscopy

Preparation of samples

Bundles of fast fibres (10-20) were isolated from rostral and caudal myotomes and pinned out on small blocks of silicone elastomer base (Sylgard 184, Dow Corning, Midland MI, USA). Initial trials showed that shrinkage was minimised if the fibres were fixed at long sarcomere lengths. Tissue was pre-fixed using a 2% solution of gluteraldehyde in 0.15 M sodium cacodylate buffer, 10 mM $CaCl_2$, pH 7.2 at 4°C for 1 hour and then rinsed in three changes of cacodylate buffer of 15 mins each. Small pieces of muscle 2-3 mm in length containing 1-3 fibres were dissected from the surface of the fixed bundles and placed in fresh cacodylate buffer. The material was post-fixed for 1 hour in 2% osmium tetroxide, 10 mM $CaCl_2$, 0.8% potassium ferricyanide, 0.15 M sodium cacodylate, pH 7.2 and then rinsed overnight in cacodylate buffer. Samples were dehydrated in a series of alcohols from 50% through to absolute and embedded in Araldite CY212. In initial trials, samples were also dehydrated in an acetone series in an attempt to minimise filament shrinkage (Page and Huxley 1963). The best results were obtained using alcohols.

Sectioning

Longitudinal sections were cut on an ultramicrotome (OM-U2, Reichert, Austria) at right angles to the long axis of the muscle fibre to reduced filament compression (Page and Huxley 1963). Semi-thin (1 μm) sections stained with Toluidine blue were used to check the orientation and progress of sectioning. Thin sections showing a silver to gold interference pattern

(80-90 nm) were picked up on 400 mesh copper grids and double-stained with uranyl-acetate and lead citrate. This method did not give sufficient contrast to observe the I filament troponin periodic repeat so grids were pre-stained with a 1% solution of $KMnO_4$ in an attempt to improve contrast. Sections were viewed under a Phillips 301B electron microscope at 80 kV and 5 micrographs per block at a magnification of x 9100 (actual magnification x 7776) were randomly photographed giving a total of 10 micrographs per fish (5 rostral and 5 caudal).

Measurement of sarcomere dimensions

Micrographs were projected directly onto the pad of a digital planimeter (Kontron Elektronic GmbH, West Germany) using a photographic enlarger (x 4). The order in which the micrographs were traced was randomised, each micrograph being identified by plate number only in order to reduce any bias on the part of the measurer. The lengths of the A-band (l_{myo}), Z-disc (l_z), I filament ($l_{act}+l_z$), M-line (l_m), crossbridge free zone (l_{cbf}) and the sarcomere length (l_{sarc}) were measured for ten randomly chosen sarcomeres on each micrograph, giving a total of 250 measurements for each muscle position (fig. 5.1). The results were expressed as the mean ± standard deviation (SD).

Statistics

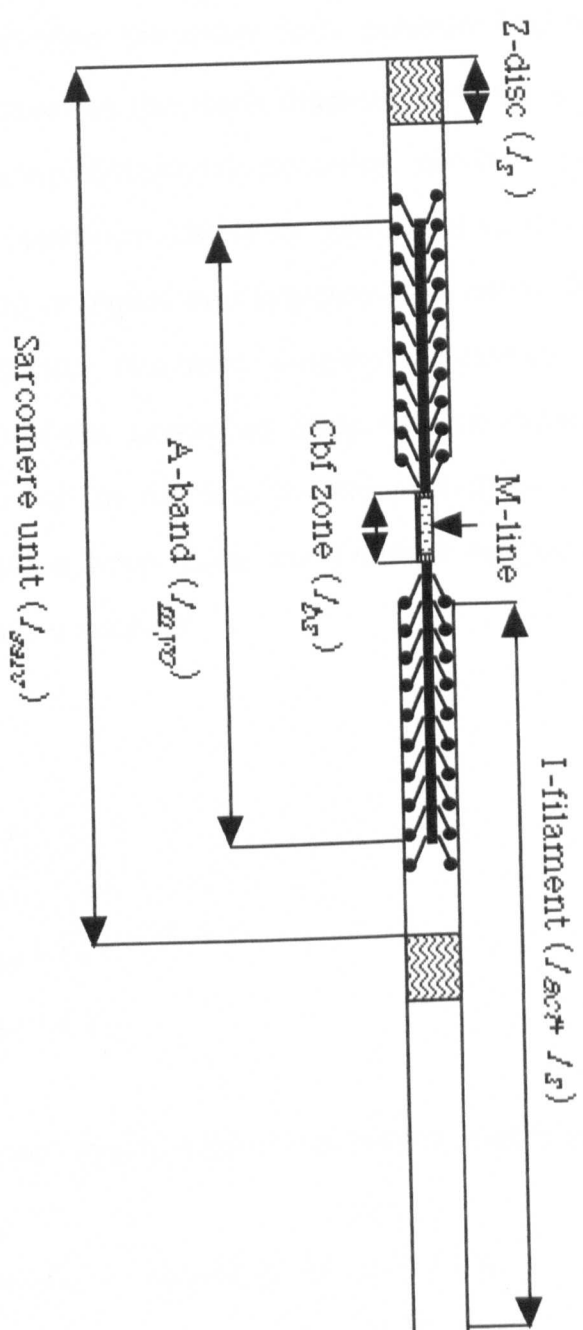All comparisons between rostral and caudal muscles were made using paired t-tests ($\alpha_{(2)} = 0.05$) (Zar 1984).

Figure 5.1

Figure 5.1

Diagram showing the sarcomere dimensions which were measured from electron micrographic plates for both rostral and caudal fast muscle samples.

Z-disc (l_Z)

M-line

A-band (l_{myo})

Cbf zone (l_{bf})

Sarcomere unit (l_{sarc})

I-filament ($l_{act} + l_Z$)

Determination of theoretical sarcomere length-tension curve

The relative force at five different sarcomere lengths was calculated after Van Leeuwen (1991) using the equations applying to design range I (where $l_{myo} \leq l_{act}$). The equations calculate the active force generated by one half of the *sarcomere sub-unit* (defined as the thick filament with the overlapping parts of the surrounding actin filaments) assuming maximal crossbridge activation under isometric conditions. The force generated in the other half of the sub-unit is assumed to be equal and opposite. Sarcomere length (fig. 5.2) was calculated from the filament lengths measured from the micrographs at (i) the base of the ascending limb; (ii) the shoulder of the ascending limb; (iii) the start of the plateau; (iv) the end of the plateau and (v) the base of the descending limb using the filament lengths measured from both rostral and caudal sarcomeres:

(i) $l_{sarc} = l_{min}$ (5.2)

(ii) $l_{sarc} = l_{myo} + l_z$ (5.3)

(iii) $l_{sarc} = l_{act} + l_z$ (5.4)

(iv) $l_{sarc} = l_{act} + l_{bz} + l_z$ (5.5)

(v) $l_{sarc} = l_{myo} + l_{act} + l_z$ (5.6)

The theoretical <u>active</u> force (F_{Ta})at a given sarcomere length is given by:

(a) $F_{Ta} = f_o \lambda. [(l_{myo} - l_{bz}) - D_{act}.(l_{act} - (l_{sarc} - l_z))$

$- D_{myo}.(l_{myo} - (l_{sarc} - l_z))] / 2$ for (i) (5.7)

(b) $F_{Ta} = f_o \lambda. [(l_{myo} - l_{bz})$

$- D_{act}.(l_{act} - (l_{sarc} - l_z))] / 2$ for (ii) (5.8)

Figure 5.2

Figure 5.2

(a) Theoretical sarcomere length-tension diagram indicating the points (1-5) for which active force and sarcomere length were calculated from sarcomere measurements of rostral and caudal fast muscle fibres. (b) Pictorial representation of sarcomere length, showing the degree of filament overlap at the points numbered 1-5 in (a).

l_{min}

1

$l_{myo} + l_z$

2

$l_{act} + l_z$

3

$l_{act} + l_{bz} + l_z$

4

$l_{myo} + l_{act} + l_z$

5
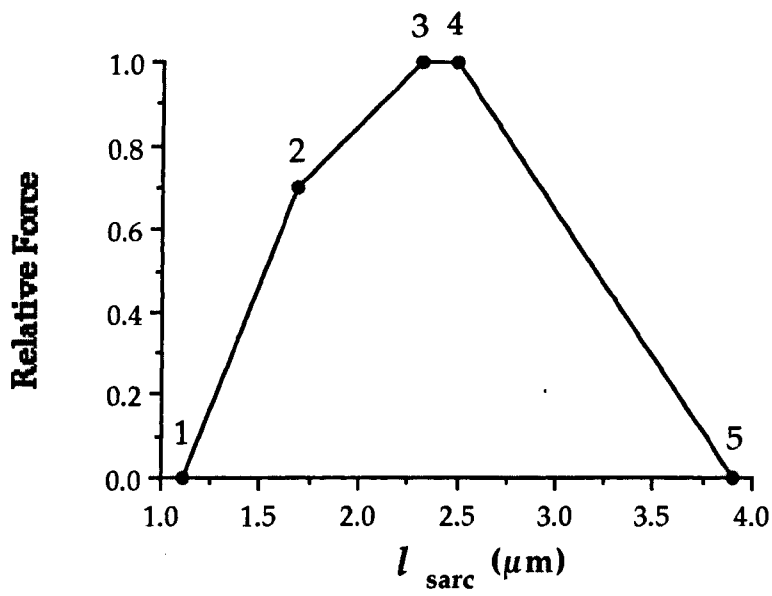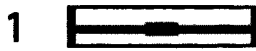
(c) $F_{Ta} = f_0 \cdot \lambda \cdot (l_{myo} - l_{bz})/2$ for (iii) & (iv)   (5.9)

(d) $F_{Ta} = f_0 \cdot \lambda \cdot [l_{myo} + l_{act} - (l_{sarc} - l_z)]/2$ for (v)   (5.10)

Where:

f_0 = the average crossbridge force under the specified conditions (taken to be 4.3 pN; Van Leeuwen 1991)

λ = the number of myosin heads on one half of the filament (calculated from measured filament lengths assuming 187 myosin heads per μm (Offer 1987, cited in Van Leeuwen 1991)).

D_{act} and D_{myo} correct for crossbridge losses due to overlap of the actin filament and collision of the myosin filament with the z-disc and are assigned the values 0.68 and 1.9 respectively (Van Leeuwen 1991).

The parts within square brackets in equations 5.7 to 5.10 represent the *filamentary overlap function.*

Passive forces at short sarcomere lengths due to the interference to crossbridge formation by both actin filament overlap and the collision of the myosin filament with the Z-disc oppose the active force and must be subtracted. These are given by:

$$F_{Tpas} = [-C_{act} \cdot (l_{act} - (l_{sarc} - l_z))$$
$$- C_{myo} \cdot (l_{myo} - (l_{sarc} - l_z))]/2 \text{ for (i) and}   (5.11)$$

$$F_{Tpas} = C_{act} \cdot [l_{act} - (l_{sarc} - l_z)]/2 \text{ for (ii)}   (5.12)$$

C_{act} is taken to be 0 and $C_{myo}/(f_0 \cdot \lambda) = 0.44$ and account for resistive forces due to actin and myosin filaments at short sarcomere lengths respectively.

The theoretical maximum force (F_{To}) occurs at the plateau of the length-tension curve and is given by:

$$F_{To} = f_o.\lambda.(l_{myo} - l_{bz})/2 \qquad (5.13)$$

allowing the calculation of relative active force:

$$F_{Ta}^* = (F_{Ta} - F_{Tpas})/F_{To} \qquad (5.14)$$

The optimum sarcomere length for force production is given by:

$$l_{Tosarc} = 0.5 l_{bz} + l_{act} + l_z \qquad (5.15)$$

and the peak tension at l_{osarc} in $kN.m^{-2}$ was calculated using:

$$P_{To} \text{ at } l_{Tosarc} = [((4.3 \times 10^{-12}.\eta_{acb})/(A_{ss}.1000)).1 \times 10^{18}].M_f \qquad (5.16)$$

where η_{acb} = number of attached crossbridges in overlap region in one half of the thick filament (calculated from measured filament lengths assuming 187 crossbridges/ μm)

A_{ss} = cross-sectional area occupied by one thick filament bounded by the centres of its associated actin filaments (taken to be 1750 nm^2; Van Leeuwen 1991)

M_f = myofibrillar fraction per muscle fibre cross-sectional area [assumed to be approximately 0.80 (Dogfish = 77.8%, Bone *et al.* 1986; *Notothenia neglecta* = 86.3%, Camm and Johnston 1985)]

5.3. Results

Experimental length-tension curves

Isometric force showed a strong dependence on sarcomere length in both rostral and caudal muscle fibres (fig. 5.3 - solid curves). Force output at a

Isometric force showed a strong dependence on sarcomere length in both rostral and caudal muscle fibres (fig. 5.3 - solid curves). Force output at a given sarcomere length was highly reproducible during an experiment and typical traces for rostral fibres at sarcomere lengths of 2.1 μm, 2.3 μm and 2.7 μm are presented in fig. 5.4 (a-c). The caudal length-tension curve was offset to lower sarcomere lengths by approximately 0.10 μm in comparison to the rostral curve above 2.1 μm (fig. 5.3).

A steep ascending limb was followed by a narrow plateau, which was less distinct in caudal than in rostral fibres. At short sarcomere lengths, the laser diffraction pattern was frequently disrupted resulting in a lack of data points for the ascending limb.

The form of the descending limb was linear between 2.7 to 3.1 μm, in agreement with the sliding filament hypothesis (Gordon *et al*.1966*b*). Rostral and caudal peak forces declined from around 2.65 μm and 2.5 μm respectively at a rate of 64%.μm^{-1}, with force reduced to zero (by extrapolation) at 3.6 μm and 3.54 μm respectively (fig. 5.3).

The optimum sarcomere length in rostral fibres (where peak force was maximal) was 4% longer than in caudal fibres ($p < 0.05$; paired t-test) but the mean isometric force at these lengths was the same (table 5.1). Greater than 80% of maximum active force was generated over a potential sarcomere excursion of $\pm$ 9.5 - 10.6% l_{osarc}, reducing to 4.2 - 5.3 % when isometric force was $\geq$ 90% of F_o (table 5.1; fig. 5.3).

Above 2.4 μm, a decrease in relaxation rate was observed. HFT increased by 74 and 88% for rostral and caudal fibres respectively between 2.4 μm and 3.0 μm, while HPT reduced slightly over the same range (fig. 5.5a). Passive force (F_{pas}; resting tension) also increased at lengths above 2.4 μm, reaching approximately 100% of maximum active force at 3.2 μm (fig. 5.5.b).

Figure 5.3

Figure 5.3

Sarcomere length-tension diagrams comparing curves determined experimentally (solid lines. Symbols: ● rostral, ▢ caudal) and theoretically (dashed lines; Symbols: ▲ rostral, △ caudal) using measurements of sarcomere geometry. Experimental curves in (a) and (b) are the same (mean ± SEM (n = 9)). Theoretical curves were calculated using filament lengths uncorrected for shrinkage (a) and corrected for shrinkage (b).

a.

Uncorrected

b.
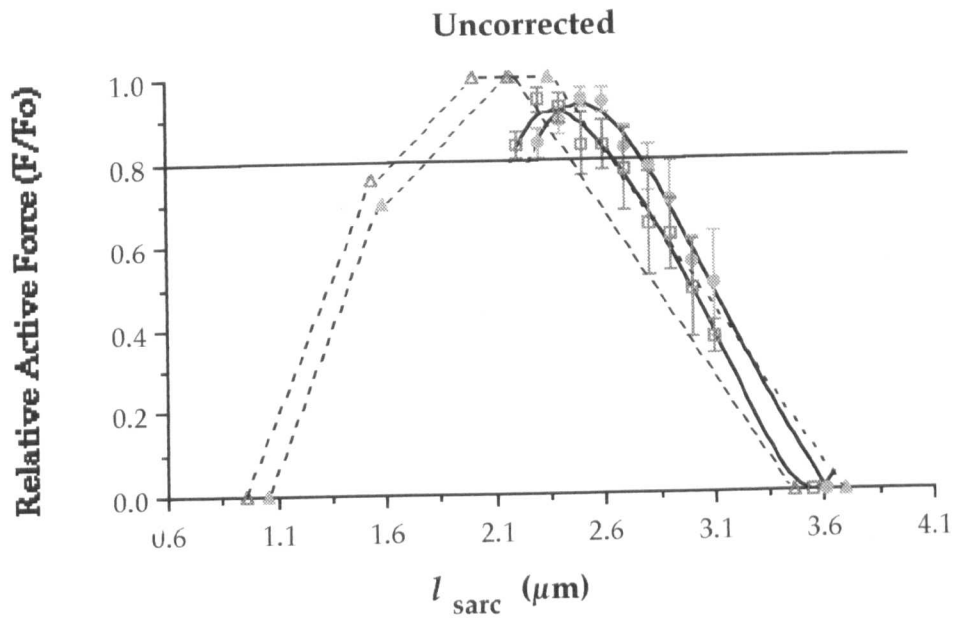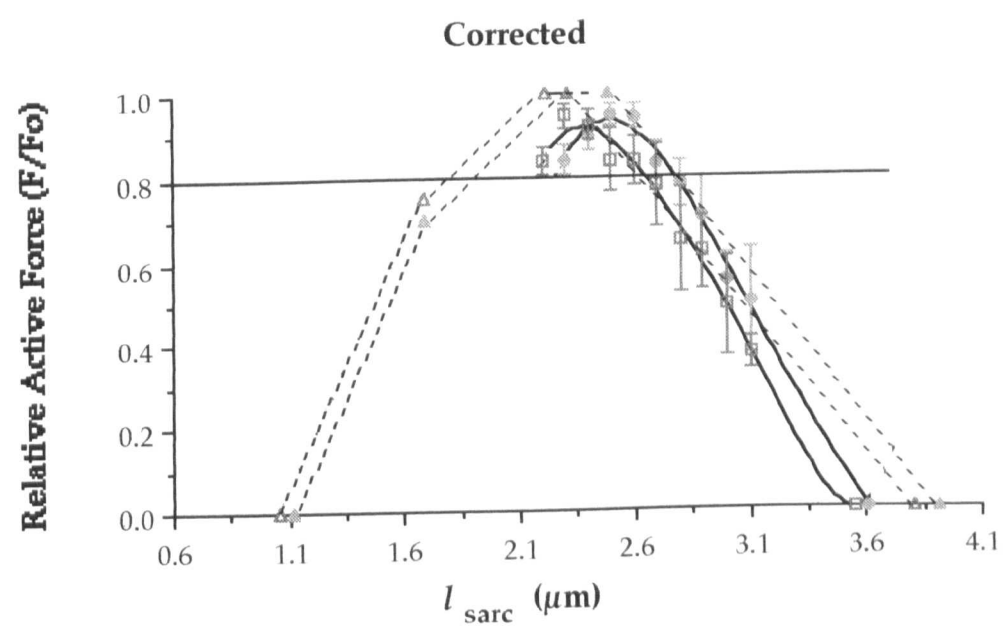
Corrected

Figure 5.4

Figure 5.4

Force output of rostral muscle fibres at sarcomere lengths of (a) 2.1 μm ; (b) 2.3 μm and (C) 2.7 μm. Diagrams showing the filament overlap at these respective sarcomere lengths were constructed using corrected sarcomere measurements (d to f).

a.

b.

c.

2.1μm

2.3μm

2.7μm

2 mN

80 ms

d.

e.

f.
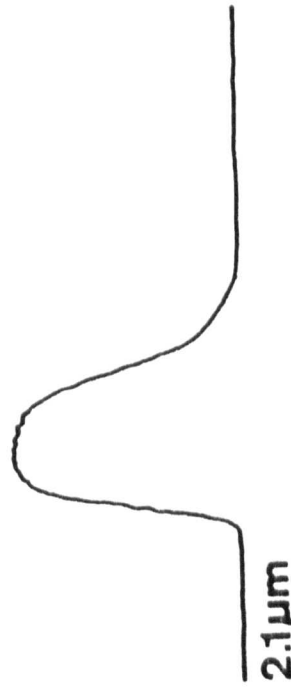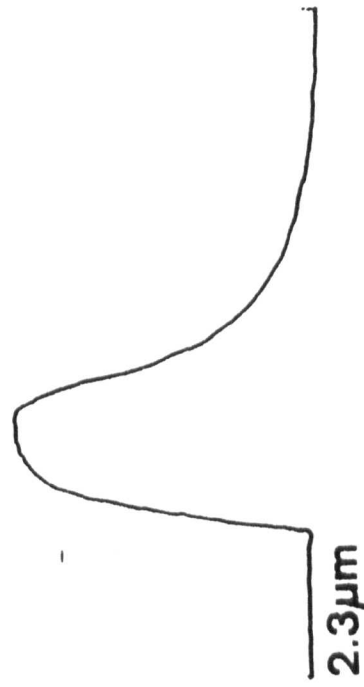
1 μm

Figure 5.5

Figure 5.5

(a) Change in half-time to peak tension (HPT) and half-time to relaxation (HFT) with sarcomere length in rostral and caudal muscle fibres. F_{pas} first appears at 2.4 μm. Values = mean ± SEM (n = 9). Symbols: ● rostral HPT; ■ caudal HPT; ○ rostral HFT; □ caudal HFT. (b) The effect of increasing sarcomere length on passive force (F_{pas}) as proportion of active force.

a.
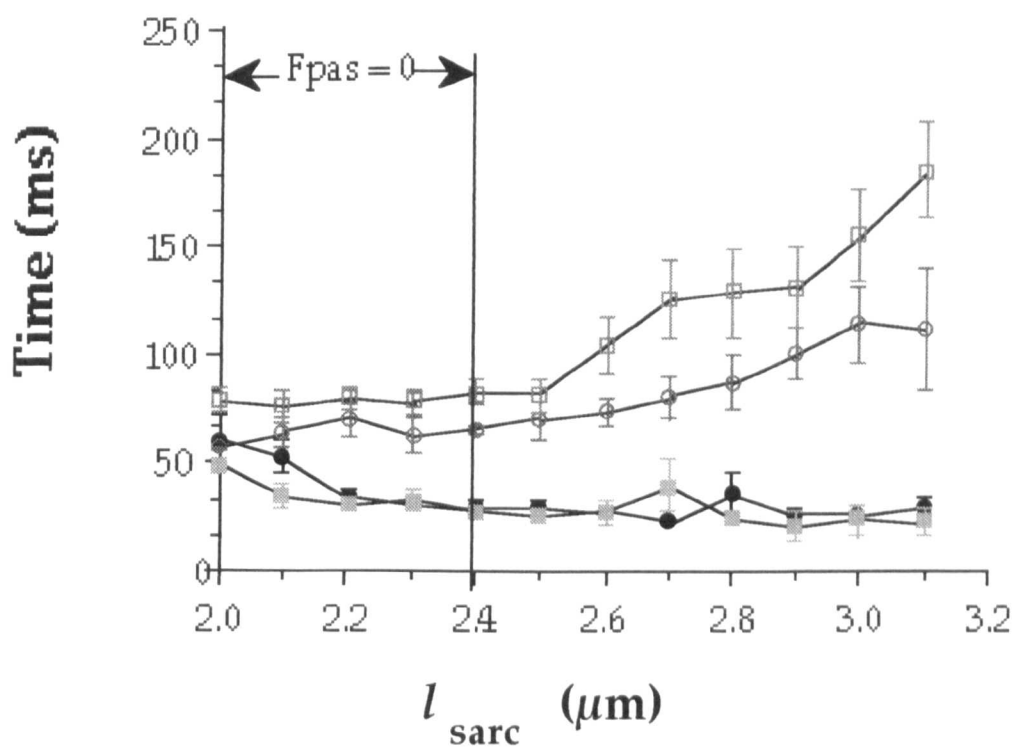
b.
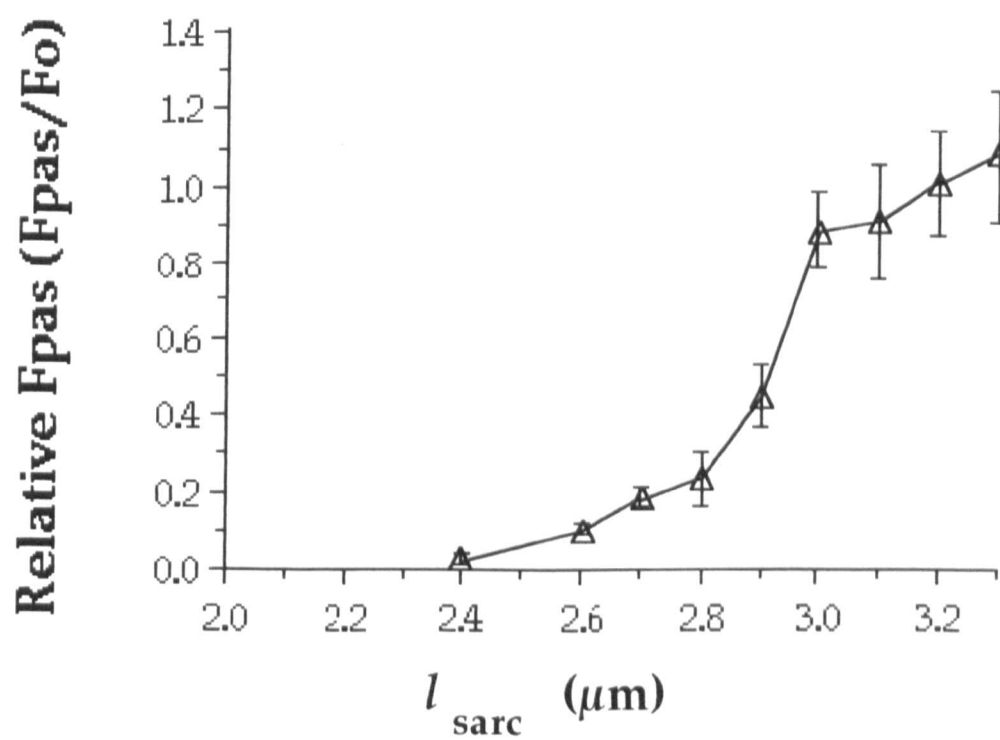
Sarcomere geometry

There was no significant difference between rostral and caudal fibres in any of the sarcomere components that were measured (paired t-test; $p > 0.05$). Good structural definition was achieved (fig. 5.6) but several different approaches failed to clearly reveal the 38.5 nm troponin repeat. A myosin length of 1.6 μm was therefore used as a reference to estimate filament shortening. Total thick filament shrinkage was estimated to be 6% and 10.4% in rostral and caudal muscle samples respectively (table 5.2); all measurements were then assumed to have shortened by a similar amount and were corrected accordingly (table 5.2). Z-disc widths compared well to those in the literature (table 5.3) but the length of the crossbridge free zone (0.171-0.174 μm) was closer to that reported for human muscle (0.17 μm; Walker and Schrodt 1973) than for fish fast (0.14 μm; Akster, Granzier and ter Keurs 1984) and slow muscle (0.124 to 0.145 μm; Van Leeuwen et al. 1990).

Fish actin filament lengths quoted for a variety of muscle fibre types ranged from 2(0.80) to 2(0.99) μm (table 5.3) which was on average only 80 to 84% of that found in sculpin muscle fibres after correction for shrinkage (table 5.3). The mean ratio of l_{myo}/l_{act} was 0.72 for rostral and 0.76 for caudal sarcomeres - 8.9 and 3.8% less respectively than the average values for fish fast fibres (0.79; table 5.3).

Prediction of the length-tension curve

The sarcomere length-tension relationship for rostral and caudal muscle fibres was calculated using both uncorrected and corrected filament lengths

Figure 5.6

Figure 5.6

Electron micrograph of longitudinal section of rostral fast muscle fibres. LS = sarcomere; A = A-band; I = I filament; M = M-line; Z = Z disc and Cbf = cross-bridge free zone. Scale bar = 1 μm.
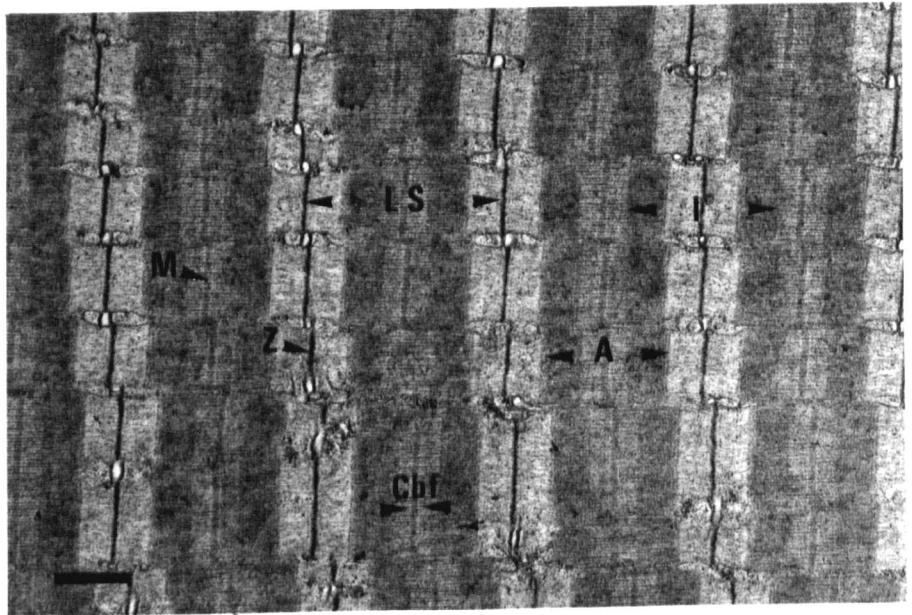
(figs. 5.3a & b - dashed lines). It was noticeable that the ascending limb of these 'theoretical' curves extended to much shorter sarcomere lengths than the experimental curves, increasing the total length range over which force was generated from 1.6 μm to approximately 2.5 μm (fig. 5.3). The corrected curves agree closely to the experimental curves between sarcomere lengths of 2.1 and 3.1 μm but diverge at longer sarcomere lengths (fig. 5.3b). The uncorrected curves are offset to lower lengths and only agree with the experimental curves between 3.1-3.6 μm (fig. 5.3a).

Diagrams of the filament overlap at sarcomere lengths corresponding to the force recordings in figures 5.4 a-c were constructed using the corrected sarcomere measurements for rostral fibres (figs. 5.4 d-f). At 2.1 μm (the top of the ascending limb) the actin filaments are beginning to overlap, causing the active force to drop below maximum (fig. 5.4 a & d). At 2.3 μm (on the plateau), force is maximal as all of the crossbridges have unimpeded access to an actin binding site (fig. 5.4 b & e). As the sarcomere is lengthened further to 2.7 μm (the top of the descending limb), the central crossbridges remain unattached during activation and force is once again sub-maximal (fig. 5.4 c & f).

The longest sarcomere length for which active force was $\geq$ 80% of F_o in rostral or caudal fibres was the same for both corrected and experimental curves (table 5.1) and differed by less than 1% when force was $\geq$ 90% F_o. By comparison, active force declined below 80% in the uncorrected curves when sarcomere was 6-8% shorter than those derived experimentally. Since the lower part of both theoretical curves extended to lower sarcomere lengths than the experimentally determined curves, the theoretical potential sarcomere excursion range where force was greater than 80 or 90% of F_o was double that obtained experimentally (table 5.1).

Table 5.1

Table 5.1

Summary of the potential strain at ≥ 80 and 90% of F_0 (derived from figure 5.3), the optimum sarcomere length for force production and the peak tetanic tension at this length for rostral and caudal muscle fibres derived both theoretically and experimentally. Where applicable, values displayed as mean $\pm$ SEM. l_{sarc} at ≥ 80 and 90% of F_0 displayed as minimum-maximum (range).

		Position	
		Rostral	Caudal
Experimental	l_{sarc} F80 (μm)	2.28-2.80 (0.52)	2.20-2.65 (0.45)
	Strain ($\pm\% l_{osarc}$)	10.6	9.5
	l_{sarc} F90 (μm)	2.40-2.66 (0.26)	2.30-2.50 (0.20)
	Strain ($\pm\% l_{osarc}$)	5.3	4.2
Theoretical			
Uncorrected	l_{sarc} F80 (μm)	1.75-2.65 (0.90)	1.60-2.45 (0.85)
	Strain ($\pm\% l_{osarc}$)	19.8	20.4
Corrected	l_{sarc} F80 (μm)	1.85-2.80 (0.95)	1.75-2.65 (0.90)
	Strain ($\pm\% l_{osarc}$)	19.8	19.6
Uncorrected	l_{sarc} F90 (μm)	1.95-2.50 (0.55)	0.83-2.35 (0.52)
	Strain ($\pm\% l_{osarc}$)	12.1	12.5
Corrected	l_{sarc} F90 (μm)	2.10-2.65 (0.55)	2.00-2.48 (0.48)
	Strain ($\pm\% l_{osarc}$)	11.5	10.4
Experimental	l_{osarc} (μm)	2.45 ± 0.05	2.33 ± 0.03
Theoretical			
Uncorrected	l_{Tosarc} (μm)	2.27	2.08
Corrected	l_{Tosarc} (μm)	2.39	2.29
Experimental	P_o at l_{osarc} (kN.m^{-2})	161.9 ± 5.66	158.2 ± 6.89
Theoretical			
Uncorrected	P_{To} at l_{osarc} (kN.m^{-2})	248.0	238.6
Corrected	P_{To} at l_{osarc} (kN.m^{-2})	262.0	262.6

Table 5.2

Table 5.2

Geometric measurements of rostral and caudal sarcomeres both before and after correction for shrinkage (using myosin length of 1.6 μm). Values are mean $\pm$ SD ($n = 250$ for each muscle position).

	Uncorrected Lengths (μm)		Corrected Lengths (μm)	
	Rostral	Caudal	Rostral	Caudal
l_{myo}	1.51±0.05	1.45±0.07	1.60	1.60
l_{act}	2.10±0.22	1.92±0.08	2.29±0.22	2.12±0.19
l_z	0.079±0.009	0.084±0.009	0.083±0.01	0.092±0.01
l_m	0.083±0.002	0.083±0.010	0.088±0.001	0.092±0.01
l_{cbf}	0.164±0.01	0.155±0.02	0.174±0.01	0.171±0.02
l_{sarc}	2.82±0.37	2.18±0.49	2.98±0.38	2.39±0.48
l_{myo}/l_{act}	0.72±0.07	0.76±0.07		
% Shrinkage	5.96±3.84	10.35±5.74		

Table 5.3

Table 5.3

Filament lengths reported for fast and slow muscles of different fish species (mean ± SD where appropriate).

a) **Present study.** Values presented as uncorrected (corrected).

b) **Sosnicki et al. 1991.** Method: (i) Fibre bundles stretched, tied to wooden rods and then fixed in 2.5% glutaraldehyde, post-fixed with 1% OsO_4 and dehydrated in acetone. (ii) Fibres fixed *in situ* with 3% glutaraldehyde (acetate buffer), post-fixed in 2% OsO_4 and dehydrated in ethanol to preserve troponin periodicity. † = corrected for shrinkage using 38.5 nm troponin periodicity (estimated to be 3.1% and 1.3% for fast and slow actin filaments respectively; n = 180). * = lengths obtained from negatively stained isolated filaments (n = 41).

c) **Van Leeuwen et al. 1990.** Method as in c. Corrected using 38.5 nm troponin periodicity (n = 7, 7, 9 and 5 for positions one to four respectively).

d) **Akster 1985.** Perch m. hyohyoideus superior (MHS). Method: Fibres fixed *in situ* with Karnovsky's for 1 h, dissected and placed in fresh Karnovsky's for 12-19 h, then post-fixed for 2 h in OsO_4 (unknown concentration) and dehydrated (solvent unknown). Corrected for shrinkage using 39 nm troponin periodicity (n = 19).

e) **Akster 1981.** Axial muscle and levator operculi anterior (LOP). Method: Fibres fixed *in situ* with Karnovsky's, dissected and placed in fresh Karnovsky's overnight, post-fixed in 2% OsO_4 and dehydrated (solvent unknown); results not corrected for shrinkage. Values taken from fig. 10: n = 19 and 16 (slow) and 15 and 14 (fast) for opercular and axial fibres respectively.

f) **Akster et al. 1984.** Hyohyoid (HH) and levator operculi anterior (LOP). Fibre bundles fixed after length tension curve measured; fixation method is unknown but results corrected for shrinkage using troponin periodicity (n = 15).

Sarcomere Dimensions (μm)

		Slow Muscle			Fast Muscle		
		Actin/2	Myosin	Z-disc	Actin/2	Myosin	Z-disc
M. scorpius [a]	Axial: 0.35 L_s				1.05(1.11)	1.51(1.60)	0.08(0.08)
	0.90 L_s				0.96(1.06)	1.51(1.60)	0.08(0.09)
C. carpio [b]	Axial	0.96†	1.52±0.009	0.10±0.003	0.97†	1.50±0.037	0.08±0.002
C. carpio [c]	Axial: 0.33 L_s	0.88	1.53±0.08	0.094±0.01	0.99±0.02*	1.56±0.03*	
	0.50 L_s	0.86	1.58±0.10	0.091±0.01			
	0.70 L_s	0.86	1.44±0.14	0.088±0.01			
	0.88 L_s	0.89	1.59±0.06	0.072±<0.01			
C. carpio [d]	MHS	0.95	1.72	0.10±0.03			
P. fluviatilis [e]	LOP	0.95	1.30		0.85	1.31	
	Axial	0.80	1.30		0.80	1.31	
[f]	LOP	1.19±0.11	1.40±0.07				
[f]	HH				0.85±0.04	1.31±0.06	0.13±0.01

The theoretical values for l_{osarc} determined using corrected measurements were 94% and 98% of the experimental rostral and caudal values respectively (table 5.2). Predicted peak tensions at l_{osarc} were 6-10% greater using corrected as opposed to uncorrected filament lengths but mean experimental peak tensions were only 61% of the corrected theoretical values (table 5.1). The observed similarity of rostral and caudal tensions was predicted using corrected filament lengths but caudal peak tensions were 4% lower than rostral when uncorrected filament lengths were used (table 5.1).

5.4. Discussion

The length-tension relationship

The shape of the length-tension relationship between 2.1 to 3.1 μm in sculpin fast muscle fibres corresponds well to that predicted by filament overlap (fig. 5.3b). Rostral fibres produced relatively more force than caudal fibres at a given sarcomere length but the maximum peak tension at respective optimum sarcomere lengths was the same in both fibre groups (fig. 5.3b; table 5.1). A simple sarcomere model was found to reproduce these results if the thick filament and the crossbridge free zone lengths were the same in rostral and caudal muscle fibres (see equation 5.13) while rostral actin filament length was 8% greater (fig. 5.3b; table 5.2).

Experimental peak tensions measured at l_{osarc} were only 61% of those calculated from the sarcomere model (table 5.1). The mean tetanic P_o at l_{osarc} for rostral fibres (10°C acclimated sculpin) was intermediate to those found for fibres isolated from 5 and 15°C acclimated sculpin (Beddow 1993) suggesting that mechanical performance of the muscle fibres in this study

was within the range expected from previous results. Sub-maximal activation of some or all of the isolated muscle fibres would result in reduced peak tensions. Damage to the motoneurone end-plates of external fibres during dissection (Johnson, Altringham and Johnson 1991) or a reduction in fish condition following acclimation (e.g. Beddow 1993) reduces the degree of fibre activation and could account for sub-maximal performance in isolated fibres.

Alternatively, theoretical peak tensions may be overestimated as the model used to calculate peak tension in this study is simplistic. Only the interaction between a single thick filament and its surrounding overlap of thin filaments is considered assuming maximal activation with zero inter-filamentary velocity. These conditions may not be fulfilled during an experiment. Theoretical peak tensions would be overestimated if:

(i) the force generated per crossbridge was less than 4.3 pN.

(ii) the number of attached crossbridges at any one time were less than the total possible. Theoretical and experimental peak tensions would be the same, if only 60% of the crossbridges were attached at any one time during activation.

(iii) the myofibrillar content of sculpin fast fibres was less than 80%.

(iv) the contractions were not truly isometric (i.e. interfilamentary velocity $\neq$ 0). Muscle fibres could shorten slightly during a fixed-end contraction at the expense of in-series compliant elements. The force-velocity relationship for sculpin fast fibres suggests that a mean shortening of 0.1 muscle lengths.s^{-1} would depress peak force to approximately 0.8 P_o (see figure 4.1b and Hill 1951).

The form of the ascending limb determined experimentally would not have accurately represented the mechanical ability of sculpin fibres as the

curves for bundles of muscle fibres isolated from the rat and perch also show a lack of points for the ascending limb, suggesting that this problem is commonly encountered for this type of muscle preparation (Akster *et al.* 1984; ter Keurs *et al.* 1984). Therefore, it is not known how accurately that the model predicts the length-tension relationship at shorter sarcomere lengths.

Above l_{osarc}, the length-tension relationship determined using intact fibre bundles often shows more force at a given length than would be expected on the basis of filament overlap (e.g. ter Keurs *et al.* 1984; Phillips and Woledge 1992) - curves determined using single fibres are generally closer to theoretical predictions by comparison (e.g. Gordon *et al.* 1966*b*). Sculpin fast fibres did not demonstrate more <u>relative</u> force than predicted above l_{osarc} and produced less force at the longest sarcomere lengths (fig. 5.3b). Passive forces first occurred at shorter sarcomere lengths (2.4 μm, fig. 5.5b) in comparison to those found for bundles of rat EDL fibres (approximately 3.2 μm; ter Keurs, Luff and Luff 1984) and rose steeply to 100% of l_{osarc} at around 3.2 μm. As this passive force component acts in opposition to the active force during a contraction, high passive forces may account for the deviation of the experimental and theoretical curves at long sarcomere lengths. The source of this force is likely to be the extension of tendons and other elastic elements, despite the care taken to reduce such components during the preparation of the fibre bundle.

Relaxation times increased significantly as sarcomere length increased in accordance with the findings of Jewel and Wilkie (1960), despite a concomitant increase in passive forces acting to extend the fibre (fig. 5.5a). It is possible that at long sarcomere lengths there is an effect on the rate of calcium uptake, or an increase in troponin calcium affinity, as found in

isolated cardiac cells, which would tend to prolong muscle relaxation (e.g. Hibberd and Jewell 1982; Fabiato and Fabiato 1978).

Accuracy of filament length measurements

Slow axial muscles isolated from four positions along the trunk of the carp did not demonstrate a difference in thick and thin filament lengths (Van Leeuwen *et al.* 1990) supporting the findings here for fast fibres. Thick filament lengths, Z-disc widths and the length of the crossbridge free zone concurred well with the range previously reported for fish muscles, but actin filaments were found to be 10 to 15% longer than the average of previously reported values (table 5.3).

The precise amount of shrinkage that occurs during preparation of muscle samples for electron microscopy is difficult to standardise and will depend on a wide variety of factors. Even the same authors can give widely different results for filament lengths for the same muscle type in the same species prepared in a similar way (e.g. table 5.3; Akster 1981; Akster *et al.* 1984). Thick filament shrinkage in sculpin muscle fibres was estimated to be 6 to 10% when compared to a myosin reference length of 1.6 μm (table 5.2) but as thick and thin filament shrinkage during processing may vary (e.g. Page and Huxley 1963), using thick filament length as a reference for actin filament shrinkage may result in the miscalculation of actin filament length. In mouse muscle, myosin-corrected and troponin-corrected actin filament lengths were found to differ by 3.5% (Phillips and Woledge 1992) showing that only a small error may be introduced by the former method. An actin filament of 5-6% (compared to isolated filament lengths) was found using a double fixation method similar to the one employed in this study in the axial

muscle of the carp (Sosnicki *et al.* 1991). The similarity of this shrinkage estimate to that found for sculpin muscle suggests that the measurements presented here are likely to be reasonable estimates of the sarcomere geometry in sculpin fast fibres.

Estimated 'shrinkage' will also include errors due to the deviation of the sectioning plane from longitudinal and measurement error. The contribution of these to total shrinkage will be less than the effects of processing: a 10° deviation from the longitudinal during sectioning (from basic trigonometry) results in an apparent shrinkage of 1.5% while measurement error (calculated as in chapter 3) was found to be less than 2% for both actin and myosin filament lengths (fig. 5.7). Measurement error rose to around 10% for distances equivalent to the Z-disc, M-line and crossbridge free zone but the large sample size, small standard deviation and good correlation with previously reported values give confidence in the precision of these estimates (fig. 5.7; table 5.2).

The ratio of thick and thin filament length (l_{myo}/l_{act}) will determine the range of strains over which power output is optimal - the value of 0.80 is typical for many small vertebrates (Van Leeuwen 1991). Using a modelling approach, Van Leeuwen (1991) found that the ratio of l_{myo}/l_{act} for maximal power output increased with decreasing strain, a finding which supported by the relatively high ratios found in sculpin fast muscles and fish axial muscles in general, where excursion amplitude is generally small (Van Leeuwen 1991; Alexander 1969).

Figure 5.7

Figure 5.7

Change in coefficient of variation (V) with object length.
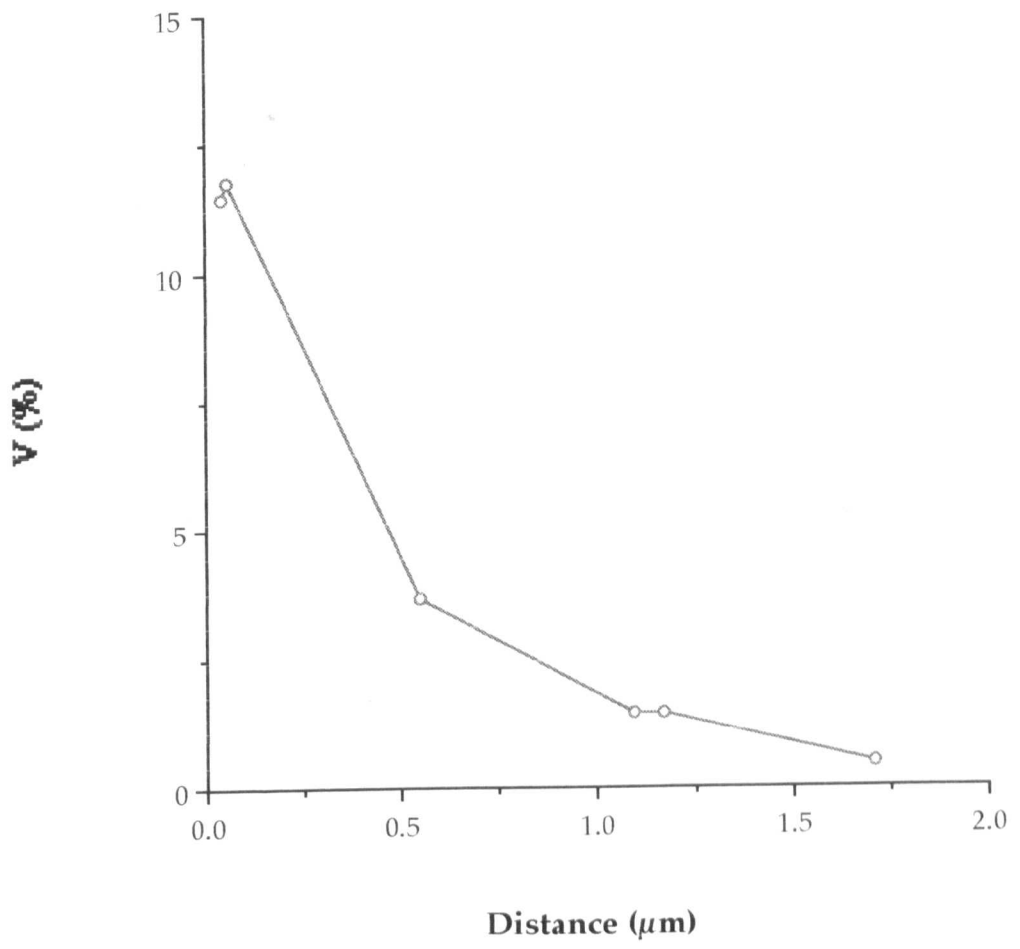
Power output during swimming - are filament lengths optimal?

The length-tension curve provides information about the performance of isolated sculpin fibres under static conditions but under the conditions found during swimming, muscle sarcomere length is constantly changing. Under these dynamic conditions, force output at a specific sarcomere length will strongly depend on both the direction and velocity of muscle strain.

In fish, sarcomere excursions during swimming calculated using kinematic data range from $\pm$ 1.6% to around $\pm$ 10.0% l_{0sarc} in slow and fast fibres respectively (table 5.4) while the optimum strain amplitude for power output in isolated fibre bundles under imposed sinusoidal strains generally ranges from 3-5% (table 5.4). Sculpin rostral and caudal fast fibres generate $\geq$ 80% of maximum tetanic force under isometric conditions within the range of sarcomere lengths occurring during swimming and $\geq$ 90% within the optimum excursion range for isolated fibres (tables 5.1 and 5.4). The strains which occur *in vivo* are thus limited to the regions of filament overlap where force output is potentially high. Since maximum shortening velocity is independent of sarcomere length over the same range (Edman 1979), power output for a given strain rate and amplitude will remain relatively constant.

The complex orientation of fast fibres results in equal shortening within an individual myotome for a given bend of the spine (Alexander 1969). Due to the mechanical advantage conferred by this arrangement, fast fibres only have to shorten approximately 25% of the amount shortened by the parallel oriented slow fibres to produce a given backbone curvature, allowing them to operate at higher strain rates (Alexander 1969). Sarcomere excursion in fast muscle fibres measured during swimming powered by slow muscle are indeed approximately one quarter of that of slow fibres - around $\pm$ 1.65 % compared

to 5% (Leiber *et al.* 1992) while slow fibres can experience a shortening of up to 20% during burst swimming (Van Leeuwen *et al.* 1990) in comparison to the 5-7% undergone by fast fibres (table 5.4). However, <u>within</u> their respective range of operating frequencies fast and slow fibres undergo similar strains (table 5.4). Since filament lengths in fish fast and slow muscle are also similar (table 5.3), fish muscle fibres of different types maintain filament overlap where force production is high to maximise power output. As swimming speed increases, power demands are met by the recruitment of fibres with faster maximum contraction velocities and different orientations designed to keep strain amplitude within the range where force output is high.

Table 5.4

Table 5.4

Muscle strains estimated using filmed sequences (kinematic), measured *in vivo* (measured) or optimised for power output under imposed sinusoidal strains of isolated fibre preparations (*in vitro*).

a. Van Leeuwen *et al.* 1990. *Cyprinus carpio.* †= Slow muscle strain during kick-and-glide manoeuvre; b. Rome *et al.* 1988. *Cyprinus carpio;* c. Rome and Sosnicki 1991. *Cyprinus carpio;* d. Altringham *et al.* 1993. *Pollachius virens* after Hess and Videler 1984; e. Rome *et al.* 1993. *Stenotomus chrysops;* f. Lieber *et al.* 1992. *Kryptopterus bicirri.* Considered to be fast muscle strain during swimming powered by slow muscle; g. Covell *et al.* 1991. *Onchorhynchus mykiss.* Mean maximum shortening during 'startle response' measured using ultrasound strain gauges surgically implanted 5mm into rostral epaxial fast muscle; h. Curtin and Woledge 1993*b. Scyliorhinus canicula;* i. Curtin and Woledge 1993*a. Scyliorhinus canicula;* j. Altringham and Johnston 1990*a. Myoxocephalus scorpius;* k. Johnston *et al.* 1993. *Myoxocephalus scorpius;* l. Altringham and Johnston 1990*b. Gadus morhua;* m. Josephson and Stokes 1989. *Carcinus maenus* - scaphognathite levator muscle; n. Josephson 1985. *Neoconocephalus triops.* Invertebrate synchronous muscle - first tergocoxal muscle (wing elevator); o. Dimery 1985. *Oryctolajus cuniculus* hindlimb; p. Cutts 1986. Wing muscles in two species of bird.

TYPE	Species	Dist. from Snout ($L_s = 1.0$)	Slow Muscle Strain ($\pm \% \, l_{osarc}$)	Fast Muscle Strain ($\pm \% \, l_{osarc}$)
Kinematic	Carp a		-4.5 to +4.0	
			-20.0†	
	Carp b	0.38-0.80	7.0	
	Carp c	0.38	6.0	6.0
		0.52	6.0	8.0
		0.68	7.5	10.5
	Saithe d	0.35	3.0	
		0.65	6.0	
	Scup e	0.29	1.6	
		0.40	2.9	
		0.54	4.8	
		0.70	5.7	
Direct	Glass catfish f			1.65
	Trout g	0.45		-9.4
		0.64		-11.2
In vitro	Dogfish h, i	Post-anal	3.5	4.5
	Sculpin j			5.0
	Sculpin k			3.0-9.0
	Atlantic Cod l			5.0
			Types unknown	
	Shore crab m		4.0	
	tettigonid n		3.0	
	Rabbit o		23.0	
	Bird p		23.0	

POWER OUTPUT OF FAST MUSCLE FIBRES ISOLATED FROM THE SHORT-HORNED SCULPIN UNDER CONDITIONS SIMULATING PREY CAPTURE EVENTS.

6.1. Introduction

Short-horned sculpin (*Myoxocephalus scorpius* L.) are sedentary marine fish which are specialised in the capture of prey by ambush. A typical prey capture event begins with a phase of stalking along the sea bed as the fish closes with its intended prey to an appropriate strike distance (e.g. 15-25 cm for fish measuring around 24 cm total length; Johnston, Franklin and Johnson 1993). The body is then bent into a preparatory S-stroke immediately followed by a propulsive stroke (a single, rapid tail beat) which accelerates the fish forwards, with extension of the jaws occurring during the final moments of approach to suck in the prey (Beddow 1993; Johnston *et al.* 1993). The mean duration of a prey strike in sculpin acclimated to 5°C was 246 and 343 ms at 15°C and 5°C respectively (total length 24 ± 2 cm; $n = 16$), with both velocity and acceleration attaining their maximum values during the propulsive stroke (Beddow, Van Leeuwen and Johnston 1995).

The work loop technique was developed to measure the power output of insect flight muscle under conditions of strain and activation approximating those experienced *in vivo* (Josephson 1985) and has subsequently been used

to study the performance of isolated fish muscle fibres under strains simulating those occurring during steady periodic swimming (Altringham and Johnston 1990*a*). To date, the power output of fish muscle fibres have been explored using this approach in relation to muscle fibre type (Altringham and Johnston 1990*b*), temperature (Johnson and Johnston 1991*a*; Johnson and Johnston 1991*b*) and body size (Anderson and Johnston 1992). Regional differences in power output for fast fibres have been documented in some species of marine fish (Chapter 2; Altringham, Wardle and Smith 1993) but in the sculpin, fibres isolated from rostral and caudal myotomes have similar contractile properties (Johnston *et al.* 1993).

Sculpin use their fast muscle almost exclusively to power unsteady swimming movements, such as prey capture events, where changes in muscle length are not sinusoidal but vary continuously in both amplitude and frequency. The aim of the present chapter was to assess the relative contributions of rostral and caudal muscle fibres to power output under strains more closely related to those found during unsteady swimming manœuvres. The experimental system enabled the mechanical performance of muscle fibres to be studied under conditions of muscle strain and activation measured from actual prey capture events. Strain sequences calculated for 0.35 L_S, 0.60 L_S and 0.93 L_S (where L_S is standard length) were used to compare rostral and caudal fibre power output. Since swimming ability and muscle contractile performance in sculpin are affected by both acute and long-term changes in temperature (Beddow 1993), swimming sequences and mechanics experiments were conducted using fish which had been acclimated to 5°C.

6.2. Materials and methods

Fish

Short-horned sculpin were caught in the Firth of Forth between May and June 1991 (swimming experiments)(total length = 24 ± 2 cm; n = 16; Beddow 1993) and April/May 1994 (mechanics experiments) and held in sea-water aquaria at ambient temperature (10°C) prior to acclimation.

For the mechanics experiments, groups of healthy, feeding fish were transferred to separate tanks and the ambient water temperature was adjusted at a rate of 1°C every two days until either 5°C or 15°C was reached (the upper and lower sea surface temperatures in the Firth of Forth; Beddow and Johnston 1995). Fish were then acclimated to their respective temperatures for 6-8 weeks prior to use. Mean standard lengths (L_s) and wet weights (W_w) of the two acclimation groups were: 5°C, L_s = 20.5 ± 0.9 cm and W_w = 315.6 ± 68.7 g; 15°C, L_s = 18.7 ± 1.3 cm and W_w = 213.2 ± 59.6 g. Photoperiod was constant throughout (12 h dark: 12 h light) and fish were fed regularly on shrimps and fish flesh.

Kinematic analysis

Prey capture sequences were filmed for a 5°C acclimated fish swimming at 5°C and 15°C and analysed at 5 ms intervals (Beddow 1993). At each interval, the outline of the fish was traced onto an acetate sheet and, after enlargement, converted in to (x,y) co-ordinates using a digital planimeter (SigmaScan, Jandel Scientific).

Strain calculation

The change in muscle strain during prey capture events was calculated for two attack sequences: one at 5°C and one at 15°C. Strains were calculated from the local curvature of the body axis, estimated from the digitised sequence of fish outlines at three points on the trunk: 0.35, 0.60 0.93 L_S (see fig. 6.1)[1].

Isolation of muscle fibres

Fast muscle fibres were isolated following the method described in Chapter 4 from rostral (0.35 L_S) and caudal (0.90 L_S) myotomes of sculpin which had been acclimated to 5 and 15°C.

Experimental Apparatus

Fibre preparations were mounted in a stainless steel chamber (5 x 1 x 1 cm) between a servo-motor and a silicon beam strain gauge (as in Chapter 2). Ringer was circulated through the chamber by a peristaltic pump (Watson-Marlow) passing through a coil of silicon rubber tubing immersed in a thermostatically controlled bath (Grant LTD 6) containing a methanol:water mixture. A second pump circulated fluid from the water bath through a metal jacket adjacent to the fibre chamber to maintain an even temperature throughout the chamber. Chamber temperature was maintained at the

---

[1] Strain sequences courtesy of Johan Van Leeuwen, University of Leiden, Netherlands; see Appendix 1 for a summary of calculations.

Figure 6.1

Figure 6.1

Strain sequences at 0.35 Ls (solid line), 0.60 L_S (short-dash) and 0.93 L_S (long-dash) calculated from attack sequences of a 5°C acclimated fish swimming at a) 5°C and b) 15°C.

a. 5°C fish at 5°C

b. 5°C fish at 15°C

Time (ms)
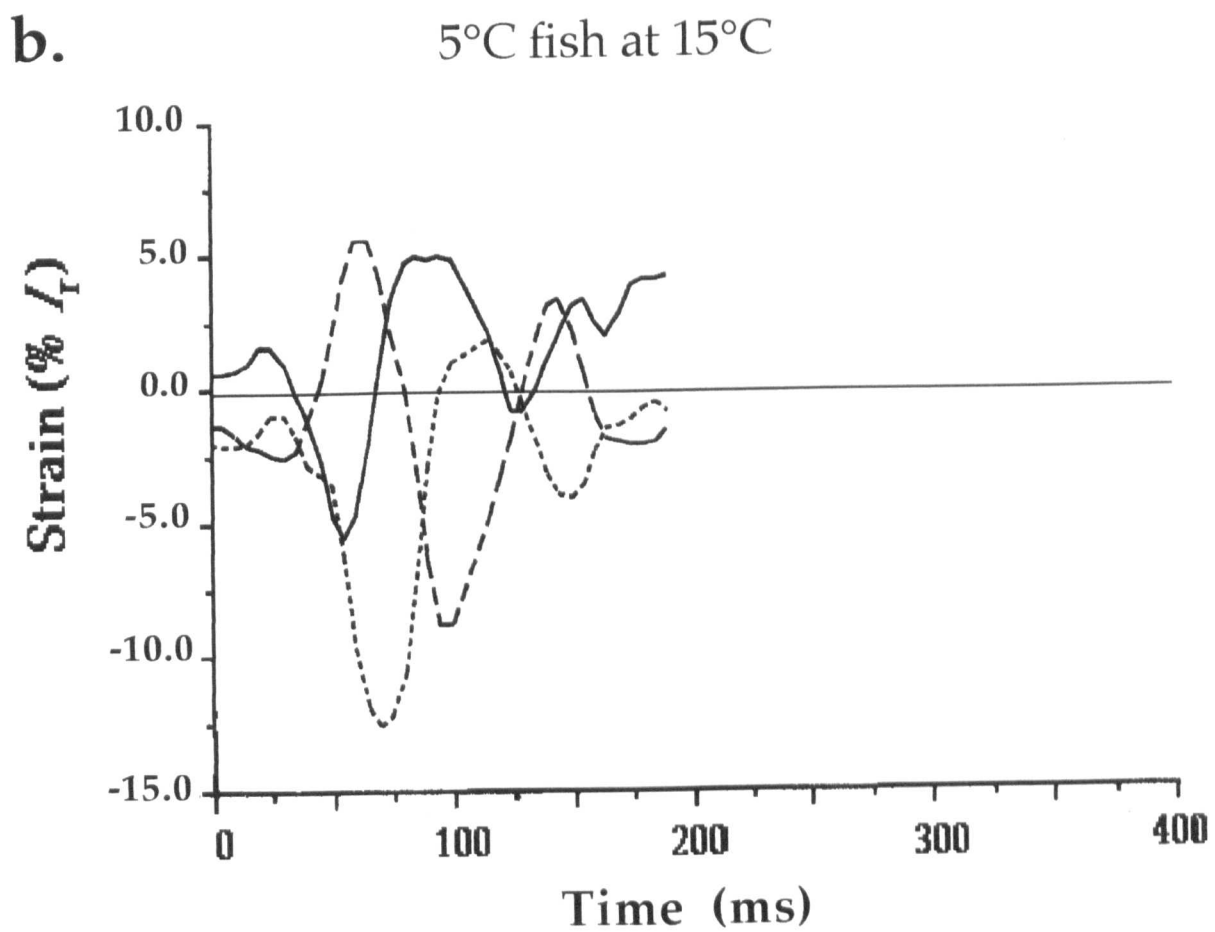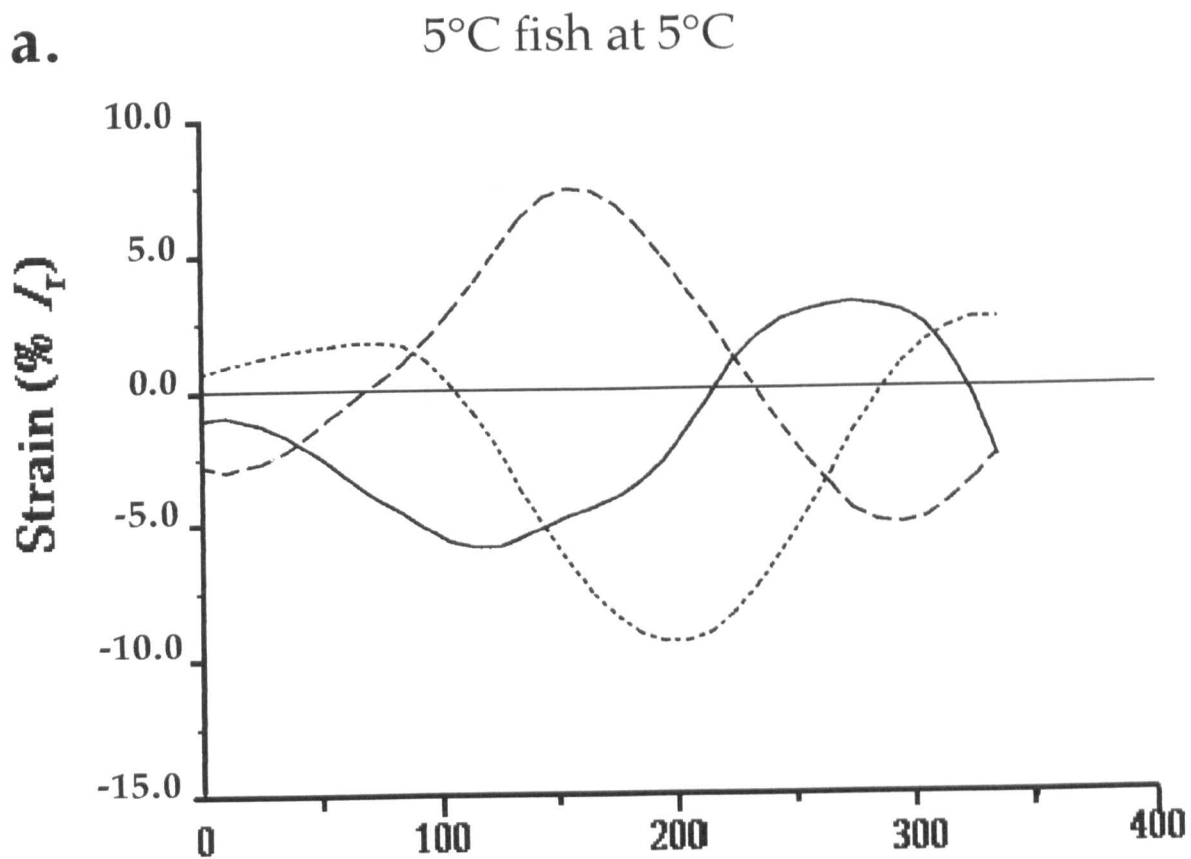
experimental temperature (5, 10 or 15°C) ± 0.1°C and was regularly checked using a thermal probe (Fissons). Ringer solution was changed every 1-2 h during the course of an experiment to compensate for increasing pH.

During *in vivo* strain (oscillatory) experiments, the amplitude and frequency of muscle oscillation and the timing and duration of the stimulus train were controlled with an in-house program run on an IBM compatible PC. The first complete cycle of each strain sequence was digitised and installed as a waveform within the program. For compatibility with the program, the start of the strain sequences at 0.35 and 0.60 L_s were extrapolated to the x axis so that the cycle would commence from fibre resting length. At 0.93 L_s, the strain sequence was digitised from the point where the fibres passed through their resting length while lengthening (i.e. offset by 180°) in order to obtain a complete cycle of muscle activity during an experiment. The 180° offset was then simply re-included in the final analysis as the muscle was not activate during this period.

Isometric contractions

Fibre length was adjusted to give the maximum isometric twitch - this length was taken as the resting length of the preparation (l_r). The optimal stimulus parameters for both isometric twitch and fused tetanus were systematically determined at 5, 10 and 15°C and the peak force (F_o) and the half-activation (HPT) and half-relaxation (HFT) times were recorded in each case (see figure 2.3).

Cyclical contractions

Rostral and caudal preparations were subjected to the abstracted strain sequences (from anterior, anal and posterior positions) about *in situ* resting length and stimulated within each cycle. The strains obtained from the sculpin attack sequence at 5°C were run at an experimental temperature of 5°C while those obtained from the 15°C attack sequence were run at 15°C (figure 6.1) - each preparation was run at both temperatures after allowing peak tetanic tension to stabilise between temperature changes. The work done during each experimental run was obtained by the numerical integration of plots of force against muscle length. The duty cycle was fixed at 25% (Johnston *et al.* 1993) and the number and frequency of stimulus pulses were optimised for work output at the initial activation phase for each position. Stimulus pulse width and amplitude were set at the optimum found for the isometric tetanus at that temperature. For each strain sequence, activation phase was defined in degrees from resting length (0°) at the start of the abstracted waveform, a full cycle being equal to 360°. From the start of the attack sequence (t = 0 ms), the activation phase was initially set at 0° (0.35 L_s), 70° (0.60 L_s) and 240° (0.93 L_s) [calculated from co-ordinated kinematic analysis and electrical recordings (EMG) during sculpin prey capture events (Johnston *et al.* 1995)] and was then systematically varied to find maximum work output. Strain amplitude (as a percentage of l_r) and cycle frequency were measured directly from strain sequences: for the 5°C event, these were 5.9%/ 3 Hz, 9.4%/ 3.4 Hz and 7.4%/ 3.6 Hz and for the 15°C event, 5.6%/ 14.5 Hz, 12.5%/7.78 Hz and 8.8%/11.56 Hz for sequences at 0.35 L_s, 0.60 L_s and 0.93 L_s respectively (fig. 6.1). As a quality control criterion, tetanic peak tension was compared both before and after a set of experimental runs at a particular

before and after a set of experimental runs at a particular temperature and before and after a temperature change. If F_o varied by more than 10%, the results were excluded from the final analysis.

Determination of cross-sectional area

The cross-sectional area (CSA) was determined following the method described in Chapter 2. The CSA and l_r associated with a particular muscle number was then installed in the computer program which returned absolute values of muscle power output (W.kg^{-1}).

Statistics

Experimental values are presented as mean ± standard error (SEM).

(i) Isometric contractile properties

Within acclimation temperature, the effect of experimental temperature (k = 3) and muscle isolation site (k=2) on isometric contractile properties was tested using a two-factor analysis of variance, with fish as replicates (H_o: $\mu_1 \neq \mu_2$; α = 0.05). Note that the effect of experimental temperature was not independent of fish (since for each fish, the effect of temperature on contractile properties was studied using the same fibre preparation at each temperature). If the null hypothesis was rejected, a Tukey multiple comparison test (Zar 1984) was used to discover between which pairs of means the differences occurred (α =0.05).

Between acclimation temperatures, a Student's t-test was used at each experimental temperature to determine which means were significantly different ($\alpha_2 = 0.05$).

(ii) Power output

The effect of muscle isolation site on power output was tested for each strain sequence using a paired t-test. If no significant difference was found between rostral and caudal fibres, their data were combined for the rest of the analysis.

Mean power output under strain sequences at 0.35 L_s, 0.60 L_s and 0.93 L_s were compared for each experimental temperature using a two-factor analysis of variance with fish (5 levels) and strain position (3 levels) as factors. If strain position had a significant effect, Tukey pair-wise comparisons were used to determine which pairs of means were statistically different (Zar 1984). Power output at each strain position was compared between experimental temperatures using a paired t-test, since the same fibre preparation was used at both temperatures. The effect of temperature acclimation on power output at 15°C was compared with a Student's t-test using the data for the 0.60 L_s strain sequence.

In all cases, the level of significance was set at $\alpha \leq 0.05$; the alternative hypothesis for t-tests and paired t-tests was $\mu_1 \neq \mu_2$. All analyses were performed using the statistical package MINITAB 8.1 (Minitab Inc., Philadelphia, USA) and Tukey tests were performed by hand.

6.3. Results

Isometric contractile properties

Fast fibres isolated from sculpin did not show regional differences in peak tension (P_O), half-time to activation (HPT) or half-time relaxation (HFT). The data for rostral and caudal fibres were therefore combined for further analysis (table 6.1). In 5°C (cold) acclimated fish, twitch and tetanic P_O were significantly reduced by a 10°C rise in temperature, declining by 70 and 55% respectively. The reduction in P_O at 15°C did not appear to be caused by thermal damage of the myofibrillar proteins as there was no significant difference between P_O measured at 5 or 10°C before and after heating the fibres to 15°C. In 15°C (warm) acclimated fish, P_O proved to be relatively temperature independent (table 6.1).

Thermal acclimation significantly affected the ability of the fibres to generate tension at each temperature (Student's t-test; $p \leq 0.05$). Fibres from warm acclimated fish consistently gave higher peak tensions than those from cold acclimated fish and this difference was observed to be temperature dependent. Fibres from warm acclimated fish generated 50% more tension at 5°C and 177% more tension at 15°C than fibres from cold acclimated fish (table 6.1). The stimulation frequency required to obtain a fused tetanus increased from approximately 70 Hz to 90 Hz between 5°C and 15°C; fibres isolated from warm acclimated fish generally required a longer pulse duration (1.5 compared to 0.8-1.0 in cold fish) to optimise isometric contractions.

Acclimation did not affect the rates of muscle activation and relaxation at 5 and 15°C (Student's t-test; ; $p \leq 0.05$). Twitch HPT, HFT and tetanic HFT were

significantly reduced by a 10°C rise in experimental temperature while tetanic HPT remained unaffected (table 6.1). The temperature coefficient (Q_{10}[5-15°C]) for the rates of activation (twitch only) and relaxation were in general between 1.6 and 1.7. Tetanic HFT in warm acclimated fish showed greater temperature dependence with a Q_{10} of 2.2 (table 6.1).

Cyclical contractions - work output

All experiments involving cyclical contractions were carried out on cold acclimated fish. Each strain sequence produced work loops of a characteristic shape - typical examples of loops for the strain sequences at 5°C are displayed in fig. 6.2. Net work output was positive in all cases (shown by the anticlockwise direction of the loops). The amplitude of shortening for strain sequences at 0.60 and 0.93 L_s was over twice that at 0.35 L_s (figure 6.1): at 5°C, shortening from maximum fibre extension (as a % l_r) was 5.7%, 11% and 12.5% while at 15°C, shortening was 7.4%, 14% and 14.8% for 0.35, 0.60 and 0.93 L_s respectively. Within the defined duty cycle of 25%, variations in pulse number and frequency had little effect on work output. Optimum stimulus frequencies were between 70 and 80 Hz at 5°C and between 80 and 100 Hz at 15°C for both warm and cold acclimated fish. The optimum activation phase for work output was 0°, 70-85° and 260-270° at 5°C, and 0°, 40-50° and 180-200° at 15°C for sequences at 0.35, 0.60 and 0.93 L_s respectively. The activation phase for maximum work at 0.35 L_s coincided with high peak force but maximum work (and therefore power) was increasingly delayed in the tail-beat cycle relative to maximum force when progressing from 0.35 to 0.93 L_s (fig. 6.3). This can clearly be seen in fig. 6.4 (using the strain sequence at 0.93 L_s as an example). At 180° phase, peak force is maximal before

Table 6.1

Table 6.1

Change in the isometric contractile properties with experimental temperature of fast muscle fibres isolated from rostral and caudal myotomes of the short-horned sculpin.

Values are mean $\pm$ SEM ($n = 10$). Symbols: $t15$ = significant difference between mean value of isometric variable at 5 or 10°C with that at 15°C; $t10$ = significant difference between mean value of isometric variable at 5°C with that at 10°C (Analysis of variance with Tukey paired comparison).

A Student's t-test was used at each experimental temperature to determine if mean values of isometric variable varied significantly with acclimation temperature ($\alpha_2 = 0.05$). A significant difference between acclimation temperatures was found for twitch and tetanic P_o at all temperatures and twP$_o$: tetP$_o$ at 15°C.

Parameter	Temperature (°C)		
	5	10	15
5°C FISH			
twitch P_O (kN.m^{-2})	85.9 ± 9.3 ^{t15}	52.8 ± 12.1	26.0 ± 5.7
twitch HPT (ms)	22.3 ± 1.1 ^{t15}	19.1 ± 0.5 ^{t15}	12.9 ± 3.4
twitch HFT (ms)	45.5 ± 3.4 ^{t15}	42.4 ± 6.0	27.1 ± 5.37
tetanic P_O (kN.m^{-2})	133.4 ± 11.1 ^{t15}	97.5 ± 15.8	60.1 ± 11.3
tetanic HPT (ms)	29.8 ± 2.3	27.6 ± 4.0	27.9 ± 3.8
tetanic HFT (ms)	117.3 ± 8.1 $^{t10\,t15}$	72.6 ± 6.6	64.9 ± 6.1
twitchP_O:tetanicP_O	0.65 ± 0.03 ^{t15}	0.44 ± 0.06	0.37 ± 0.04
15°C FISH			
twitch P_O (kN.m^{-2})	120.3 ± 11.9	124.5 ± 13.9	101.9 ± 17.8
twitch HPT (ms)	21.6 ± 1.0 $^{t10\,t15}$	17.0 ± 0.7 ^{t15}	13.2 ± 0.3
twitch HFT (ms)	44.0 ± 7.0 ^{t15}	34.4 ± 4.0	25.7 ± 3.1
tetanic P_O (kN.m^{-2})	201.2 ± 12.3	231.4 ± 18.3	166.8 ± 21.2
tetanic HPT (ms)	29.1 ± 2.8	25.1 ± 3.2	19.6 ± 1.9
tetanic HFT (ms)	123.1 ± 8.8 $^{t10\,t15}$	84.9 ± 4.8 ^{t10}	57.3 ± 5.1
twitchP_O:tetanicP_O	0.64 ± 0.04	0.55 ± 0.05	0.58 ± 0.05

Figure 6.2

Figure 6.2

Examples of the work loops produced by sculpin fast fibres under optimum conditions of activation under strain sequences calculated from a prey capture event at 5°C (single rostral preparation). Strains were calculated at three positions down the trunk: 1 = anterior (0.35 L_s); 2 = anal (0.60 L_s); 3 = posterior (0.93 L_s). Work loops are arranged so that their resting lengths (l_r) are aligned (dashed line) and the direction of muscle shortening and lengthening are indicated by - and + respectively. The horizontal arrow beneath each loop indicates the direction of the loop (anticlockwise = positive work) and stimulus pulses are marked on each loop by small squares. The work done (= area of loop) is displayed within each loop with the power output (work per unit muscle mass x cycle frequency) below. The outline of the sculpin was traced from video footage of a prey capture event (courtesy of T. Beddow).
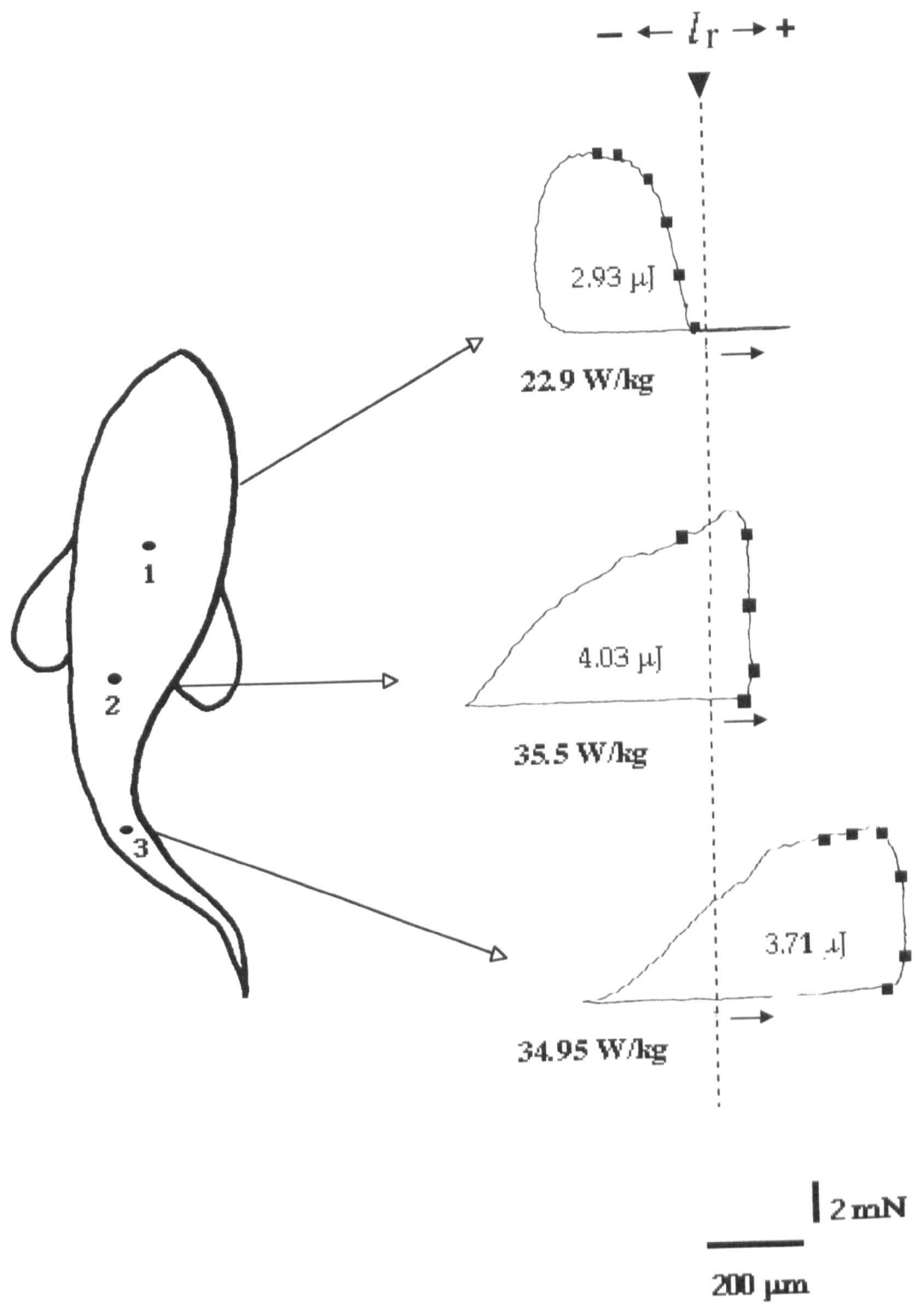
$- \leftarrow l_r \rightarrow +$

2.93 µJ

22.9 W/kg

4.03 µJ

35.5 W/kg
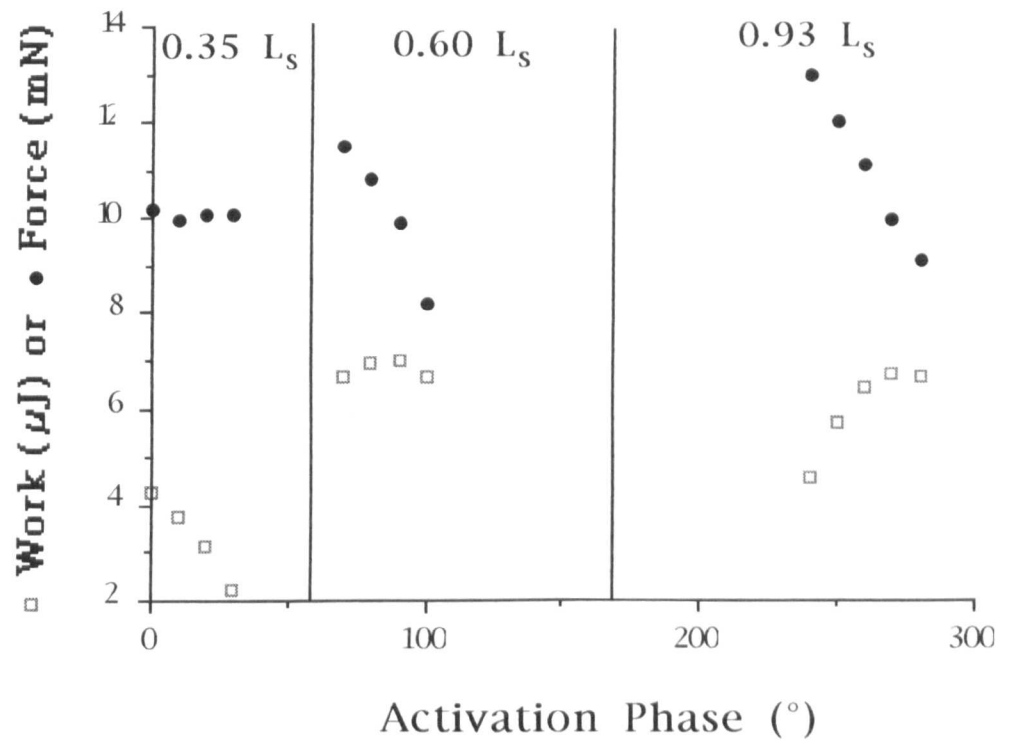
3.71 µJ

34.95 W/kg

2 mN

200 µm

Figure 6.3

Figure 6.3

Change in peak force (mN) and work output (μJ) with activation phase under strain sequences calculated from the 5°C prey capture sequence at 0.35 L_S, 0.60 L_S and 0.93 L_S (single rostral preparation).

shortening commences, producing a tall but thin work loop (fig. 6.4a). As the activationphase is increased peak force is reduced, as the fibres start to shorten before maximum force is generated. However, the period where the highest force is generated now coincides with muscle shortening, producing a more rounded loop and a high work output (fig. 6.4b). A further increase in activation phase results in both low force and low work as muscle shortening commences before force has sufficient time to develop (fig. 6.4c).

Cyclical contractions - power output

The mean power output (averaged over the whole cycle) of muscle fibres isolated from rostral and caudal myotomes was the same for each strain sequence. Between strain positions (i.e. strains at 0.35, 0.60 and 0.93 L_s), power output varied significantly in a temperature dependent manner (rostral and caudal data combined; fig. 6.5). At 5°C, mean power output the strain sequence for 0.35 L_s was 12 W.kg^{-1}, some 45-50% less than that generated using the sequences for 0.60 and 0.93 L_s at the same temperature (21-23 W.kg^{-1}; fig. 6.5). At 15°C this situation was reversed: power output using 0.35 L_s was more than twice that produced using the more posterior sequences (fig. 6.5). Power output at 0.35 L_s varied little with temperature, while at 0.60 and 0.93 L_s power output at 15°C was only around one-quarter of that produced at 5°C (fig. 6.5). As a result, the highest mean power output obtained at 15°C (13 W.kg^{-1} at 0.35 L_s) was only 56% of the highest value obtained at 5°C (23 W.kg^{-1} at 0.93 L_s; fig. 6.5).

A comparison of the relative timing of instantaneous power output (calculated as the product of force and velocity at each time interval) at the three strain positions shows that power peaks sequentially from 0.35 to 0.93

Figure 6.4

Figure 6.4

Example of a typical change in work output with activation phase under the posterior waveform at 15°C: a) 180° phase (work = 1.13 μJ), b) 210° phase (work = 2.1μJ) and c) 240° phase (work = 2.03 μJ). Resting length (l_r) is aligned and the direction of the loop is indicated by a horizontal arrow. Stimulus pulses are marked on each loop by small squares. All loops are from the same rostral fibre preparation. Caudal preparations behaved similarly.

a. 180° phase

l_r

+

b. 210° phase

l_r

+

c. 240° phase

l_r

+

2mN

100 μm
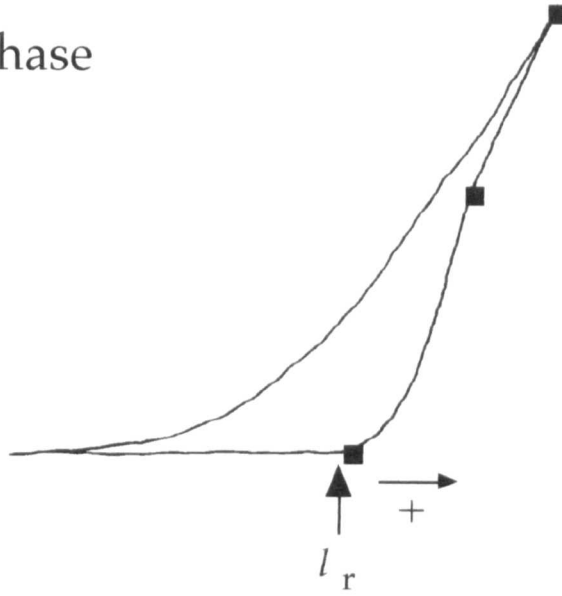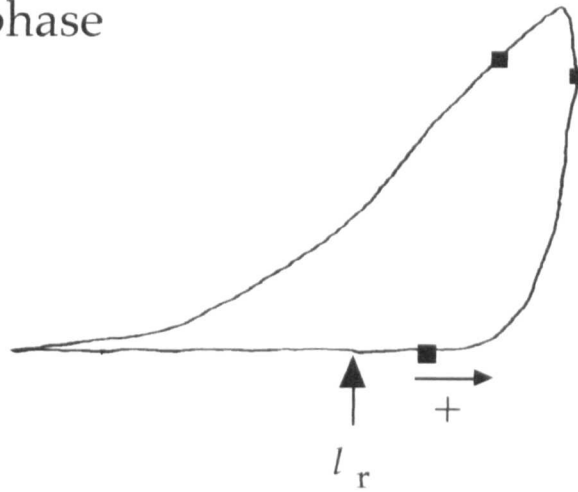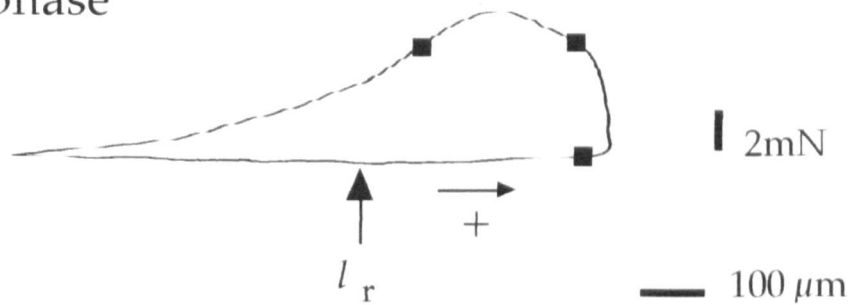
Figure 6.5

Figure 6.5

Power output of fast muscle fibres isolated from 5°C acclimated sculpin under strain sequences calculated at three positions on the trunk (■ = 0.35 L_s, ▨ = 0.60 L_s and ▢ = 0.93 L_s) from attack sequences of a 5°C acclimated fish swimming at 5°C and 15°C. 5°C and 15°C strains were run at experimental temperatures of 5 and 15°C respectively. Mean values are displayed with error bars (SEM). Symbols: * = significant difference in mean power output between strain sequences within experimental temperature.
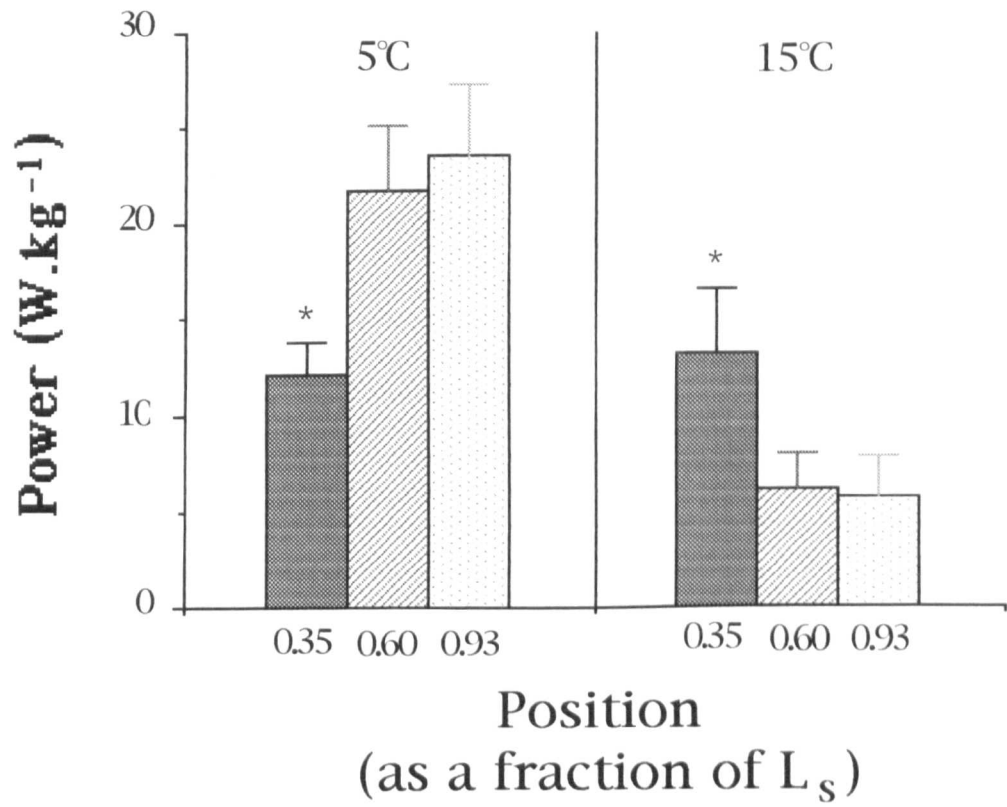
Figure 6.6

Figure 6.6

An example of the relative timing of instantaneous power output $(W.kg^{-1})$ at 0.35 L_s ($\square$), 0.60 L_s ($\blacktriangle$) and 0.93 L_s ($\bigcirc$) during the first tail beat of a prey strike (single rostral preparation). Power is the product of force and velocity at each time interval.

0.35 L$_s$ 0.60 L$_s$ 0.90 L$_s$

0.35   0.60   0.93

Instantaneous Power (W/kg^{-1})
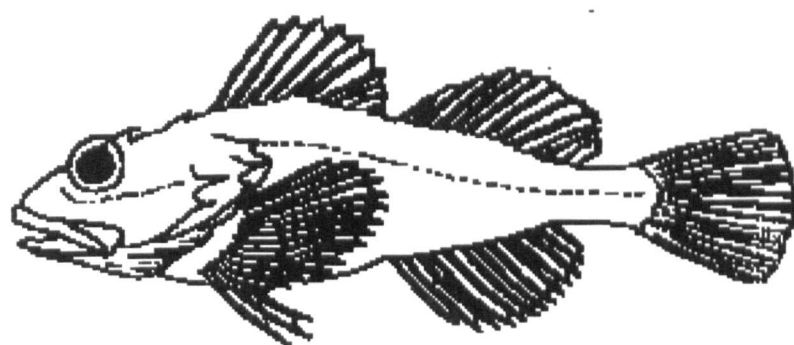
Time (ms)
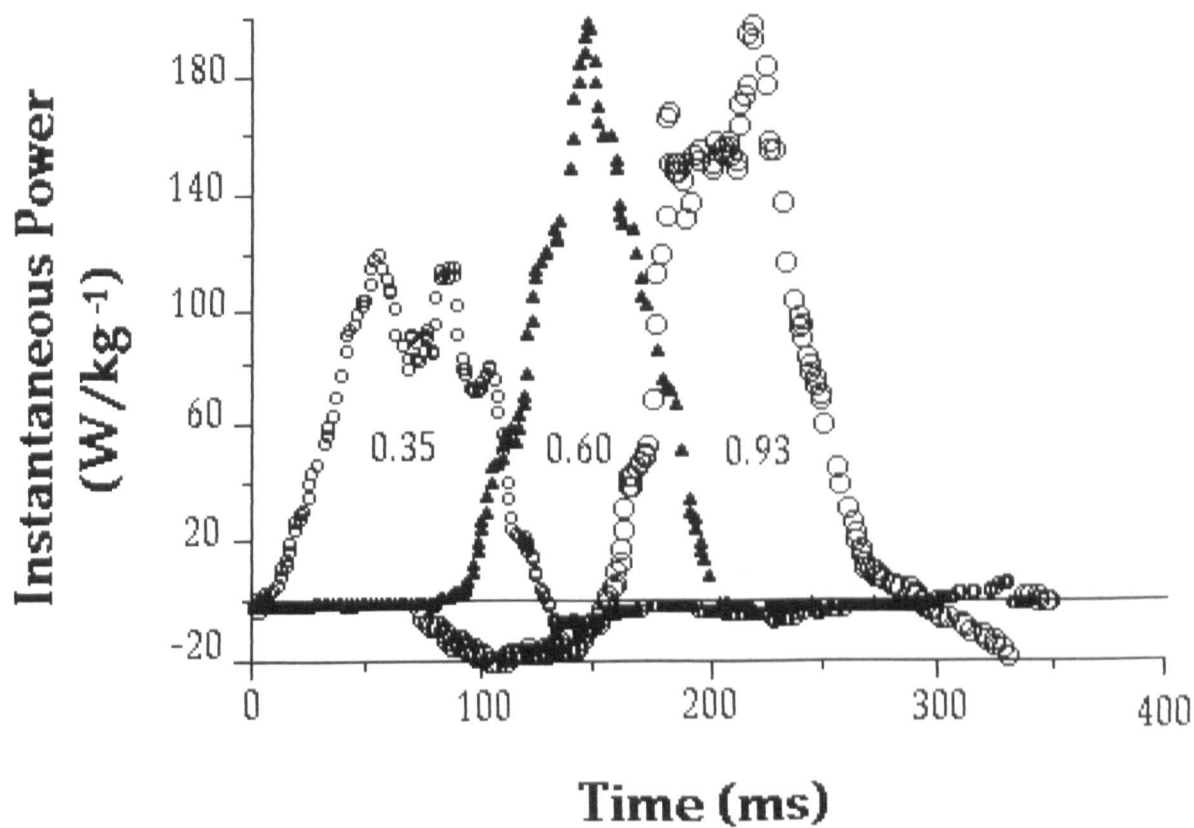
Figure 6.7

Figure 6.7

Power output under the strain sequence from 0.60 L_S in fibres isolated from sculpin acclimated to 5 (solid bars) and 15°C (hatched bar). 5°C acclimated fibres were run under waveforms from 5°C fish swimming at 5 and 15°C (at 5 and 15°C respectively); 15°C acclimated fibres were run under waveform of 15°C acclimated fish swimming at 15°C. Mean ± SEM; n = 10). * represents a significant difference between the power output of fibres from 5°C fish at 15° when compared to 15°C acclimated fish at 15°C (Student's t-test; p=0.0013) and 5°C acclimated fish at 5°C (paired t-test; p=0.0008).
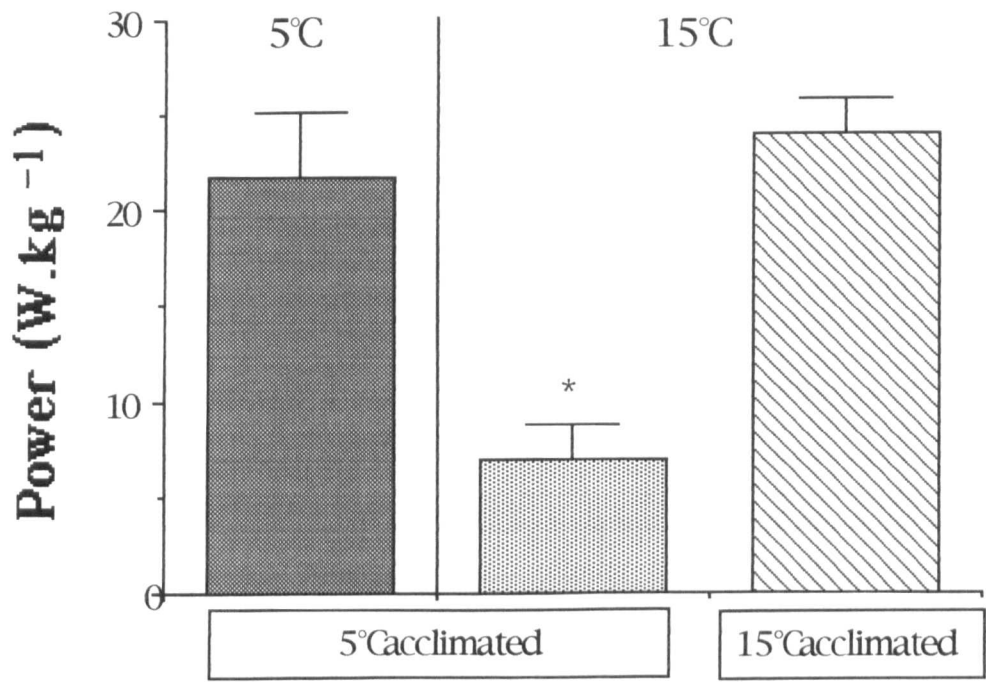
L_s (fig. 6.6). Peak power output at 5°C in this example was around 200 W.kg^{-1} (0.60 and 0.93 L_s; fig. 6.6).

The effect of temperature acclimation on power output was examined for the 0.60 L_s sequence by comparing the results for cold acclimated fish with a parallel study on warm acclimated fish (Johnston *et al.* 1995). The power output of fibres from cold and warm acclimated fish were similar when measured at their respective acclimation temperatures (fig. 6.7). However power output at 15°C was around 70% lower in fibres from cold fish than from warm acclimated fish (fig. 6.7).

6.4. Discussion

Thermal dependence of isometric properties

The contractile properties of sculpin fast fibres isolated from rostral and caudal myotomes are similar under isometric conditions, agreeing with the findings of Johnston *et al.* (1993)(table 6.1). Contractile performance is temperature dependent with the effect of temperature on the ability of the fibres to generate tension being modified by thermal acclimation. Warm acclimation did not result in an improvement in P_0 at 15°C relative to P_0 at 5°C. By contrast, cold acclimation impaired the ability of fibres to generate force at the warmer temperature: tetanic P_0 was reduced by 55% by a 10°C increase in temperature (table 6.1). In the carp (*Cyprinus carpio*), acclimation to cold temperatures (2-8°C) leads to a reduction in peak tensions at warm temperatures (20-30°C). However, this is generally accompanied by improvements in P_0 and maximum shortening velocity (V_{max}) at cold temperatures relative to fibres from warm acclimated fish, showing a partial

compensation of contractile performance (Johnston, Sidell and Driedzic 1985; Langfeld, Crockford and Johnston 1991; Flemming *et al.* 1990; table 6.1). The compensation of P_O and V_{max} at low temperatures following cold acclimation in carp muscle results in part from changes in the myosin heavy chain (MHC; Gerlach *et al.* 1990) and light chain (MLC; Crockford and Johnston 1990; Langfeld *et al.* 1991) isoform composition. Maximally activated skinned fibres isolated from 5°C and 15°C acclimated sculpin develop similar tensions at 15°C indicating that differences in the myosin protein isoform compostion alone are not sufficient to account for the effects of acclimation on contractile performance. Fibres from 5°C acclimated fish also generate significant residual tension at 15 and 20°C (Ball and Johnston 1995). These results, in combination with the present study, suggest that cold acclimation in sculpin may affect one or more of the processes that regulate and control muscle contraction. Changes in the ability of the troponin/tropomyosin complex to regulate the cross-bridge is one possibility (as proposed for cardiac muscle; Landesberg and Sideman 1994).

Half-times to activation (HPT) in twitches and half-times to relaxation (HFT) for both twitches and tetani showed $Q_{10}s[5-15°C]$ of 1.8-2.0, a value which is typical for many physiological processes (Bennett 1990)(table 6.1). Similar $Q_{10}s$ have been reported for contraction times in sculpin (Beddow 1993; Langfeld, Altringham and Johnston 1989) and in the muscle fibres of various Antarctic, temperate and tropical teleosts (Altringham and Johnston 1989; Johnson and Johnston 1991 *b*). Acclimation does not alter the influence of temperature on either HPT or HFT in sculpin fibres (table 6.1) suggesting that changes in the rates of calcium release and uptake from the

sarcoplasmic reticulum (SR) membrane are not involved in the response of sculpin fibres to cold acclimation.

The effect of muscle strain on work output

The shape of the work loop is determined by the characteristics of the imposed strain sequence (figure 6.2). At 5°C, the optimum activation phase lies within the range found *in vivo* during prey capture events by cold acclimated fish at the same temperature (i.e. 0°, 70-85°, and 260-270° 0.35, 0.60 and 0.93 L_s sequences respectively; Johnston *et al.* 1995). At 0.60 and 0.93 L_s, this corresponded to the fibres being given a short active pre-stretch before shortening began. Active pre-stretch was also required for maximum work output in sculpin fast fibres under sinusoidal strains (Johnson and Johnston 1991a). Fibres under strains from 0.60 and 0.93 L_s shorten over twice the distance (as a % l_r) experienced under 0.35 L_s strains at both temperatures, giving a greater potential for positive work output at 0.60 L_s and 0.93 L_s (fig. 6.1). As the cycle frequency at 15°C was greater than that at 5°C (fig. 6.1) the relationship between force and shortening at 0.60 and 0.93 L_s could only be maintained if activation occurred earlier in the strain cycle (fig. 6.5). During continuous periodic swimming, the timing of EMG onset at a given point on the trunk relative to the wave of mechanical bending is independent of swimming speed (e.g. Grillner and Kashin 1976). However, during the escape response in the goldfish, variation in the degree of lateral displacement and the final escape trajectory were achieved by altering the relative timing of muscle activation down each side of the fish (Foreman and Eaton 1993). Thus, during transient (unsteady) swimming manoeuvres in the sculpin, it is possible that the adjustment of the timing and duration of

muscle activation is important in adjusting work output down the trunk to the requirements of different swimming behaviours.

Power output during prey capture events

Power output under each strain sequence was the same for fibres isolated from rostral and caudal myotomes. Under sinusoidal strains, both power output and the conditions of strain and activation optimum for power were also found to be the same for rostral and caudal fibres (Johnston *et al.* 1993). A comparison of *in vitro* power output with the relative timing of muscle activation measured *in vivo* suggested that power output would be positive down the trunk of the fish under most conditions, which has been confirmed in the present study (Johnston *et al.* 1993). This situation is unlike that found for steady swimming in the saithe, where muscle activation during fibre lengthening results in net negative work in caudal myotomes (Altringham *et al.* 1993). The results of the present study, combined with the findings of Johnston *et al.* (1993), suggest that muscle fibres in rostral and caudal myotomes may both function as generators of positive power under most conditions.

Average power output of fibres from winter acclimatised sculpin at 4-5°C is 20-30 W.kg^{-1} (Johnson and Johnston 1991*a*) and the 23 W.kg^{-1} at 5°C found here lies within this range (0.93 L$_s$; fig. 6.5). At 15°C the highest power achieved was only 13 W.kg^{-1} (a reduction of 45-50%) compared to a maximum of 9 W.kg^{-1} produced under sinusoidal strains (Johnson and Johnston 1991*a*). The reduction in power output at 15°C in the present study is likely to be due to the reduced performance of cold acclimated fish muscle at 15°C (table 6.1). The average power output of scallop adductor muscle measured under

sinusoidal or *in vivo* strains was also similar (34 ± 1 and 29 ± 1 W.kg^{-1}, $n = 4$; mean $\pm$ SEM) but the distribution of power within each cycle was different (Marsh and Olson 1994). At the optimum activation phase for work output, instantaneous power output in the sculpin peaks sequentially down the trunk during each tail-beat cycle, showing a smooth transition of mechanical power corresponding to the passage of the wave of mechanical bending towards the tail (fig. 6.6). Peak instantaneous power at 5°C was around 200 W.kg^{-1} at 0.60 and 0.93 L$_s$ (fig. 6.6) which is 65% greater than the instantaneous power output calculated from the force-velocity (P-V) relationship with the same combination of acclimation and experimental temperatures (121.1 W.kg^{-1}; Beddow and Johnston 1995). The ability of muscle fibres to generate power during an oscillatory cycle tends to exceed that estimated from the P-V curve as force production during cyclical oscillations is enhanced by active pre-stretch (Stevens 1993).

At 5°C, fibres isolated from cold acclimated sculpin generate maximum power under 0.60 and 0.93 L$_s$ strain sequences (fig. 6.5). With these two sequences the fibres undergo around twice the total amplitude of shortening experienced with 0.35 L$_s$ strains, giving a greater potential for the production of positive power. This 'extra' shortening during the propulsive stroke is possible due to the adoption of the S-start position at the start of the strike. The S-start additionally allows the fish to accelerate in any chosen direction and gives a better balance of recoil forces along the body (Webb and Weihs 1983) which may increase the chance of a successful prey strike. At 15°C, the situation is reversed: maximum power is produced 0.35 L$_s$ with a substantial reduction in power output at 0.60 L$_s$ and 0.93 L$_s$ even though total muscle shortening is still substantially greater at these two positions (fig. 6.5). The calculated strain sequences used *in vitro* were originally produced

by muscle contractions in a swimming fish. The poor performance of the fibres *in vitro* at 15°C could thus be due to a difference in muscle performance between the fish used for the swimming and mechanics parts of the experiment or a greater thermal sensitivity of contractile performance *in vitro* in comparison to that under *in vivo* conditions.

As with fibres from cold acclimated fish at 5°C, the mean power output of fibres isolated from 15°C acclimated fish measured at their acclimation temperature was greatest at 0.60 and 0.93 L_S (Beddow 1993; Johnston *et al.* 1995). This indicates a tendency for the kinematics of a prey strike measured at the temperature of acclimation to result in the greatest power output (per kg of muscle) in the post-anal region. In the pike (*Esox lucius*), another acceleration specialist, the majority of thrust during fast start manoeuvres is generated in the tail, aided by a deep body/fin profile in this region (Frith and Blake 1991). The increase in mass specific muscle power output towards the tail is thus likely to relate to large rapid thrust requirements during the propulsive stage of an attack sequence.

Warm acclimation resulted in a combination of kinematics and muscle contractile properties at 0.60 L_S which gave over 3.5-times the power produced by fibres from cold acclimated fish at the same temperature (fig. 6.7). However at 5°C, the power output of fibres from cold acclimated fish was similar to that produced by fibres from warm acclimated fish at 15°C. Thus in sculpin, cold acclimation leads to reduced muscle performance at higher temperatures relative to warm acclimated fish. Cold acclimation has a positive affect on instantaneous power output at low temperatures: fibres from cold acclimated fish generated more than twice the power (calculated from force-velocity (P-V) relationship) at 5°C than fibres from warm acclimated fish (Beddow and Johnston 1995). This relative increase in performance was due

to a significant decrease in the curvature of the force-velocity relationship (Beddow 1993), which improves power output by increasing the shortening velocity for a given load. Ranatunga (1984) suggested that differences in the shape of the force-velocity curve were due to changes in the relative rates of cross-bridge attachment and detachment - an decrease in the rate of detachment corresponding to a decrease in curvature. This corresponds to the proposal that acclimation in sculpin fibres primarily affects the regulation of the cross-bridge cycle.

Prey capture success in 5°C acclimated fish swimming at 15°C is decreased relative to fish acclimated to 15°C but the maximum acceleration and velocity attained during a prey strike was independent of temperature (Beddow *et al.* 1995). Fish acclimated to 15°C have a lower success rate at 5°C compared to cold acclimated fish (Franklin and Johnston, unpublished results), despite similarities in isometric contractile properties (table 6.1) and V_{max} (Beddow and Johnston 1995) at that temperature. Since sculpin probably continue to feed throughout the year in the wild (King *et al.* 1983), maintaining the percentage success rate of strikes at both high and low temperatures is essential. During thermal acclimation, compensation occurs in the conditionability of behaviours (Rahmann, Schmidt and Schmidt 1980; Zerbolis 1973) and in the ability to co-ordinate swimming manœuvres at low temperatures (Roots and Prosser 1962 - see Prosser and Nelson 1981 for a review). Therefore acclimatory compensation of the processes affecting the judgement and co-ordination of attack sequences may be equally important as muscle performance to the success of prey strikes in sculpin affected by seasonal changes in temperature.

GENERAL DISCUSSION

The main finding of this thesis is that fast muscle fibres isolated from rostral and caudal myotomes of the Atlantic cod differ significantly in their contractile properties while those isolated from the short-horned sculpin do not. Cod fast fibres show clear regional differences in peak tension (Chapter 2), half times to activation (HPT) and relaxation (HFT) (Chapters 2 and 4), maximum contraction speed (V_0 in Chapter 2 and V_{max} in Chapter 4) and peak power output (Chapter 4) while sculpin rostral and caudal fibres possess similar isometric contractile properties (Chapters 4, 5 and 6) and generate equivalent amounts of positive power during both isovelocity shortening (Chapter 4) and under imposed cycles of lengthening and shortening (Chapter 6). In order to understand the significance of these results to the generation of thrust in each species, an attempt will be made in the following sections to interpret *in vitro* contractile properties in light of *in vivo* muscle function.

7.1 The Atlantic cod

Based on observations of morphology, Videler (1981) suggested that propulsion in cod could be described by a 'reactive' hydrodynamic model. In this model, thrust ultimately depends on three things: the size of the added mass of water accelerated by movements of the fish's body (dependant on the depth of the fish's silhouette), the rate at which this mass is shed from the trailing edge of the tail blade (determined by the

lateral velocity of the tail sweep) and its direction in the wake of the fish (determined by the angle that the rearward face of the tail blade makes with the direction of motion)(Lighthill 1960, 1971; Webb 1975a). Fish that use steady swimming at high speeds, such as Scombroidae, Xiphiidae and Istiophoridae, have a body form and locomotory style that results in the generation of the majority of the propulsive force at the edge of the tail blade (Fierstine and Walters 1968). Cod are less streamlined and have a more tapered body form than these specialist cruisers but it is likely that a large fraction of the propulsive force is still shed to the water *via* the trailing edge of the caudal fin (Wardle and Videler 1980). What are the possible consequences of this to the conversion of muscle force into propulsive force?

Theoretical evidence based on EMG data and calculated muscle strains (Van Leeuwen *et al.* 1990; Van Leeuwen 1994) and experimental evidence (e.g. Wardle and Videler 1993; Altringham, Wardle and Smith 1993) suggest that rostral and caudal myotomes play different roles in the transformation of mechanical power into thrust. Under *in vivo* conditions of activation, muscle fibres isolated from rostral myotomes of the saithe (*Pollachius virens*) generate maximum positive power when caudal fibres on the same side are producing maximum force as they actively resist lengthening (Altringham *et al.* 1993). The effect of this will be to stiffen the tail along its outer bend, effectively converting muscle fibre shortening in rostral myotomes into a lateral movement of the tail blade. The moment when both rostral power and caudal force are maximal (and the transmission of rostral power to the tail blade is also maximal) coincides with the passage of the tail tip across the direction of travel (Videler 1994). I propose that in fish which use this style of swimming the 'caudal transmission' of rostral power is linked to the importance of shedding the added mass at the trailing edge of the tail-blade in the

generation of thrust. Other factors such as the increasing localisation of muscle fibres in rostral myotomes, the helical orientation of fibres within rostral myotomes (Alexander 1969), body form (e.g. body depth and fineness ratio) and kinematics (e.g. tail-beat amplitude and body wavelength) will all play integral parts in the way in which muscle force is channelled and controlled. If the relative timing of muscle activation in rostal and caudal myotomes *in vivo* in the cod is similar to that of the saithe, the association between high rostral power and high caudal force would be the same (Chapter 2). However, experimental evidence from co-ordinated EMG and kinematic data is needed to prove this. In addition, cod fast fibres are used to power unsteady swimming movements (Videler 1981) so the relationship between rotral power and caudal force under conditions simulating steady swimming proposed in Chapter 2 may not hold under more realistic strains.

In the cod, muscle fibres in caudal myotomes have longer activation and relaxation times than fibres from rostral myotomes (Chapter 2). A similar caudal increase in activation and relaxation times has also been found in fast fibres isolated from the saithe (Altringham *et al.* 1993 and in cod, saithe, haddock and mackerel myotomes *in situ* (Wardle 1985). Longer caudal contraction times could have two main consequences:

(i) An increase in the positive power generated during the tail beat cycle in caudal myotomes. Caudal fibres are mainly active while lengthening but are active while shortening for a short period before EMG offset occurs. A longer contraction duration would extend the duration of active shortening (see Van Leeuwen 1994). Caudal muscle shortening occurs as the tail tip begins its return sweep. If the duration of positive power output is prolonged during this period, it may help to accelerate the tail in its return sweep. Indeed in a steadily swimming cod, the lateral path of the tail tip is

not perfectly sinusoidal as velocity tends to be greatest at the start of the tail sweep (Videler and Wardle 1978).

(ii) The maximum tail-beat frequency is limited by the minimum muscle contraction time (Wardle 1975). Cod rostral fibres are capable of shortening more quickly than caudal fibres (Chapters 2 and 4) and so may define the maximum tail-beat frequency. In this case, a longer contraction duration in caudal myotomes, combined with a lower shortening velocity (Chapters 2 and 4) will tend to increase resistance to lengthening (and therfore the stiffness of the tail) as swimming speed increases to maximum.

If a stiff tail is important to effective propulsion, why not simply replace the muscle in caudal myotomes with tendons, which do not require ATP to resist lengthening? Thuniform swimmers which are specialised for swimming at a high, fairly constant speed have adopted this strategy: muscle shortening is translated into lateral movements of the tail *via* a system of tendons, confining lateral oscillations to the tail and caudal peduncle (Lindsey 1978; Webb 1984). The disadvantage of this arrangement is that rapid changes in speed or direction are not possible so the ability to manoeuvre is poor in these fish. Cod are voracious predators of crustacea and other fish (Macer 1991) and need muscle fibres caudally (in combination with a large variable area of dorsal, anal and caudal fins) to give them the flexibility to turn or vary their speed quickly in pursuit of prey. The kinematics of a swimming fish depend on its body form and the physical properties of the surrounding water. For any one individual, the resistance of the surrounding water mass to the passage of the tail increases with the velocity of the tail sweep. As tail-beat frequency can be linearly related to swimming speed over a range of velocities (Bainbridge 1958), resistance to the passage of the tail will therefore vary with swimming speed. The efficiency with which the

mechanical wave of bending is propagated caudally (and thus propulsive efficiency) will depend on the resistance the body of the fish meets from the water relative to its own stiffness (Blight 1977). A stiff tail is a good propagator of body movements at high speeds where fluid resistance is also high. At low speeds or during turns, flexibility of the tail may be more important to control the direction of the propulsive force so the resistance of the tail should be relatively low. Tendons fix the stiffness of the tail but muscle provides a stiffness modulator whose stiffness can be varied by the degree of muscle activation. By varying the degree of muscle activation in caudal myotomes, cod may be able to control the stiffness of their tails to suit their swimming speed thereby ensuring an effective use of muscle power.

7.2 The Short-horned sculpin

Fast and slow fibres in the sculpin show differences in power output and shortening velocity that match well with their velocity of recruitment during swimming (Chapter 4). Sculpin primarily use their fast fibres to power standing starts, either during prey strikes or escape responses. Both behaviours occur over a short time period (100-200 ms), involve a tail beat of large amplitude and have the purpose of generating maximum rates of acceleration, regardless of the drag costs incurred. During a startle response in the pike, another lunging specialist, the majoity of thrust was generated by the tail because of its large median and caudal fins and the large amplitude of the tail beat. The stereotypical kinematics associated with a prey strike and the emphasis on fast rates of acceleration may greatly reduce the importance of shedding the added mass at the trailing edge of the tail-blade to the generation of thrust. In isolated sculpin fibres, the maximum potential for power is in post-anal

myotomes (Chapter 6). The cross-sectional area of myotomes is reduced caudally (see Wardle 1985) but sculpin have large dorsal and anal median fins which, combined with the large tail-beat amplitude, suggest that thrust is high over a larger area of the caudal region - not just at the trailing edge of the caudal fin.

During isovelocity shortening, rostral and caudal fibres produce similar amounts of power at the same velocity of shortening (Chapter 4) and under conditions approximating steady swimming, rostral and caudal fibre maximum power output was similar and required the same optimum conditions of strain and activation (Johnston, Franklin and Johnson 1993). On the basis of EMG recordings from prey capture events, Johnston and co-workers proposed that muscle generated positive power down the trunk under most conditions. The results of chapter 6 support this view. During a prey strike the delay between rostral and caudal activation during a prey strike was around 10 ms (Johnston *et al.* 1993) suggesting that rostral and caudal fibres would be activated nearly simultaneously. As the fish's body is bent into an S-shape during the preparatory stroke, all the fibres down one side will initially shorten on activation. Thus both rostral and caudal fibres in the sculpin have the same role: the generation of positive power. In keeping with this, fast fibres isolated from rostral and caudal myotomes show a similar ability to generate positive power (Chapters 4 and 6).

7.3 Conclusions and proposals for future work

Fast fibres in both cod and sculpin show mechanical characteristics which may be interpreted favourably in terms of the locomotory behaviour of the species. However, this is definitely not enough evidence to argue that these properties are adaptive (Garland and Adolph 1994). It is

widely accepted that mechanical characteristics of a structure are an indication of their functional demand, as evidenced by the studies linking the swimming speeds at which different fibre types are recruited to their *in vitro* mechanical properties (e.g. Rome *et al.* 1988). However, a much greater understanding of the relationship between kinematics and hydrodynamics is needed before muscle contractile properties can be clearly related to all observed swimming movements.

By having a specific set of mechanical characteristics built in to its muscle fibres (and musculoskeletal system), a fish can control muscle power output simply by varying the numbers and type of fibres which are activated. The change in locomotory requirements in fast fibres is more subtle and harder to detect since there is not an obvious division of roles at different swimming speeds. In this case, the modification of muscle power output is more likely to be related to the relative timing of power output during the tail-beat cycle. But again, by hard-wiring fibre mechanical characteristics, variation in timing and duration of activation can be used to finely control power output and body stiffness as hydrodynamical constraints change with swimming speed. Given the tight link shown between function and requirements in other components of the locomotory system, it is likely that regional differences in *in vitro* contractile properties are related to their operation *in vivo*.

With the latest developments in co-ordinated EMG and sonomicrometry combined with custom computer software, there are many exciting possibiltites for studying *in vitro* muscle function under a range of simulated swimming behaviours. For the future, the convergence of a range of disciplines on the same goal may one day yield a complete answer to the elusive question that has been the subject of fascination for centuries, namely how *do* fish swim?

Appendix 1

A1.1 Calculation of muscle strain sequences from prey-capture events[1]

Outlines of the fish in successive frames were traced, enlarged on a Xerox machine, and digitised (Jandel Scientific, California) relative to fixed reference points in order to provide a series of x-y co-ordinates. A computer program was written to display the digitised outline data on screen and to transform the data into a suitable format for further calculations.

Another program was written for the calculation of the shape of the axis of the fish during the swimming event from the digitised outlines. Each axis calculation was started at the most rostral point and was finished at the most caudal point. Following Van Leeuwen *et al.* (1990) it was assumed that the projected areas left and right of the axis were equal for each element of the axis. This was supported by radiography of swimming carp (van Leeuwen *et al.* 1990). The calculated axis followed closely the central canal of the vertebral column as projected on the radiograph. In order to calculate the fish axis it was divided into a number of straight-line segments. The (mathematical) segment length Δs was defined to vary linearly down the trunk of the fish:

$$\Delta s = (L - s)/ s_1 + s/s_2 \qquad (A1.1)$$

where L is the total length of the fish, s is the distance along the axis from the snout and s_1 and s_2 are the most rostral and caudal segment lengths respectively. The variable segment length was chosen to improve the stability of the applied algorithm, while allowing enough flexibility to approach the actual curvature as much as possible. Therefore, the largest segment length chosen was in the head region (typically 0.1 BL), which is very stiff so that bending is negligible, whereas the smallest segment length was in the tail region (typically 0.03 BL) where bending is largest. These variable lengths correspond approximately to the anatomical segment lengths of the fish (skull, vertebrae, and fin-ray segments respectively).

A computer program was written to describe the axis data in parametric form, so that x = F(s,t), and Y = G(s,t). For each of the selected instants, the functions F and G were smoothed as a function of position down the trunk using cubic spline functions. For this purpose, the spline function package by Woltring (1986) was used. Smoothing was by choosing an appropriate values of the smoothing parameter. The parameter was chosen such that (1) the axis in the head region was kept as straight as possible, (2) unrealistic small scale fluctuations in the curvature were removed as much as possible, and (3) the fundamental characteristics of the wave of lateral curvature were preserved. With $F_{sp}(s,t)$ and $G_{sp}(s,t)$ as the smoothed functions, the absolute curvature at a particular position down the trunk was calculated as described by Lipschutz (1969):

$$k = ((d^2F_{sp}/ds^2)^2 + (d^2G_{sp}/ds^2)^2)^{0.5} / ((dF_{sp}/ds)^2 + (dG_{sp}/ds)^2) \qquad (A1.2)$$

For convenience, we defined the curvature c(s,t) as positive (c = k) for bending to the right-hand side and *visa versa*. Using quintic spline functions and the generalised cross validation criterion as described by Woltring (1986), the curvature function c(s,t) was smoothed as a function of time to obtain a function c_{st}(s,t), which was used for the strain calculations. To calculate the strains of the selected muscle fibres, formulae (4) to (7) from van Leeuwen *et al.* (1990) were applied. These formulae take into account the thickening and thinning of the body at the concave and the convex side respectively, as well as the position and orientation of the muscle fibres.

The computer programs were written for the Macintosh family of computers, using either Think Pascal 4.0.2 (Symantec Corp.) or Mac Fortran II 3.2 (Absoft Corp.) as programming languages. ANSI standards were used as much as possible (except for graphic routines).

A1.2 Determination of muscle fibre geometry

Fish were placed flat on their lateral surface and the skin carefully removed to reveal the musculature An incision was made with a sharp razor blade at the mid-point of the dorsal fast muscle at points 0.32 L, 0.52 L and 0.77 L along the body (where L is total length).The angles of the fibres were measured with respect to the median and horizontal plane of the fish (Alexander 1969). The range of angles measured for fast muscle fibres in the median plane were 14-24° for the 5th myotome at 0.32 L (measured from the snout), 19-26° for the 15th myotome at 0.52 L and 10-14° for the 29th myotome at 0.77 L (angles inclined towards the tail). In the horizontal plane, fast muscle fibres 2-3 mm deep made angles with respect to the longitudinal axis of 13° and 0.32 L, 17° at 0.52 L and 36° at 0.77 L. These

angles were used to correct strain calculations for the orientation of fast
fibres (see above).

References

Aidley, D. A. (1971). *The physiology of excitable cells.* Cambridge University Press, Cambridge. pp 468.

Akster, H. A. (1981). Ultrastructure of muscle fibres in the head and axial muscles of the perch (*Perca fluviatilis* L.): A quantitative study. *Cell and Tissue Research* 219:111-131.

Akster, H. A. (1985). Morphometry of muscle fibre types in the carp (*Cyprinus carpio* L.): relationships between structural and contractile characteristics. *Cell and Tissue Research* 241:193-201.

Akster, H. A., H. L. M. Granzier and H. E. D. J. ter Keurs (1984). Force-sarcomere length relations vary with thin filament length in muscle fibres of the perch (*Perca fluvatilis* L.). *Journal of Physiology (London)* 653: 61P.

Akster, H. A., H. L. M. Granzier and H. E. D. J. ter Keurs (1985). A comparison of quantitative ultrastructural and contractile characteristic of muscle fibre types of the perch, *Perca fluvatilis* L. *Journal of comparative Physiology B* 155:685-691.

Alexander, R. McNiell (1967). *Functional design in fishes.* Hutchinson, London. 160 pp.

Alexander, R. McNiell (1969). The orientation of muscle fibres in the myomeres of fishes. *Journal of the Marine Biological Association U.K.* 49:263-290.

Allen, P. D. and W. N. Stainsby (1983). A 5 parameter curve: the best fit for the force-velocity relationship of *in situ* dog skeletal muscle. *Physiologist* 16:252.

Altringham, J. D. and I. A. Johnston (1982). The pCa-tension curve and force velocity characteristics of skinned fibres isolated from fish fast and slow muscles. *Journal of Physiology (London)* 333:421-449.

Altringham, J. D. and I. A. Johnston (1986). Energy cost of contraction in fast and slow muscle fibres isolated from an elasmobranch and an antarctic teleost fish. *Journal of experimental Biology* 121:239-250.

Altringham, J. D. and I. A. Johnston (1988a). Activation of multiply innervated fast and slow myotomal muscle fibres of the teleost *Myoxocephalus scorpius. Journal of experimental Biology* 140:313-324.

Altringham, J. D. and I. A. Johnston (1988b). The mechanical properties of polyneuronally innervated, myotomal muscle fibres isolated from a teleost fish. *Pflügers Archiv* 412:524-529.

Altringham, J. D. and I. A. Johnston (1990a). Modelling muscle power output in a swimming fish. *Journal of experimental Biology* 148:395-402.

Altringham, J. D. and I. A. Johnston (1990b). Scaling effects on muscle function: power output of isolated fish muscle fibres performing oscillatory work. *Journal of experimental Biology* 151:453-467.

Altringham, J. D. and G. H. Pollack (1984). Sarcomere length changes in single frog muscle fibres during tetani at long sarcomere lengths. Pages 473-493 in G. H. Pollack and H. Sugi, eds. *Contractile mechanisms in muscle.* Plenum Press, London.

Altringham, J. D., C. S. Wardle and C. I. Smith (1993). Myotomal muscle function at different points on the body of a swimming fish. *Journal of experimental Biology* 182:191-206.

Andersen, P., J. K. S. Jensen and Y. Løyning (1969). Slow and faast muscle fibres in the Atlantic hagfish (*Myxine glutinosa*). *Acta Physiolgica Scandinavica* 57:167-179.

Anderson, M. E. and I. A. Johnston (1992). Scaling of power output in fast muscle fibres of the Atlantic cod during cyclical contractions. *Journal of experimental Biology* 170:143-154.

Archer, S. D. and I. A. Johnston (1989). Kinematics of labriform and subcarangiform swimming in the antarctic fish *Notothenia neglecta*. *Journal of experimental Biology* 143:195-210.

Archer, S. D., J. D. Altringham and I. A. Johnston (1990). Scaling effects on the neuromuscular system, twitch kinetics and morphometrics of the cod, *Gadus morhua*. *Marine Behavioural Physiology* 17:137-146.

Bainbridge, R. (1958). The speed of swimming of fish as related to size and to the frequency and amplitude of the tail beat. *Journal of experimental Biology* 35:109-133.

Ball, D. and I. A. Johnston (1995). Plasticity of muscle contractile properties following temperature acclimation in the marine fish *Myoxocephalus scorpius*. In preparation.

Barnard, R. J., V. R. Edgerton, T. Furukawa and J. B. Peter (1971). Histochemical, biochemical, and contractile properties of red, white, and intermediate fibres. *American Journal of Physiology* 220:410-414.

Beamish, F. W. H. (1966). Swimming endurance of some northwest Atlantic fishes. *Journal of the Fisheries Research Board of Canada* 23:341-347.

Beamish, F. W. H. (1978). Swimming capacity. Pages 101-187 in W. S. Hoar and D. J. Randall, eds. *Fish physiology (VII): Locomotion*. Academic Press, London. pp. 576.

Beardall, C. H. and I. A. Johnston (1983). Muscle atrophy during starvation in a marine teleost. *European Journal of Cell Biology* 29:209-217.

Beddow, T. A. (1993). The influence of temperature acclimation on isolated muscle properties and burst swimming performance of the sculpin

PAGE MISSING IN ORIGINAL

Bone, Q. (1964). Patterns of muscular innervation in the lower chordates. *International Review of Neurobiology* 6: 99-147.

Bone, Q. (1966). On the function of the two types of myotomal muscle fibre in elasmobranch fish. *Journal of the Marine Biological Association U.K.* 46: 321-349.

Bone, Q. (1970). Muscular innervation and fish classification. *Simp. Int. Zoofil. 1st Univ. Salamanca*: 369-377.

Bone, Q. (1972). The dogfish neuromuscular junction: dual innervation of vertebrate striated muscle fibres? *Journal of Cell Science* 10: 657-665.

Bone, Q. (1978). Locomotor muscle. Pages 361-424 in W. S. Hoar and D. J. Randall, eds. *Fish physiology (VII): Locomotion.* Academic Press, London. pp. 576.

Bone, Q. and R. D. Ono (1982). Systematic implications of innervation patterns in teleost myotomes. *Brevoria* 470: 1-23.

Bone, Q., J. Kiceniuk, and D. R. Jones (1978). On the role of the different fibre types in fish myotomes at intermediate swimming speeds. *Fisheries Bulletin* 76: 691-699.

Bone, Q., I. A. Johnston, A. Pulsford and K. P. Ryan (1986). Contractile properties and ultrastructure of three types of muscle fibre in dogfish myotomes. *Journal of Muscle Research and Cell Motility* 7: 47-56.

Bossen, E. J., J. R. Sommer and R. A. Waugh (1978). Comparative stereology of the mouse and finch left ventricle. *Tissue and Cell* 10:773-784.

Bragg, W.L. (1913). The structure of some crystals as indicated by their diffraction of X-rays. *Proceeding of the Royal Society A* 89:248-277.

Breder, C. M. (1926). *The locomotion of fishes.* Zoologica (N.Y.) 4: 159-297.

Brett, J. R. (1964). The respiratory metabolism and swimming performance of young sockeye salmon. *Journal of the Fisheries Research Board of Canada* 21:1183-1226.

Burton, K. (1992). Myosin step size: estimates from motility assays and shortening muscle. *Journal of Muscle Research and Cell Motility* 13: 590-607.

Caiozzo, V. J., R. E. Herrick and K. M. Baldwin (1992). Response of slow and fast muscle to hyperthyroidism - maximal shortening velocity and myosin isoforms. *American Journal of Physiology* 263:86-94.

Camm, J. P. and I. A. Johnston (1985). Developmental changes in the differentiation of muscle fibres in the Antarctic teleost *Notothenia neglecta. Journal of Physiology (London)* 367: 98P.

Cavagna, G. A., N. C. Heglund and C. R. Taylor (1977). Mechanical work in terrestrial locomotion: two basic mechanisms for minimising energy expenditure. *American Journal of Physiology* 233: R243-R261.

Cochran, W. G. and G. M. Cox (1957). *Experimental Designs.* 2nd ed. Wiley, New York. 617 pp.

Crockford, T. C. and I. A. Johnston (1990). Temperature acclimation and the expression of contractile protein isoforms in the skeletal muscles of the common carp (*Cyprinus carpio* L.). *Journal of comparative Physiology B* 160: 23-30.

Curtin, N. A. and R. E. Davies (1975). Very high tension with very little ATP breakdown by active skeletal muscle. *Journal of Mechanochemical Cell Motility* 3: 147-154.

Curtin, N. A. and R. C. Woledge (1988*a*). Energetic cost of power output by isolated fibre bundles from dogfish white muscle. *Journal of Physiology (London)* 407: 74P.

Curtin, N. A. and R. C. Woledge (1988*b*). Power output and force-velocity relationship of live fibres from white myotomal muscle of the dogfish, *Scyliorhinus canicula*. *Journal of experimental Biology* 140: 187-197.

Curtin, N. A. and R. C. Woledge (1991). Efficiency of energy conversion during shortening of muscle fibres from the dogfish *Scyliorhinus canicula*. *Journal of experimental Biology* 158: 343-353.

Curtin, N. A. and R. C. Woledge (1993*a*). Efficiency of energy conversion during sinusoidal movement of white muscle fibres from the dogfish *Scyliorhinus canicula*. *Journal of experimental Biology* 183: 137-147.

Curtin, N. A. and R. C. Woledge (1993 b). Efficiency of energy conversion during sinusoidal movement of red muscle fibres from the dogfish *Scyliorhinus canicula. Journal of experimental Biology* 185:195-206.

Cutts, A. (1986). Sarcomere length changes in the wing muscles during the wing beat cycle of two bird species. *Journal of Zoology* 209:183-185.

Daxboeck, C., D. J. Randall and D. R. Jones. 1982. Cardiac output redistribution during swimming exercise in a teleost fish, *Salmo gairdneri. Journal of experimental Biology.* Cited in Johnston 1983.

Diamond, J. (1971). The mauthner cell. Pages 265-346 in W. S. Hoar and D. J. Randall, eds. *Fish physiology (V).* Academic Press, London.

Dimery, N. J. (1985). Muscle and sarcomere lengths in the hindlimb of a rabbit (*Oryctolajus cuniculus*) during a galloping stride. *Journal of Zoology* 205:373-383.

Driedzic, W. R. and P. W. Hochachka (1978). Metabolism in fish during exercise. Pages 503-543 W. S. Hoar and D. J. Randall, eds. *Fish physiology (VII): Locomotion.* Academic Press, London.

Dulhunty, A. F. (1986). A freeze-fracture study of extensor digitorum ongus and soleus muscles from thyroxic rats. *Journal of Ultrastructural Research* 94:121-130.

Dulhunty, A. F. (1990). The rate of tetanic relaxation is correlated with the density of calcium ATPase in the terminal cisternae of thyrotoxic skeletal muscle. *Pflügers Archiv* 415:433-439.

Duthie, G. G. (1982). The respiratory metabolism of temperature-adapted flatfish at rest and during swimming activity and the use of anaerobic metabolism at moderate swimming speeds. *Journal of experimental Biology* 97:359-373.

Eaton, R. C., R. A. Bombardieri and D. L. Meyer (1977). The Mauthner-initiated startle response in teleost fish. *Journal of experimental Biology* 66:65-81.

Ebashi, S. (1975). Regulatory mechanism of muscle contraction with special reference to the Ca-troponin-tropomyosin system. *Essays Biochem.* 10: 1-36.

Ebashi, S. (1991). Excitation-contraction coupling and the mechanism of muscle contraction. *Annual Review of Physiology* 53: 1-16.

Edman, K. A. P. (1979). The velocity of unloaded shortening and its relation to sarcomere length and isometric force in vertebrate muscle fibres. *Journal of Physiology (London)* 291:143-159.

Edman, K. A. P., G. Elzinga and M. I. M. Noble (1978). Enhancement of mechanical performance by stretch during tetanic contractions of vertebrate skeletal muscle fibres. *Acta Physiologica Scandinavica* 109:15-26.

Edman, K. A. P., L. A. Mulieri, and B. Scubon-Mulieri (1976). Non-hyperbolic force-velocity relationship in single muscle fibres. *Acta Physiologica Scandinavica.* 98:143-156.

Eggington, S. and I. A. Johnston (1982a). Quntitative analyses of ultrastructure and vascularisation of the slow muscle fibres of the anchovy. *Tissue and Cell* 14: 319-328.

Eggington, S. and I. A. Johnston (1982b). A morphometric analysis of regional differences in myotomal muscle ultrastructure in the juvenile eel (*Anguilla anguilla* L.). *Cell and Tissue Research* 222:579-596.

Eisenberg, B. R. and R. S. Eisenberg (1982). The T-SR junction in contracting single skeletal muscle fibres. *Journal of General Physiology* 79: 1-19.

Eisenberg, B. R. and A. M. Kuda (1975). Stereological analysis of mammalian skeletal muscle. II. white vastus muscle of the adult guinea pig. *Journal of Ultrastructural Research* 51:176-187.

Eisenberg, B. R. and S. Salmons (1981). The reorganisation of subcellular structure in muscle undergoing fast-to-slow type transformation. A stereological study. *Cell and Tissue Research* 220:449-471.

Eisenberg, B. R., A. M. Kuda and J. B. Peter (1974). Stereological analysis of mamalian skeletal muscle. I. soleus muscle of the adult guinea pig. *Journal of Cell Biology* 60:732-754.

Fabiato, A. and F. Fabiato (1978). Myofilament-generated tension oscillations during partial calcium activation and activation

dependence of the sarcomere length tension relation of skinned cardiac cells. *Journal of General Physiology* 72:667-669.

Fierstine, H. L and V. Walters (1968). Studies in locomotion and anatomy of scombroid fishes. *Mem. South Calif.Acad.Sci.* 6: 1-31.

Finer, J. T., R. M. Simmons and J. A. Spudich (1994). Single myosin molecule mechanics: piconewton forces and nanometre steps. *Nature* 368:113-119.

Flemming, J. R., T. C. Crockford, J. D. Altringham and I. A. Johnston (1990). Effects of temperature on muscle relaxation in the carp: a mechanical, biochemical, and ultrastructural study. *Journal of experimental Zoology* 255:286-295.

Focant, B., F. Huriaux and I. A. Johnston (1976). Subunit composition of fish myofibrils: the light chains of myosin. *International Journal of Biochemistry* 7:129-133.

Ford, L. E., A. F. Huxley and R. M. Simmons (1985). Tension transients during steady shortening of frog muscle fibres. *Journal of Physiology (London)* 361:131-150.

Foreman, M. B. and R. C. Eaton (1993). The direction change concept for reticulospinal control of goldfish escape. *Journal of Neuroscience* 13(10):4101-4113.

Frith, H. R. and R. W. Blake (1991). Mechanics of the startle response in the northern pike, *Esox lucius. Canadian Journal of Zoology* 69:2831-2839.

Full, R. J. (1991). The concepts of efficiency and economy in land locomotion. Pages 97-132 in R. W. Blake, ed. *Efficiency and economy in animal physiology.* Cambridge University Press, Cambridge.

Gans, C. (1991). Efficiency, effectiveness, perfection, optimisation: their use in understanding vertebrate evolution. Pages 1-12 in R. W. Blake, ed. *Efficiency and economy in animal physiology.* Cambridge University Press, Cambridge.

Garland, T. and S. C. Adolph (1994). Why not do two species comparative studies: limits on inferring adaptation. *Physiological Zoology* 67(4): 797-828.

Gerday, C. and J. M. Gillis (1976). The possible role of parvalbumins in the control of contraction. *Journal of Physiology (London)* 258:96-97P.

Gerlach, G-F., L. Turay, K. T. Malik, J. Lida, A. Scutt and G. Goldspink (1990). Mechanisms of temperature acclimation in the carp: a molecular biology approach. *American Journal of Physiology* 259:R237-R244.

Goolish, E. M. (1991). Aerobic and anaerobic scaling in fish. *Biological Reviews* 66:33-56.

Gordon, A. M., A. F. Huxley and F. J. Julian (1966). The variation in isometric tension with sarcomere length in vertebrate muscle fibres. *Journal of Physiology (London)* 184:170-192.

Grabarek, Z., T. Tao and J. Gergely (1992). Molecular mechanism of troponin-C function. *Journal of Muscle Research and Cell Motility* 13: 383-393.

Gray, J. (1933). Studies in animal locomotion: II. The relationship between waves of muscular contraction and the propulsive mechanism of the eel. *Journal of experimental Biology* 10:386-390.

Greaser, M. L., R. L. Moss and P.J. Reiser (1988). Variations in contractile properties of rabbit single muscle fibres in relation to troponin T isoforms and myosin light chain. *Journal of Physiology (London)* 406:85-98.

Greer-Walker, M. and G. A. Pull. (1975). A survey of red and white muscle in marine fish. *Journal of Fish Biology* 7:295-300.

Griffiths, R. I. (1991). Shortening of muscle fibres during stretch if the active cat medial gastrocnemius muscle: the role of tendon compliance. *Journal of Physiology (London)* 436:219-236.

Grillner, S. and S. Kashin (1976). On the generation and performance of swimming in fish. Pages 181-201 in R. M. Herman, S. Grillner, P. S. G. Stein and D. G. Stuart, eds. *Neural control of locomotion.* Plenum Press, New York.

Grillner, S., J. T. Buchanan, P. Wallén and L. Brodin (1988). Neural control of locomotion in lower vertebrates - from behaviour to ionic mechanisms. Pages 1-40 in A. H. Cohen, S. Rossignol and S. Grillner, eds. *Neural control of rhythmic movements in vertebrates.* Wiley, New York.

Grillner, S., P. Wallén, L. Brodin and A. Lansner. 1993. Pages 39-63 in C. M. C. Bakker, M. A. M. Berger, C. A. M. Doorenbosch, C. E. Peper, M. E. T. Willems and F. T. J. M. Zaal, eds. *Neural aspects of human movement - implications for control and coordination.* Swets and Zeitlinger, Amsterdam.

Harden-Jones, F. R., G. P. Arnold, M. Greer-Walker and P. Scholes (1978). Selective tidal stream transport and the migration of Plaice (*Pleuronectes platessa* L.) in the southern North Sea. *Journal du Conseil International pour Exploration de la Mer* 38:331-337.

Harada, Y., K. Sakurada, T. Aoki, D. D. Thomas and T. Yanagida (1990). Mechanochemical coupling in actomyosin energy transduction studied by *in vitro* movement assay. *Journal of Molecular Biology* 216:49-68.

He, P., C. S. Wardle and T. Arimoto (1991). Electrophysiology of the red muscle of maxkerel, *Scomber scombrus* L. and its relation to swimming at low speed. Pages 469-472 in R. Hirano and I Hanyu, eds. *The second Asian fisheries forum.* Asian Fisheries Society, Manilla.

Heglund, N. C. and G. A. Cavagna (1985). Efficiency of vertebrate locomotory muscles. *Journal of experimental Biology* 115:283-292.

Hess, F. and J. J. Videler (1984). Fast continuous swimming of saithe (*Pollachius virens*): a dynamic analysis of bending movements and muscle power. *Journal of experimental Biology* 109:229-251.

Hibberd, M. G. and B. R. Jewell (1982). Calcium- and length- dependent force production in rat ventricular muscle. *Journal of Physiology (London)* 329:527-540.

Hidaka T. and N. Toida (1969). Biophysical and mechanical properties of red and white muscle fibres in fish. *Journal of Physiology (London)* 201: 49-59.

Hill, A. V. (1938). The heat of shortening and the dynamics constant of muscle. *Proceedings of the Royal Society of London Series B* 126:136-195.

Hill, A. V. (1951). The effect of series compliance on the tension develped in a muscle twitch. *Proceedings of the Royal Society of London Series B* 138:325-329.

Hill, A. V. (1964). The efficiency of mechanical power development during muscular shortening and its relation to load. *Proceedings of the Royal Society of London Series B* 159:319-324.

Hoyle, G. (1957). *Comparative physiology of the nervous control of muscular contraction.* Cambridge University Press, Cambridge. pp. 147.

Hudson, R. C. L. (1969). Polyneuronal innervation of the fast uscles of the marine teleost *Cottus scorpius* L. *Journal of experimental Biology* 50: 47-67.

Hudson, R. C. L. (1973). On the function of the white muscles in teleosts at intermediate swimming speeds. *Journal of experimental Biology* 58: 509-522.

Huriaux, F. and B. Focant (1977). Isolation and characterisation of the three light chains from carp white muscle myosin. *Archives of International Physiology and Biochemistry* 85:917-929.

Huxley, A. F. (1957). Muscle structure and theories of contraction. *Prog. Biophys. biophys. Chem.* 7:255-318.

Huxley, A. F. (1974). Muscular contraction. *Journal of Physiology (London)* 243:1-43.

Huxley, A. F. and R. Niedergerke (1954). Interference microscopy of living muscle fibres. *Nature (London)* 173:971-973.

Huxley, A. F. and R. M. Simmons (1971). Proposed mechanism of force generation in striated muscle. *Nature(London)* 233:533-538.

Huxley, H. E. and J. Hanson (1954). Changes in the cross-striation of muscle during contraction and stretch and their interpretation. *Nature (London)* 173:973-976.

Jayne, B. C. and G. V. Lauder (1993). Red and white muscle activity and kinematics of the escape response of the bluegill sunfish during swimming. *Journal of comparative Physiology A* 173:495-508.

Jayne, B. C. and G. V. Lauder (1994). how fish use slow and fast muscle fibres: implications for models of vertebrate muscle recruitment. *Journal of comparative Physiology A* 175:123-131.

Jewell, B. R. and D. R. Wilkie (1958). An analysis of the mechanical component of frog's striated muscle. *Journal of Physiology (London)* 143:515 540.

Jewell, B. R. and D. R. Wilkie (1960). The mechanical properties of relaxing muscle. *Journal of Physiology (London)* 293:30-47.

Johnson, T. P. and I. A. Johnston. (1991a). Power output of fish muscle fibres performing oscillatory work: effects of acute and seasonal temperature change. *Journal of experimental Biology* 157:409-423.

Johnson, T. P. and I. A. Johnston (1991b). Temperature adaptation and the contractile properties of live muscle fibres from teleost fish. *Journal of comparative Physiology B* 161:27-36.

Johnson, T. P., J. D. Altringham and I. A. Johnston (1991). The effects of Ca^{2+} and neuromuscular blockers on the activation of fish muscle fibres. *Journal of Fish Biology* 38:789-790.

Johnson, T. P., I. A. Johnston and T. W. Moon (1991). Temperature and the energy cost of oscillatory work in teleost fast muscle fibres. *Pflügers Archiv* 419:177-183.

Johnston, I. A. (1981). Structure and function of fish muscles. Pages 71-113 in M. H. Day, ed. *Vertebrate locomotion*. Symposia of the Zoological Socety of London no.48. Academic Press, London.

Johnston, I. A. (1983). On the design of fish myotomal muscles. *Marine Behavioural Physiology* 9:83-98.

Johnston, I. A. and L. M. Bernard (1982). Routine oxygen consumption and characteristics of the myotomal muscle in tench: effects of long-term acclimation to hypoxia. *Cell and Tissue Research* 227:161-177.

Johnston, I. A. and J. Dunn (1987). Pages 67-93 in K. Bowler and B. J. Fuller, eds. *Temperature and animal cells*. Symposia of the Society for experimental Biology XXXXI. Cambridge University Press, Cambridge.

Johnston, I. A. and G. Goldspink (1973a). A study of glycogen and lactate in the myotomal muscles and liver of the coalfish (*Gadus virens* L.) during sustained swimming. *Journal of the Marine Biological Association U.K.* 53:17-26.

Johnston, I. A. and G. Goldspink. (1973b). Quantitative studies of muscle glycogen utilisation in the crucian carp (*Carassius carassius* L.) during sustained swimming. *Journal of experimental Biology* 59:607-615.

Johnston, I. A. and T. W. Moon (1980) Endurance training in the fast and slow skeletal muscles of a teleost fish (*Pollachius virens*). *Journal of comparative Physiology* 135:147-156.

Johnston, I. A. and T. W. Moon (1981). FIne structure and metabolism of multiply innervated fast muscle fibres in teleost fish. *Cell and Tissue Research* 219:93-109.

Johnston, I. A. and J. Salmonski (1984). Power output and force-velocity relationship of red and white muscle fibres from the pacific blue marlin (*Makaire nigricans*). *Journal of experimental Biology* 111: 171-177.

Johnston, I. A., W. Davison and G. Goldspink (1977). Energy metabolism of carp swimming muscles. *Journal of comparative Physiology* 114: 203-216.

Johnston, I. A., C. E. Franklin and T. P. Johnson (1993). Recruitment patterns and contractile properties of fast muscle fibres isolated from rostral and caudal myotomes of the short-horned sculpin. *Journal of experimental Biology* 185:251-265.

Johnston, I. A., N. Frearson and G. Goldspink (1973). The effects of environmental temperature on the properties of myofibrillar adenosine triphosphatase from various species of fish. *Biochemistry Journal* 133:735-738.

Johnston, I. A., B. D. Sidell and W. R. Driedzic (1985). Force-velocity characteristics and metobolism of carp muscle fibres following

temperature acclimation. *Journal of experimental Biology* 119:239-249.

Johnston, I. A., P. S. Ward and G. Goldspink (1975). Studies on the swimming musculature of the rainbow trout. I. fibre types. *Journal of Fish Biology* 7:451-458.

Johnston, I. A., S. Patterson, P. S. Ward and G. Goldspink (1974). The histochemical demonstration of myofibrillar adenosine triphosphatase activity in fish muscle. *Canadian Journal of Zoology* 52:871-877.

Johnston, I. A., J. L. Van Leeuwen, M. L. F. Davies and T. Beddow (1995). Muscle power output in a fish under conditions simulating prey capture. In preparation.

Josephson, R. K. (1985). Mechanical power output from striated muscle during cyclical contraction. *Journal of experimental Biology* 114: 493-512.

Josephson, R. K. (1993). Contraction dynamics and power output of skeletal muscle. *Annual Review of Physiology* 55:527-546.

Josephson, R. K. and D. R. Stokes (1989). Strain, muscle length and work output in a crab muscle. *Journal of experimental Biology* 131:265-287.

King, P. A., J. M. Fives and J. Dunne (1983). Littoral and benthic investigations on the west coast of Ireland - XVIII. The biology of the

short-spined sea scorpion *Myoxocephalus scorpius*(L.) in the Galway Bay area. *Proc. R. Ir. Acad.* 83B:325-334.

Korneliussen, H., H. A. Dahl and J. E. Paulsen (1978). Histochemical definition of muscle fibre types in the trunk musculature of a teleost fish (cod, *Gadus morhua* L.). *Histochemistry* 55:1-16.

Krueger, H. M., J. B. Saddler, G. A. Chapman, I. J. Tinsley and R. R. Lowry (1968). Bioenergetics, exercise and fatty acids of fish. *American Zoology* 8:119-129.

Kryvi, H. (1977). Ultrastructure of the different fibre types in axial muscles of the sharks *Etmopterus spinax* and *Galeus melastomus*. *Cell and Tissue Research* 184:287-300.

Kryvi, H., T. Flatmark and G. H. Totland (1981). The myoglobin content in red, intermediate and white fibres of the swimming muscles in three species of shark - a comparitive study using high-performance liquid chromatography. *Journal of Fish Biology* 18:331-338

Kryvi, H., P. R. Flood and D. Gulyaev (1980). The ultrastructure and vascular supply of the different fibre types in the axial muscle of the sturgeon *Acipenser stellatus*, Pallus. *Cell and Tissue Research* 212: 117-126.

Kugelberg, E. and A. F. Thornell (1983). Contraction time, histochemical type and terminal cisternae volume of rat motor units. *Muscle and Nerve* 6:149-153.

Lackner, R., W. Weiser, M. Huber and J. Dalla Via (1988). Response of intermediary metabolism to acute handling stress and recovery in untrained and trained *Leuciscus cephalus* (Cyprinidae, Teleostei). *Journal of experimental Biology* 140:393-404.

Landesberg, A. and S. Sideman (1994). Coupling calcium-binding to troponin-C and cross-bridge cycling in skinned cardiac cells. *American Journal of Physiology* 266:1260-1271.

Langfeld, K. S., J. D. Altringham and I. A. Johnston (1989). Temperature and the force-velocity relationship of live muscle fibres from the teleost *Myoxocephalus scorpius*. *Journal of experimental Biology* 144: 437-448.

Langfeld, K. S., T. Crockford and I. A. Johnston (1991). Temperature acclimation in the common carp: force-velocity characteristics and myosin subunit composition of slow muscle fibres. *Journal of experimental Biology* 155:291-304.

Lännergren, J. (1978). The force-velocity relation of isolated twitch and slow muscle fibres of *Xenopus laevis*. *Journal of Physiology (London)* 283:501-521.

Leiber, R. L., R. Raab, S. Kashin and V. R. Edgerton (1992). Sarcomere length changes during fish swimming. *Journal of experimental Biology* 169:251-254.

Lighthill, M. J. (1960). Note on the swimming of slender fish. *Journal of Fluid Mechanics* 9:305-317.

Lighthill, M. J. (1970). Aquatic animal propulsion of high hydromechanical efficiency. *Journal of Fluid Mechanics* 44:265-301.

Lin, Y., G. H. Dobbs and A. L. De Vries (1974). Oxygen consumption and lipid content in red and white muscle of Antarctic fishes. *Journal of experimental Zoology* 189:379-385.

Lindsey, C. C. (1978). Form, function and locomotory habits in fish. Pages 1-100 in W. S. Hoar and D. J. Randall, eds. *Fish physiology (VII): Locomotion.* Academic Press, London.

Lindstedt, S. L. and J. H. Jones (1987). Symmorphosis: the concept of optimal design. Pages 289-309 in M. E. Feder, A. F. Bennett, W. W. Burggren & R. B. Huey, eds. *New directions in Ecological Physiology.* Cambridge University Press, Cambridge.

Lipschutz, M. M. (1969). *Theory and Problems of Differetial Geometry.* Schaum's outline series, McGraw-Hill, New York. 269pp.

Liu, D. W. and M. Westerfield (1988). Function of identified motoneurones and co-ordination of primary and secondary motor systems during zebra fish swimming. *Journal of Physiology (London)* 403:73-89.

Lombardi, V. and G. Piazzesi (1990). The contactile response during steady lengthening of stimulated frog muscle fibres. *Journal of Physiology (London)* 431:141-171.

Lowey, S. and D. Risby (1971). Light chains from fast and slow muscle myosins. *Nature (London)* 234: 81-85.

Lowey, S., G. S. Waller and K. M. Trybus (1993). Skeletal muscle myosin light chains are essential for physiological speeds of shortening. *Nature (London)* 365: 454-456.

Luff, A. R. and H. L. Atwood (1971). Changes in the sacoplasmic reticulum and transverse tubular system of the mouse during postnatal development. *Journal of Cell Biology* 51: 369-

McClellan, A. and S. Grillner (1984). Activation of 'fictive' swimming by electrical microstimulation of brainstem locomotor regions in an in vitro preparation of the lamprey central nervous system. *Brain Research* 300: 357-361.

Macer, C. T. (1991). The Atlantic cod. *Biologist* 38(5): 189-193.

Marsh, R. L. and A. F. Bennett (1985). Thermal dependence of isoonic contractile properties of skeletal muscle and sprint performance of the lizard *Dipsosaurus dorsalis*. *Journal of Comparative Physiology* 155: 541-551.

Marsh, R. L. and A. F. Bennett (1986). Thermal dependence of contractile properties of skeletal muscle from the lizard *Sceloporus occidentalis* with comments on methods for fitting and comparing force-velocity curves. *Journal of experimental Biology* 126: 63-77.

Marsh, R. M. and J. M. Olson (1994). Power output of scallop adductore muscle during contracions replicating the *in vivo* mechaincal cycle. *Journal of experimental Biology* 193:139-156.

Mayr, E. (1976). *Evolution and the diversity of life.* Belknap Press, Cambridge, Massechusets.

Medley, D. G. (1982). *An introduction to mechanics and modelling.* Heinemann Educational Books Ltd, London. 340 pp.

Milligan, C. L. and C. M. Wood (1986a). Tissue intracellular acid-base status and the fate of lactate after exhaustive exercise in the rainbow trout. *Journal of experimental Biology* 123:123-144.

Milligan, C. L. and C. M. Wood (1987b). Muscle and liver intracelluler acid-base metabolite status afte strenuous activity in the inactive, benthic starry flounder (*Platichthys stellatus*). *Physiological Zoology* 60:37-53.

Moon, T. W., J. D. Altringham and I. A. Johnston (1991). Energetics and power output of isolated fast fibres performing oscillatory work. *Journal of experimental Biology* 158:261-273.

Mos, W., S. Maslam and E. Armée-Horvath (1988). Changes in the distribution of synapses during growth: a quantitative morphological study of the neuromuscular system of fishes. *Neuroscience* 24(3): 1061-1069.

Munro, H. N. (1969). Evolution of protein metabolism in mammals. Pages 133-182 in H. N. Munro, ed. *Mammalian protein metabolism, vol 3.* Academic Press, London.

Nachlas, M. M., K. C. Tsou, E. De Sonza, C. S. Cheng and A. M. Seligman (1957). Cytochemical demonstration of succinic dehydrogenase by the use of a new *p*-nitrophenylsubstituted ditetrazole. *Journal of Histochem. Cytochem.* 5:420-436.

Nag, A. C. (1972). Ultrastructure and adenosine triphoosphate activity of red and white muscle fibres of the caudal region of a fish Salmo Gairdneri. *Journal of Cell Biology* 55:42-57.

Offer, G. (1987). Myosin filaments. In J. M. Squire and P. J. Vibert, eds. *Fibrous protein structure.* Academic Press, London.

Page, S. G. and H. E. Huxley (1963). filament lengths in striated muscle. *Journal of Cell Biology* 19:369-390.

Patterson, S. Johnston, I. A. and Goldspink, G. (1975). A histochemical study of the lateral muscles of five teleost species. *Journal of Fish Biology* 7:159-166.

Peachy, L. D. (1965). The sarcoplasmic reticulum and transverse tubules of the frog sartorius. *Journal of Cell Biology* 25:209-231.

Pechère, J. F., J. Derancourt and J. Harech (1977). The participation of parvalbumins in the activation-relaxation cycle of vertebrate skeletal muscle. *FEBS letters* 75:111-114.

Pennycuick, C. J. (1991). Adapting skeletal muscles to be efficient. Pages 33-42 in R. W. Blake, ed. *Efficiency and economy in animal physiology.* Cambridge University Press, Cambridge.

Phillips, S. K. and R. C. Woledge (1992). A comparison of isometric force, maximum power and isometric heat as a function of sacomere length in mouse skeletal muscle. *Pflügers Archiv* 420:578-583.

Potter, J. D. and J. Gergely (1975). The calcium and magnesium binding sites on troponin and their role in the regulation of myofibrillar adenosine triphosphatase. *Journal of Biological Chemistry* 250:4628-4633.

Prandtl, L. (1952). *Essentials of fluid dynamics.* Blackie, London.

Prosser, C. L. and D. O. Nelson (1981). The role of nervous systems in temperature adaptation of poikilotherms. *Annual Review of Physiology* 43:281-300.

Rahmann, H., W. Schmidt and B. Schmidt (1980). Influence of long-term thermal accliamtion on the conditionability of fish. *Journal of Thermal Biology* 5:11-16.

Rall, J. A. and B. A. Schottelius (1973). Energetics of contraction in phasic and tonic skeletal muscles of the chicken. *Journal of General Physiology* 62:303-323.

Ramsey, R. W. and D. F. Street (1940). The isometric length-tension diagram of isolated muscle fibres of the frog. *Journal of Cell and Comparative Physiology* 15: 11-34.

Ranatunga, K. W. (1984). The force-velocity relation of rat fast-twitch and slow-twitch muscles examined at different temperatures. *Journal of Physiology (London)* 351:517-529.

Ranatunga, K. W. and P. E. Thomas (1990). Correlation between shortening velocity, force-velocity relation and histochemical fibre-type composition in rat muscles. *Journal of Muscle Research and Cell Motility* 11:240-250.

Randall, D. and C. Brauner (1991). Effects of environmental factors on exercise in fish. *Journal of experimental Biology* 160:113-126.

Rayment, I., W. R. Rypniewski, K. Schmidt-Bäse, R. Smith, D. R. Tomchick, M. M. Benning, D. A. Winkelmann, G. Wesenberg and H. M. Holden (1993a). Three-dimensional structure of myosin subfragment-1: a molecular motor. *Science* 261:50-58.

Rayment, I., H. M. Holden, M. Whittaker, C. B. Yohn, M. Lorenz, K. C. Holmes and R. A. Milligan (1993b). Structure of the actin-myosin complex and its implications for muscle contraction. *Science* 261:58-65.

Rome, L. C. (1983). The effect of long-term exposure to different temperatures on the mechanical performance of frog muscle. *Physiological Zoology* Rome, L. C. (1990).56: 33-40.

Rome, L. C. (1990). Influence of temperature on muscle recruitment and muscle function *in vivo*. *American Journal of Physiology* 259:R210-R222.

Rome, L. C. and A. A. Sosnicki (1990). The influence of temperature on mechanics of red muscle in carp. *Journal of Physiology (London)* 427:151-169.

Rome, L. C., R. P. Funke and R. McNiell Alexander (1990). The influence of temperature on muscle velocity and sustained performance in swimming carp. *Journal of experimental Biology* 154:163-178.

Rome, L. C., A. Sosnicki and I-H. Choi (1992). The influence of temperature on muscle function in the fast swimming scup. II. the mechanics of red muscle. *Journal of experimental Biology* 163:281-295.

Rome, L. C., A. A. Sosnicki and D. O. Goble (1990). Maximum velocity of shortening of three fibre types from horse soleus muscle: implications for scaling with body size. *Journal of Physiology (London)* 431:173-185.

Rome, L. C., D. Swank and D. Corda (1993). How fish power swimming. *Science* 261:340-343.

Rome, L.C., I-H. Choi, G. Lutz and A. Sosnicki (1992). The influence of temperature on muscle function in the fast swimming scup. I. shortening velocity and muscle recruitment during swimming. *Journal of experimental Biology.* 163:259-279.

Rome, L, C., R. P. Funke, R. McNeill Alexander, G. Lutz, H. D. J. N. Aldridge, F. Scott and M. Freadman (1988). Why animals have different muscle fibre types. *Nature (London)* 355:824-827.

Romer, A. S. (1959). *The Vertebrate Story.* 4th edition. The University of Chicago Press, London. 437 pp.

Roots, B. I. and C. L. Prosser (1962). Temperature acclimation and the nervous system of fish. *Journal of experimental Biology 39:617-629.*

Rose, G. A. (1993). Cod spawning on a migration highway in the north-west Atlantic. *Nature (London)* 366:458-461.

Rüegg, J. C. (1988). *Calcium in muscle activation.* Springer-Verlag, Heidelberg. 300 pp.

Scarabello, M., G. H. J. Heogenhauser and C. M. Wood (1991). The oxygen debt hypothesis in juvenille rainbow trout after exhaustive exercise. *Respiratory Physiology* 84:245-259.

Schmidt-Nielsen, K. (1984). *Scaling: why is animal size so important?* Cambridge University Press, Cambridge. pp. 241.

Sosnicki, A. A., K. E. Loesser and L. C. Rome (1991) Myofilament overlap in swimming carp I. myofilament lengths of red and white muscle. *American Journal of Physiology* 260:C283-C288.

Squire, J. L. (1981). Muscle regulation: a decade of the steric blocking model. *Nature (London)* 291:614-615.

Stevens, E. D. (1993). Relation between work and power calculated from force-velocity curves to that done during oscillatory work. *Journal of Muscle Research and Cell Motility* 14:518-526.

Stevens, E. D. and E. C. Black (1966). The effect of intermittent exercise on carbohydrate metabolism in rainbow trout, *Salmo gairdneri. Journal of the Fisheries Research Board of Canada* 23:471-485.

Stonington, H. H. and A. G. Engel (1973). Normal and denervated muscle. *Neurology* 23:714.

Tatarczuch, L. and W. Kilarski (1982). Histochemical analysis of muscle fibres in myotome of teleost fishes (*Carassius auratus gibelio*). *Folia Histochemica et Cytochemica* 20 (3-4):143-170.

ter Keurs, H. E. D. J., A. R. Luff and S. E. Luff (1984). Force-sarcomere-length relation and filament length in rat extensor digitorum muscle. Pages 511-522 in G. H. Pollack and H. Sugi, eds. *Contractile mechanisms in muscle*. Plenum Press, London.

Totland, G. K., H. Kryvi, Q. Bone and P. R. Flood (1981). Vascularization of the lateral muscle of some elasmobranchiomorph fishes. *Journal of Fish Biology* 18:223-234.

Turner, J. D., C. M. Wood and D. Clarke (1983). Lactate and proton dynamics in the rainbow trout (*Salmo gairdneri*). *Journal of experimental Biology* 104:247-268.

Ushio, H. and S. Watabe (1993). Effects of temperature acclimation on Ca^{2+}-ATPase of the carp sarcoplasmic reticulum. *Journal of experimental Zoology* 265: 9-17.

Van Leeuwen, J. L. (1991). Optimum power output and structural design of sarcomeres. *Journal of theoretical Biology* 149: 229-256.

Van Leeuwen, J. L. (1992). Muscle function in locomotion. Pages 191-250 in R. McNeill Alexander. *Mechanics of animal locomotion*. Springer-Verlag, Heidelberg.

Van Leeuwen, J. L. (1994). The action of muscles in swimming fish. *Experimental Physiology*: under review.

Van Leeuwen, J. L., M. J. M. Lankheet, H. A. Akster and J. W. M. Osse (1990). Function of red axial muscle of carp (Cyprinus carpio): recruitment and normalised power output during swimming in different modes. *Journal of Zoology (London)* 220: 123-145.

Videler, J. J. (1981). Swimming movements, body structure and propulsion in Cod, *Gadus morhua*. Pages 1-27 in M. H. Day, ed. *Vertebrate locomotion*: Proceedings of the symposium of the zoological society of London 48. Academic Press, London.

Videler, J. J. (1993). *Fish swimming*. Chapman and Hall, London.

Videler, J. J. and C. S. Wardle (1978). New kinematic data from high speed cine film recordings of swimming cod (*Gadus morhua*). *Netherlands Journal of Zoology* 28: 465-484.

Videler, J. J. and C. S. Wardle (1991). Fish swimming stride by stride: speed limits and endurance. *Reviews in Fish Biology and Fisheries* 1:23-40.

Videler, J. J. and D. Weihs (1982). Energetic advantage of burst-and-coast swimming of fish at high speeds. *Journal of experimental Biology* 97: 169-178.

Wainwright, S. A. (1983). To bend a fish. Pages 68-91 in P. W. Webb and D. Weihs, eds. *Fish Biomechanics.* Preager Publishers, New York.

Walker, S.M. and G. Randolph-Schrodt (1973). I-segment lengths and thin filament periods in skeletal muscle fibres of the Rhesus monkey and the human. *Anatomical Research* 178:63-82.

Wallén, P. and T. L. Williams (1984). Fictive locomotion in the lamprey spinal chord in vitro compared with swimming in the intact and spinal animal. *Journal of Physiology (London)* 347:225-239.

Wardle, C. S. (1975). Limit of fish swimming speed. *Nature (London)* 225: 725-727.

Wardle, C. S. (1978). Non-release of lactic acid from anaerobic swimming muscle of plaice, *Pleuronectes platessa*: a stress rection. *Journal of experimental Biology* 77:141-155.

Wardle, C. S. (1985). Swimming activity in fish. Pages 521-540 in M. S. Laverack, ed. *Physiological adaptations of Marine Animals.* Company of Biologists, Cambridge.

Wardle, C. S. and J. J. Videler (1980). Fish Swimming. Pages 125-150 in H. Y. Elder and E. R. Trueman, eds. *Aspects of Animal Movement*. Cambridge University Press, Cambridge.

Wardle, C. S. and J. J. Videler (1993). The timing of the EMG in the lateral myotomes of mackerel and saithe at different swimming speeds. *Journal of Fish Biology* 42 (3):347-359.

Watabe, S., G. -C. Hwang, M. Nakaya, X. -F. Guo and Y. Okamoto (1992). Fast skeletal myosin isoforms in thermally acclimated carp. *Journal of Biochemistry* 111:113-122.

Webb, P. W. (1971*a*). The swimming energetics of trout II. Oxygen consumption and swimming efficiency. *Journal of experimental Biology* 55:521-540.

Webb, P. W. (1971*b*). The swimming energetics of trout I. thrust and power output at cruising speeds. *Journal of experimental Biology* 55:489-520.

Webb, P. W. (1975*a*). Hydrodynamics and energetics of fish propulsion. *Bulletin of the Fisheries Research Board of Canada* 190:1-159.

Webb, P. W. (1975*b*). Efficiency of pectoral fin propulsion of *Cymatogaster aggregata*. In T. Y. Wu, C. J. Brokaw and C. Brennen, eds. *Swimming and flying in nature*. Plenum Press, New York.

Webb, P. W. (1984). Form and function in fish swimming. *Scientific American* 251:58-68.

Webb, P. W. and D. Weihs (1983). Optimisation of locomotion. Pages 339-371 in P. W. Webb and D. Weihs, eds. *Fish Biomechanics.* Preager Publishers, New York.

Webb, P. W., P. T. Kostecki and E. D. Stevens (1984). The effect of size and swimming speed on locomotor kinematics of rainbow trout. *Journal of experimental Biology* 109:77-95.

Weibel, E. R. (1972). A stereological method for estimating volume and surface of sarcoplasmic reticulum. *Journal of Microscopy* 95:229-242.

Weibel, E. R. (1973). Stereological techniques for electron microscopic morphometry. Pages 237-296 in M. A. Hayat, ed. *Principles and techniques of electron microscopy, Vol. III.* Van Nostrand Reinhold Co., New York.

Weibel, E. R. (1979). *Stereological methods, Vol 1. Practical methods for biologcal morphometry.* Academic Press, London.

Weihs, D. (1974). Energetic advantges of burst swimming of fish. *Journal of Theoretical Biology* 48:215-229.

Weihs, D. (1975). Some hydrdynamical aspects of fish schooling. Pages 703-718 in T. Y. Wu, C. J. Brokaw and C. Brennen, eds. *Swimming and flying in nature.* Plenum Press, New York.

Weiser, W., R. Lackner, S. Hinterleitner and U. Platzer (1987). Distribution and properties of lactate dehydrogenase isoenzymes in red and white muscle of freshwater fish. *Fish Physiology and Biochemistry* 3:151-162.

Westerfield, M., J. V. McMurray and J. S. Eisen (1986). Identified motoneurones and their innervation of axial muscles in the zebrafish. *Journal of Neuroscience* 6(8):2267-2277.

Whitfield, P. (editor) (1984). *Longman illustrated animal encyclopaedia.* Marshall Editions Ltd, London. 600 pp.

Wilkie, D. R. (1960). Thermodynamics and interpretations of biological heat measurements. *Progress in Biophysical Chemistry* 10:259-298.

Wilkie, D. R. (1974). The efficiency of muscular contraction. *Journal of Mechanochemical Cell Motility* 2:257-267.

Williams, T. L., S. Grillner, V. V. Smoljaninov, P. Wallén, S. Kashin and S. Rossignol (1989). Locomotion in lamprey and trout: the relative timing of activation and movement. *Journal of experimental Biology* 143:559-566.

Winer, B. J. (1962). *Statistical principles in experimental design.* McGraw-Hill Book Company, London. 672 pp.

Wokoma, A. and I. A. Johnston (1981). Lactate production at high sustainable cruising speeds in rainbow trout (*Salmo gairdneri* Richardson). *Journal of experimental Biology* 90:361-364.

Woledge, R. C., N. A. Curtin and E. Homsher (1985). *Energetic aspects of muscle contraction.* Academic Press, London. pp. 357.

Woltring, H. J. (1986). A Fortran package for generalised, cross-validatory spline smoothing and differentiation. *Adv.Engng.Software* 8:104-113.

Wood, C. M. (1991). Acid-base and ion balance, metabolism, and thei interactions, after exhaustive exercise on fish. *Journal of experimental Biology* 160:285-308.

Zar, J. H. (1984). *Biostatistical analysis.* 2nd edition. Prentice Hall International, Inc, New Jersey. 718 pp.

Zerbolis, D. J. (1973). Temperature-dependent learning in goldfish: a multi-trial active avoidance situation. *Behavioural Biology* 8:755-761.

Acknowledgements

I owe much to Professor Ian Johnston for his unfailing help and support during my time under his supervision. I thank him for allowing me to use SUSHI, the permission to use his data set for 15°C acclimated fish in Chapter 6 and for the courage he has shown in placing his name next to mine on any joint publications arising from this thesis.

I would also like to express my gratitude to Drs. Toni Beddow and Johan van Leeuwen for allowing me to use their strains sequences for sculpin prey capture events in Chapter 6. In addition, a medal must go to Johan, who bravely chaperoned me during my stay in Leiden and helped me to appreciate (and occasionally understand) the elegance of Newtonian physics.

Thanks also to Professor Cormack of the Department of Maths & Statistics, St. Andrews who helped me wrestle with 5 factor nested and crossed analyses of variance and listened to me witter about fish on numerous occasions.

A big thank you to Malcolm McCandless and Ken Munro of the Psychology Workshop at the University of St. Andrews who are responsible for turning the concept of SUSHI into a reality and who, together with Murray Couttes, were always ready to help me cope with all those 'little' technical problems.

I wish I was able to properly thank everyone in St. Andrews and in Leiden: in one way or another you have all helped to make the last three years memorable. I have thought of something to say to everyone, but unfortunately as most of it is unprintable a big group

hug will have to suffice. However, there are a few that I would like to specially mention: the co-members and conspirators of the 'Gatty Foreigner's Society'; Bel, my porno twin, and her partner in nose-sucking, Ken Müller; the Hardege family for convincing me that you <u>can</u> eat raw herring (and live!); the Lamberts, my fellow Mainiacs, for sharing their evenings with me; Mr. Pete Baxter for putting up with my pestering and Mr. Iain Johnston for saying 'nee bother' more often than 'get stuffed you mouthy Welsh git'; Christina and Jane for always having time for someone else's problems in spite of your own; Capn' Bob Wilson who is awarded the Fish *of Merit for* obtaining cod above and beyond the call of duty; Marguerite, Lisa, Ann, Irvine, Kirsten, Mary, Isabel, Tjeerd, Janette, Craig, the Great Waldini, Boy Wonder, Nick and Mark - thank you for laughter (and many, many other things).

I would also like to mention my mother, father, Mam-Gu and my wonderful brothers for all their support and for understanding my long absences from home.

And finally to Barry, who I love very much, for waiting for three long years and always being there to encourage me and give support when I most needed it.